



Universidad de Valladolid



**ESCUELA DE INGENIERÍAS
INDUSTRIALES**

**UNIVERSIDAD DE VALLADOLID
ESCUELA DE INGENIERIAS INDUSTRIALES**

Grado en Ingeniería mecánica

Robot tool calibration equipment

Autor:

Palomero del Castillo, Luis

Responsable de Intercambio en la Uva

Marta Herráez Sánchez

Universidad de destino

Vilnius Gediminas Technical University

Valladolid, mes y año.

TFG REALIZADO EN PROGRAMA DE INTERCAMBIO

TÍTULO: Robot tool calibration equipment
ALUMNO: Luis Palomero del Castillo
FECHA: 03/06/2025
CENTRO: Faculty of Mechanics
UNIVERSIDAD: Vilnius Gedeminas Technical University
TUTOR: Vytautas Bučinskas

Resumen

El proyecto consiste en el diseño de un dispositivo de calibración fabricado para integrarse en el robot Yaskawa HC20SDTP. Las medidas de contacto se realizan mediante seis sensores piezorresistivos proporcionados por la Vilnius Tech University encerrados en una matriz de dos piezas dispuesta correctamente para analizar y diferenciar entre seis grados de libertad. El dispositivo se fija al brazo robótico mediante dos tornillos que también ensamblan la matriz, además de otros dos diseñados para calibrar el dispositivo y disponer de otro componente de fijación, lo que le confiere rigidez y precisión.

Cuando se produce el contacto, el brazo comprime estos sensores en una secuencia descrita por el algoritmo de trabajo. La señal se envía a la unidad de control para describir la dirección del palpado y, después, a la unidad del robot para su análisis, como puede ser conocer el entorno o la detección y posición de una pieza concreta.

Palabras clave: Diseño calibración de robot, 6 grados de libertad, sensores piezorresistivos, palpador de contacto, Impresión 3D.

Abstract

The project consists on the design of a touch calibration device made for being integrated in the Yaskawa HC20SDTP robot. Contact measures are made by using 6 piezo resistive sensors provided by Vilnius Gediminas Technical University, enclosed in a two-piece matrix, correctly disposed to analyse and to differentiate between six degrees of freedom. The device is attached to the robotic arm by two screws which also assemble the matrix, in addition of other two screws designed for calibrating the device and to have another fixing component, which gives rigidity and precision.

When contact is made, the touch probe compresses these sensors in a sequence described by the working algorithm. Signal is sent to the control unit for being able to describe the direction of the sensing and therefore to the robot control unit for any robot touch calibration purposes such as environment knowing or specific part detection and position.

Keywords: Robot touch calibration, 6 degrees of freedom, piezoresistive sensors, touch probe, 3D printing.



VILNIUS GEDIMINAS TECHNICAL UNIVERSITY

FACULTY OF MECHANICS

DEPARTMENT OF MECHATRONICS, ROBOTICS AND DIGITAL MANUFACTURING

Luis Palomero del Castillo

ROBOT TOOL CALIBRATION EQUIPMENT

Final Bachelor's Project

Study programme MECHATRONICS AND ROBOTICS,

Code 6121EX048

Vilnius, 2025

VILNIUS GEDIMINAS TECHNICAL UNIVERSITY

FACULTY OF MECHANICS

DEPARTMENT OF MECHATRONICS, ROBOTICS AND DIGITAL MANUFACTURING

APPROVED BY
Head of Department

(Signature)

(Name, Surname)

(Date)

Luis Palomero del Castillo

ROBOT TOOL CALIBRATION EQUIPMENT

Final Bachelor's Project

Study programme MECHATRONICS AND ROBOTICS,

Code 6121EX048

Supervisor: _____ (Title, Name, Surname) _____ (Signature) _____ (Date)

Vilnius, 2025

VILNIUS GEDIMINAS TECHNICAL UNIVERSITY

Luis Palomero del Castillo, 71179221V

(Student name and surname, Student ID)

Faculty of Mechanics

(Faculty)

Mechatronics and Robotics, MRfu-21

(Study programme, academic group)

DECLARATION OF AUTHORSHIP IN FINAL DEGREE PROJECT

2025_ 05-18

(Date)

I confirm, that my final degree project, which topic is **Robot tool calibration equipment**

is written independently. The material presented in this final degree project is not plagiarized. Quotations from other sources used directly or indirectly are indicated in the literature references.

The final degree project was inspected by: **prof. dr. Vytautas Bučinskis**

There is no contribution of other persons to the final degree project. I have not paid any statutory sums of money for this work.

Luis Palomero
(Student's Name,
Surname)

2025-05-18

Signature

LUIS PALOMERO DEL
CASTILLO

(Name and Surname)

VILNIUS GEDIMINAS TECHNICAL UNIVERSITY
FACULTY OF MECHANICS
DEPARTMENT OF MECHATRONICS ROBOTICS AND DIGITAL MANUFACTURING
APPROVED BY

Production and Manufacturing engineering study field

Head of Department

Mechatronics and robotics study programme,

State code 6121EX048

(Signature)

Vytautas

Bučinskas

(Name, Surname)

(Date)

TASK FOR BACHELOR THESIS

13 February 2025 No. 1

Vilnius

For student Luis Palomero

Bachelor Thesis title: Robot tool calibration equipment

Approved on _____.

The Final work has to be completed by _____.

TASK FOR FINAL THESIS:

Initial data:

The robot calibration tool should be suitable for use in an industrial robot. Such a device shall be capable for sensing all types of obstacles and holes. It should have 6 degrees of freedom. System should be mounted directly on robot arm. The system has been developed to be able to operate with real robotic movement errors.

Explanatory part:

1. Introduction. Analysis of analogical devices. Substantiation of the taken technical decision.
2. Calculations needed for the design process.
3. Description of the design and working principle. Electric-block scheme. Algorithm of management of device.
4. Work safety. General provisions and requirements for safe working and environmental protection. Work safety of specific devices.
5. Evaluation of economic indicators of the designed or upgraded device.
6. Final conclusions and recommendations.
7. Literature reference list.

Drawings:

1. General drawing of the device (1 sheet A1);
2. Assembly drawing of the device (node) (1 sheet A1);
3. Algorithm of management of device (0,5 sheet A1);
4. The work drawings of the chosen part (3 sheets A3);
6. Economic indicators (0.5 sheet A1).

Supervisor

.....
(Signature)

prof. dr. Vytautas Bučinskas
(Academic Title, Name, Surname)

Task accepted

.....
(Student's signature)

Luis Palomero

(Student's Name, Surname)

2025-05-02

(Date)

Vilnius Gediminas Technical University Faculty
of Mechanics
Department of Mechatronics, Robotics and
Digital Manufacturing

ISBN ISSN
Copies No.
Date 2025-05-17

Mechatronics and Robotics study program bachelor thesis.

Title: Robot tool calibration equipment

Author: Luis Palomero del Castillo Academic supervisor: Prof. dr. Vytautas Bučinskas

Thesis language

Lithuanian

Foreign (English)

Annotation

The project consists on a touch calibration device made for being integrated in the Yaskawa HC20SDTP robot. Contact measures are made by using 6 piezo resistive sensors provided by Vilnius Gediminas Technical University, enclosed in a two-piece matrix, correctly disposed to analyse and to differentiate between six degrees of freedom. The device is attached to the robotic arm by two screws which also assemble the matrix, in addition of other two screws designed for calibrating the device and to have another fixing component, which gives rigidity and precision.

When contact is made, the touch probe compresses these sensors in a sequence described by the working algorithm. Signal is sent to the control unit for being able to describe the direction of the sensing and therefore to the robot control unit for any robot touch calibration purposes such as environment knowing or specific part detection and position.

Structure: introduction, overview of analytic constructions, overview of specific nodes, calculations, description of construction and operating principle, work safety, economical calculation and conclusions and suggestions, references.

Thesis consist of: 58 p. text without appendixes, 30 pictures, 8 tables, 19 bibliographical entries.

Appendixes included.

Keywords: Robot calibration, touch sensor, 6 degrees of freedom, piezoresistive sensors, touch probe, mechanic design, 3D printing.

Vilnius Gediminas Technical University Faculty
of Mechanics
Department of Mechatronics, Robotics and
Digital Manufacturing

ISBN ISSN
Copies No.
Date 2025-05-17

Mechatronics and Robotics study program bachelor thesis.

Title: Robot tool calibration equipment

Author: Luis Palomero del Castillo Academic supervisor: Prof. dr. Vytautas Bučinskas

Thesis language

Lithuanian

Foreign (English)

Annotation

Projektą sudaro jutiklinis kalibravimo įrenginys, skirtas naudoti į Yaskawa HC20SDTP robotą. Jutikliai bus sukurti naudojant šešis Vilniaus Gedimino technikos universiteto pateiktus pjezo varžinius jutiklius, įtaisytus į dviejų dalių matricą, išdėstytus taip, kad jų signalai tikėtų analizuoti judesius pagal šešis laisvės laipsnius. Prietaisas prie roboto rankos tvirtinamas dviem varžtais, kurie taip pat tvirtina jutiklių matricą, be kitų dviejų varžtų, skirtų prietaisui kalibruoti ir turėti kitą tvirtinimo komponentą, kuris suteikia tvirtumo ir tikslumo.

Kai paliečiamas objektas roboto jutikliu, jutiklio svirtelė suspaudžia šiuos jutiklius atitinkama kryptimi ir procesorius suskaičiuoja koordinates darbo algoritmo aprašyta seka. Signalas siunčiamas į valdymo bloką, kad būtų galima apibūdinti jutimo kryptį, taigi ir į roboto valdymo bloką bet kokiems roboto prisilietimo kalibravimo tikslams, pavyzdžiui, aplinkos pažinimui arba konkrečios dalies aptikimui ir padėties nustatymui.

Darbą sudaro 4 dalys: įvadas, analitinių konstrukcijų apžvalga, konkrečių mazgų apžvalga, skaičiavimai, konstrukcijos ir veikimo principo aprašymas, darbų sauga, ekonominis skaičiavimas ir išvados bei pasiūlymai, literatūros sąrašas.

Darbo apimtis – 58 p. teksto be priedų, 30 iliustracijų, 8 lent., 19 bibliografinių šaltinių.

Pridedami priedai.

Keywords: Robot calibration, touch sensor, 6 degrees of freedom, piezoresistive sensors, touch probe, mechanic design, 3D printing.

CONTENT

LIST OF PICTURES	7
LIST OF TABLES	8
INTRODUCTION	9
1. OVERVIEW OF ANALOGIC CONSTRUCTIONS	11
1.1. Optimized Design of a Triangular Shear Piezoelectric Sensor	11
Using Non-Dominated Sorting Genetic Algorithm-II(NSGA-II).....	11
1.2. Development of a Six-Degree-of-Freedom Analog 3D Tactile	13
Probe Based on Non-Contact 2D Sensors.....	13
1.3 A Piezoelectric Tactile Sensor for Tissue Stiffness	14
Detection with Arbitrary Contact Angle	14
1.4 Piezoresistive tactile sensor:.....	15
1.5 Silicon Piezoresistive Six-Degree of Freedom Micro Force-Moment Sensor.....	17
1.6 Working principle and commercial Ideas	19
1.6.2 Kistler triaxial force transducer:.....	20
1.4.3 Tekscan Flexiforce standard model A502:.....	21
1.5. Substantiation of the decision	22
2. OVERVIEW OF SPECIFIC NODES.....	24
2.1. Device design, general view and function.	24
2.1. Material of the sensor and robot.....	26
3. CALCULATION OF PROJECT	27
3.1. Specifications, calculations and accuracy	27
3.2. Finite element Static analysis calculations.....	33
3.3. Frequency analysis	38
3.3. Thermal expansion calculation	39
4. DESCRIPTION OF THE CONSTRUCTION AND OPERATIONAL PRINCIPLE.....	40
4.1. Assembly construction scheme	40
4.2. Electric block scheme	43
4.2.1. Electric-block and control scheme	43
4.3. Algorithm of management of device or node	45
5. WORK SAFETY	47
5.1. General provisions and requirements for safe working and environmental protection	47
5.2. Work safety and environmental requirements of robotic calibration tool:	47
6. ECONOMIC CALCULATION.....	50

7. CONCLUSIONS	53
LIST OF LITERATURE	56
THE ANNEXES	58
Piezo resistive material provided by VGTU	58
Tensile stress-strain curves of ABS and PLA for flat and upright printing orientations	59
Drawings	¡Error! Marcador no definido.

LIST OF PICTURES

Figure 1.1 Geometric structure of the piezoelectric sensor	11
Figure 1.2 Diagram of voltage and deformation (Shi & Dai, 2025)	12
Figure 1.3 LED measuring device (Albajez et al., 2024)	13
Figure 1.4 (a) Structure of piezoelectric tactile sensor. (b) Detect tissue with contact angle α (Zhang et al., 2020)	14
Figure 1.5 Mechanical diagram (Fiorillo, 1997)	15
Figure 1.6 Electrical scheme of resistors (Fiorillo, 1997)	16
Figure 1.7 Microsensor (Dao et al., n.d.)	17
Figure 1.8 Resistance in function of stresses (Dao et al., n.d.)	18
Figure 1.9 Stress diagram and resistor distribution (Dao et al., n.d.)	18
Figure 1.10 Algorithm of the device in function of the resistances value. (Dao et al., n.d.)	19
Figure 1.11 Image of the Kistler triaxial force transducer (Group, 2021)	20
Figure 1.12 Image of the Tekscan Flexiforce device (Tekscan, n.d.)	21
Figure 2.1 General view of the device.	24
Figure 2.2 Section view of the device.	25
Figure 2.3 Yaskawa HC20SDTP robot. (Yaskawa, n.d.)	26
Figure 3.1 Angle of displacement of the probe	29
Figure 3.2 Calculation of maximum displacement	30
Figure 3.3 Calculation of the lateral arm displacement	31
Figure 3.4 Sensor placement design	32
Figure 3.5 Moment and stress calculations.	32
Figure 3.6 Origin of the assembly visualization	34
Figure 3.7 Centre of mass of the assembly visualization.	35
Figure 3.8 Self-weight stress analysis.	36
Figure 3.9 Vertical force of 30 N stress analysis	36
Figure 3.10 Combined force of 30 N stress analysis	37
Figure 3.11 Frequency stress analysis.	38

Figure 3.12 Thermal expansion displacement analysis.....	39
Figure 4.1 Kinematic movement assemble important tolerances scheme.....	42
Figure 6.1 Breakeven point visualization.....	51
Figure 6.2 Distribution pie chart of device costs.....	52

LIST OF TABLES

Table 1.1 Parameters of resistance in function of force.....	21
Table 2.1 Comparison between piezoelectric and piezoresistive options.....	22
Table 3.1 Properties of PLA.....	27
Table 3.2 Printing properties of PLA.....	28
Table 3.3 Properties of the assembly elements.....	33
Table 3.4 Inertia a centre of mass properties of the assembly.....	34
Table 6.1 Economical cost of materials.....	50
Table 6.2 Breakeven point exact parameters.....	52

INTRODUCTION

Investigation problem. In this project touch sensors will be incorporated in a robotic arm for position calibration of the robot, creating a device that permits, to detect contact with 6 degrees of freedom. In every industrial or scientific environment there is a need for the use of robotics, nowadays most of the industrial processes use them and its essential to have a kinematic sensing probe that calibrates, locates and gives sensivity to the robot, not only for completing the task which it is made, also for security reasons (let the robot know the environment) and for giving the robot a human touch sense and providing limits, defining its exact position.

For that, piezoelectric sensors are used. Piezoelectric materials generate an electric current when a mechanical stress is applied to them. Using this principle, when the touch probe is deformed in one direction, the movement is detected. In this case I'm using a piezoresistive material, which means there is a change in resistance when pressure is applied. Piezoresistive sensors are widely used in various industries due it measuring capabilities of pressure force and strain. For example, there are some key areas where these sensors are used, such as automotive industry (pressure for engine cylinders, fuel gauges), medical industry (distance surgery), prosthetics and any industrial process that involves the use of robots.

The key of this project is to implement the piezoresistive material and to properly design the touch probe, knowing that the material works in compression only, so it will be very important to calculate the possible scenarios that the touch probe will face and also the tolerances and the precision of the device.

Object of Project. The use of a piezoresistive material designed in the Vilnius tech University as a sensor for detecting contact and force of contact, with 6 degrees of freedom, creating the complete mechanical design of the device which is enclosed and the mechanical solution to implement it in a robotic arm.

The aims and purposes of the project.

The aim of these project is to create a touch probe that detects force and pressure, with the purpose of using it for robot tool calibration fabricated in a 3D printer.

To achieve the necessary goals of project, need to be fulfilled in order these tasks:

1. Analysing of literatures sources
2. Review of the advantages and disadvantages of the object that is being created.
3. Choosing necessary elements for system design according to the parameters provided.
4. Make calculations of the device or unit strengths.
5. To create and describe the control schemes of the device being developed.

6. To carry out the evaluation of economic indicators of the calibration device
7. Present conclusions, recommendations future improvements.

The novelty and relevance of the theme. The innovation of the project lies on the design and fabrication of an effective touch probe made for calibration, obtaining at the same time precise results and low-cost fabrication expenses compared to other market alternatives. Also, to have a quick assembly design and easy calibration procedure, which makes robot integration of the device simple and versatile. The use of the plastic material makes also a lightweight component which means easier transportation.

Relevance, relies on the importance of robot calibration which need precision positional accuracy without the need of expensive equipment. Also, to enhance repeatability and reliability crucial in robotic tasks, industrial or scientific purposes. For concluding this introduction is remarkable to say that this project aligns with the trends in Industry 4.0 and flexible manufacturing where adaptive, modular and cost-efficient alternatives are critical for success.

1. OVERVIEW OF ANALOGIC CONSTRUCTIONS

1.1. Optimized Design of a Triangular Shear Piezoelectric Sensor

Using Non-Dominated Sorting Genetic Algorithm-II(NSGA-II)

Device No.1. Triangular piezometric sensor.

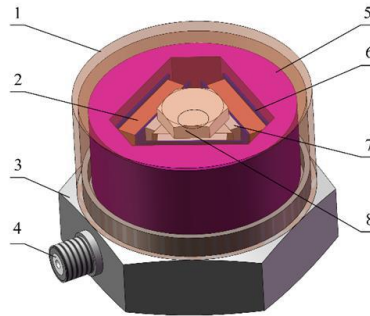


Figure 1.1 Geometric structure of the piezoelectric sensor

(1) Shell; (2) piezoelectric plate; (3) base; (4) socket core; (5) mass block; (6) conductive plate; (7) insulating plate; (8) fastener. (...) (Shi & Dai, 2025)

A new piezoelectric sensor with a triangular shear structure was designed to carry the deformation monitoring of geotechnical bodies in mining airspace. Firstly, a three-dimensional sensor model was developed to analyse the impact of structural parameters on resonant frequency and voltage, utilizing both finite element and experimental methods. Secondly, the NSGA-II genetic algorithm (multiobject solution) was employed to optimize the sensor's structural parameters, focusing on resonant frequency and voltage, resulting in a Pareto optimal solution set. Design is focused to accomplish in a mining environment.

“Mining is bound to form a mining hollow area, and the dynamic instability of the overlying rock in the mining hollow area changes the geological structure and stress nature, which may easily cause hidden disasters on the surface and underground, thus presenting a complex situation due to the impact of ground pressure, sudden water and other dynamic disasters. Therefore, it is essential to study the deformation of the geotechnical body and to understand its pattern. The deformation monitoring of a geotechnical body allows for the accurate prediction and forecasting of the deformation and stability of the overburdened rock in the mining airspace area by detecting and analysing the tiny vibration signals generated, and it is widely used in projects involving deep buried tunnels, large hydroelectric power stations, the deep mining of mines and other projects. Enhancing sensor sensitivity within the operating frequency range enables a comprehensive and accurate

acquisition of minor vibration signals, significantly improving prediction and forecasting accuracy.”(Shi & Dai, 2025)

The base centre column has a piezoelectric sheet in each plane, with polarization treated in the same direction. The mass block, piezoelectric plate, and conductive plate are secured to the centre post by a radial force created through the compression of the insulating plate using fasteners.

In this project Sensors used for the deformation monitoring of geotechnical bodies in mining airspace areas have an operating frequency range of at least 0 to 1500 Hz and sufficient sensitivity. Analysing the piezometric characteristics of the project we can find the following correlation (deformation vs voltage), piezoelectric materials work in the compression, so we can see the most compressed zones generate more voltage.

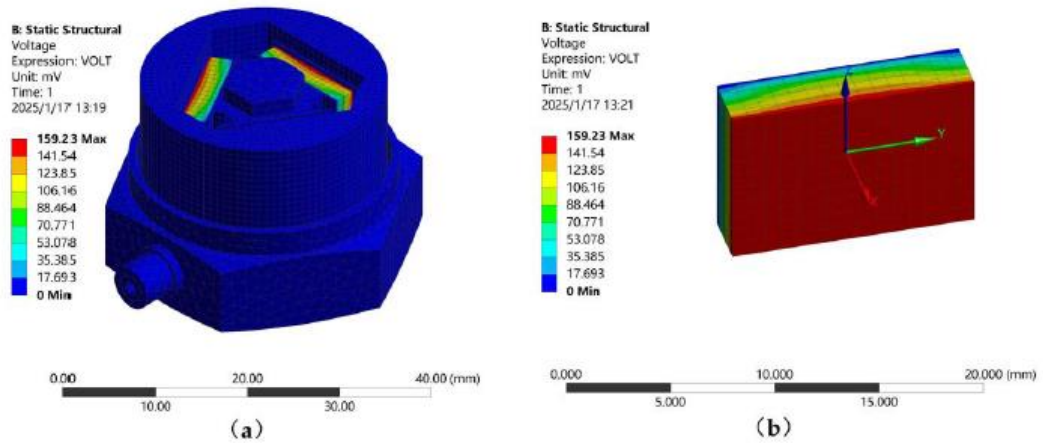


Figure 1.2 Diagram of voltage and deformation (Shi & Dai, 2025)

Regarding this project, to mine, the shape of the sensor and the analysis of voltage will be similar, but purposes and use is different and also environment. This project is orientated to frequency detection and not force, so that will be another difference. The advantages of this device are, its reduced and simple design, and its small size. Regarding the disadvantages, for my project its necessary to measure also force in the Z direction, but for having a general idea it is suitable.(Shi & Dai, 2025)

1.2. Development of a Six-Degree-of-Freedom Analog 3D Tactile Probe Based on Non-Contact 2D Sensors

Device No. 2. Six degrees of freedom measuring concept of the suspended probe body (the arrows show the light beams emitted by the LEDs).

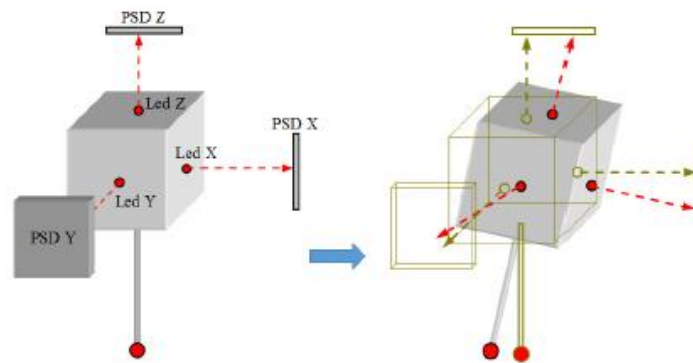


Figure 1.3 LED measuring device (Albajez et al., 2024)

In this paper, a six-degree-of-freedom analogical tactile probe with a new, simple, and robust mechanical design is presented. Its design is based on the use of one elastomeric ring that supports the stylus carrier and allows its movement inside a cubic measuring range of 3mm. “The position of the probe tip is determined by three low-cost, noncontact, 2D PSD (position-sensitive detector) sensors, facilitating a wider application of this probe to different measuring systems compared to commercial ones”(Albajez et al., 2024). However, several software corrections, regarding the size and orientation of the three LED light beams, must be carried out when using these 2D sensors for this application due to the lack of additional focusing or collimating lenses and the very wide measuring range. The development process, simulation results, correction models, experimental tests, and calibration of this probe are presented.

This project is very interesting, even if the technology for measuring is optic and not piezoelectric, the design of the touch probe is suitable to my project, in this case the probe is made of ruby, and in my case, it will be made of PLA, because of the not so high precision requirements. Regarding its advantages, we can talk about its high precision and sensitivity, also it has disadvantages, such as a very high price, and its difficulty for calibration.(Albajez et al., 2024)

1.3 A Piezoelectric Tactile Sensor for Tissue Stiffness Detection with Arbitrary Contact Angle

Device No. 3. Piezoelectric medical touch sensor tissue stiffness measurement

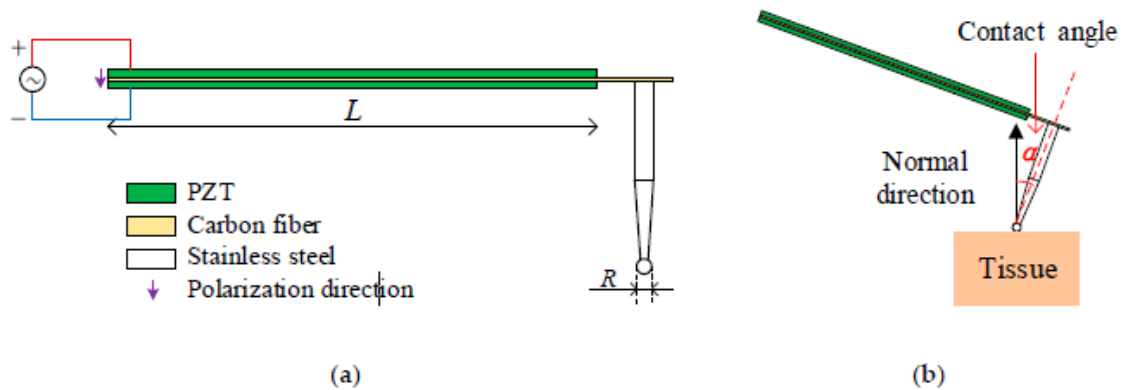


Figure 1.4 (a) Structure of piezoelectric tactile sensor. (b) Detect tissue with contact angle α

(Zhang et al., 2020)

In this paper, a piezoelectric tactile sensor for detecting tissue stiffness in robot-assisted minimally invasive surgery (RMIS) is proposed. It can detect the stiffness not only when the probe is normal to the tissue surface, but also when there is a contact angle between the probe and normal direction. It solves the problem that existing sensors can only detect in the normal direction to ensure accuracy when the degree of freedom (DOF) of surgical instruments is limited.

As we see this device applies for the medical field, which robotics are key in some situations. I think the design of the probe will be useful for my project, also the way it senses the movement will serve for inspiration to my mechanical design, using the sphere shape for collecting data in all directions. The lever-acted pressing design is also key for a mechanical touch probe as my project does. Disadvantages regarding to my thesis, this project doesn't distinguish between directions of touching, so that will need to be fixed.(Zhang et al., 2020)

1.4 Piezoresistive tactile sensor:

Device No. 4. Piezo resistive tactile sensor

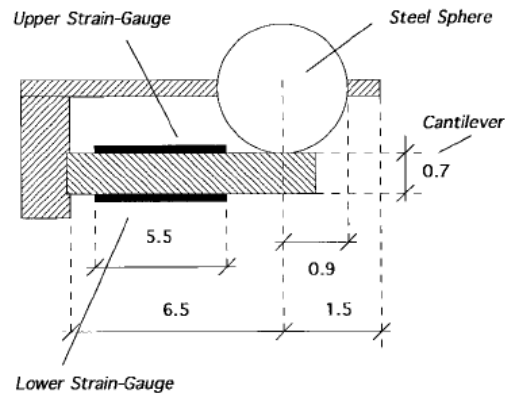


Figure 1.5 Mechanical diagram (Fiorillo, 1997)

In the present project a pressure array sensor is developed. One of the problems regarding these devices is the lack of sensitivity or linearity, and also the influence of temperature and this idea reduces them considerably. “Particular attention has been paid to the design of the geometrical structure of the device and the design of the electronic acquisition unit, to obtain a small and compact device. This feature is of primary importance for pressure sensors capable of being incorporated in a grasp-effector also equipped with proximity sensors for robotic application in unstructured environments”.(Fiorillo, 1997) Each sensing element consists of two strain gauges inserted, respectively, in two independent Wheatstone half bridges (sometimes denoted quarter bridges). The output of each bridge is connected to a current voltage converter, then to a multiplexer followed by a differential amplifier.

A Wheatstone bridge is an electrical circuit used to measure an unknown electrical resistance by balancing two legs of a bridge circuit, one leg of which includes the unknown component.

The sensor is obtained by cutting, from a thin steel sheet, sixteen cantilevers that deflect under pressure. Two metal strain gauges, having a resistance of 120 Ohms, are bonded onto the upper and lower faces, respectively, of each cantilever that induces in them opposite deformations during deflection. The upper one, is operated in tension while the lower one, is operated in compression. The maximum deflection is limited by a metallic tooth. to protect the sensing elements from overloads. By using a technique already developed for the implementation of a ferroelectric polymer tactile sensor, a second metallic sheet, with an equal number of circular holes each one corresponding to a

single sensing element, is positioned over the first sheet. In each hole, a steel sphere is directly in contact with the front side of the underlying cantilever, but sufficiently far from the strain-gauge to avoid damage. Furthermore, it is constrained at the boundary. In this way, the sphere transmits only the normal component of an external force acting on the upper face to the sensing element.

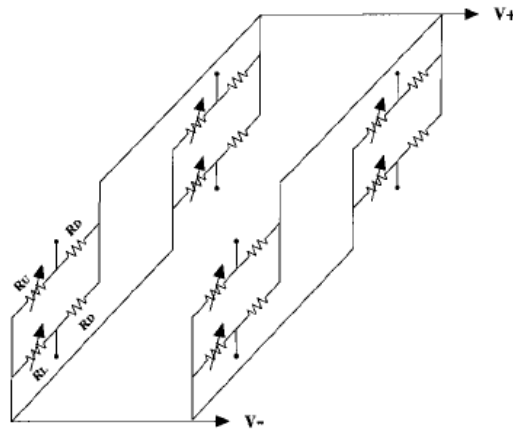


Figure 1.6 Electrical scheme of resistors (Fiorillo, 1997)

Tactile sensor configuration that shows the upper and lower piezoresistive arrays (2 x 2 elements). Each couple “dummy gauge-strain gauge” is inserted in a Wheatstone half-bridge circuit and is connected through an analog multiplexer to a differential amplifier. The advantage of this circuit topology is twofold. It allows the doubling of the electrical signal generated by the pressure on each cantilever and a drastic reduction in the noise generated by the transducers. Each pair of strain gauges bonded onto the opposite faces of the same cantilever generates pressure signals that have the same amplitude but are opposite in polarity and temperature signals that are equal in amplitude and polarity.

In conclusion this device is a good way to analyse how piezoresistive sensors work and to establish a concept of design, such as the idea of the sphere for having only normal forces. Also, the use of multiplexers in the electrical circuit will be useful for my final electrical design as a concept. (Fiorillo, 1997)

1.5 Silicon Piezoresistive Six-Degree of Freedom Micro Force-Moment Sensor

Device No. 5. Silicon piezoresistive 6 degree of freedom touch sensor

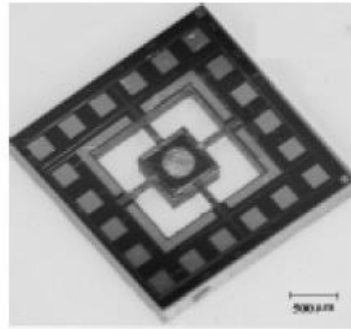


Figure 1.7 Microsensor (Dao et al., n.d.)

In this paper, we describe the design, fabrication and calibration results of a 6-degree of freedom force-moment micro sensing chip utilizing the piezo resistance effect in silicon. “The sensing chip is designed to be able to simultaneously detect three components of force and three components of moment in three orthogonal directions. Conventional p-type and four-terminal p-type piezo resistors have been combined in this single sensing chip in the (111) plane of silicon. The total number of piezo resistors is 18, much fewer than the previous art piezo resistance-based 6-component force moment sensors known to the authors. While much work has dealt with three-component force sensors, studies on six force-moment components micro sensors are rare. The three-component sensors are adequate for the tasks involving feature identification, or determining object location. However, for certain applications, they are inadequate. Examples of such applications include measuring external forces on particles in liquid flows, and grasping and manipulation by robot hand”.(Dao et al., n.d.)

The sensing chip is a single crystalline silicon crossbeam with two-terminal (conventional type) and four-terminal piezo resistors diffused on the surface of the four suspended-beams. Forces and moments applied to the sensing chip, deform the four suspended-beams and change the resistance of the piezo resistors, which leads to a change in output of corresponding measurement circuits. The beam’s size, piezo resistance coefficients and the positions of piezo resistors on the sensing chip are the main factors determining the sensitivity of the sensor. This section discusses how crystallographic orientations and piezo resistor arrangement were specified in order to obtain large sensitivity while complying with the specification in which the sensor can detect six components of force and moment independently.

The piezo resistant effect is a phenomenon in which the electrical resistivity of a material changes due to a applied stress. Talking about semiconductors, distortions in the energy band affect electrons mobility and holes distribution. Those changes modify the resistance of the semiconductor.

$$\frac{\Delta R}{R} = \pi_{11}'\sigma_1 + \pi_{12}'\sigma_2 + \pi_{13}'\sigma_3 + \pi_{14}'\tau_4 + \pi_{15}'\tau_5 + \pi_{16}'\tau_6$$

Figure 1.8 Resistance in function of stresses (Dao et al., n.d.)

When the force is applied in every direction, the stress is distributed along the central axes, and the moment applied to de central part of the plate point O. Sigma 1 is the normal to direction stress, t for the tangent and the numbers are the directions, here is an example of the force distribution for X axe due to My, and the arrangement of the piezo resistors on the crossbeam:

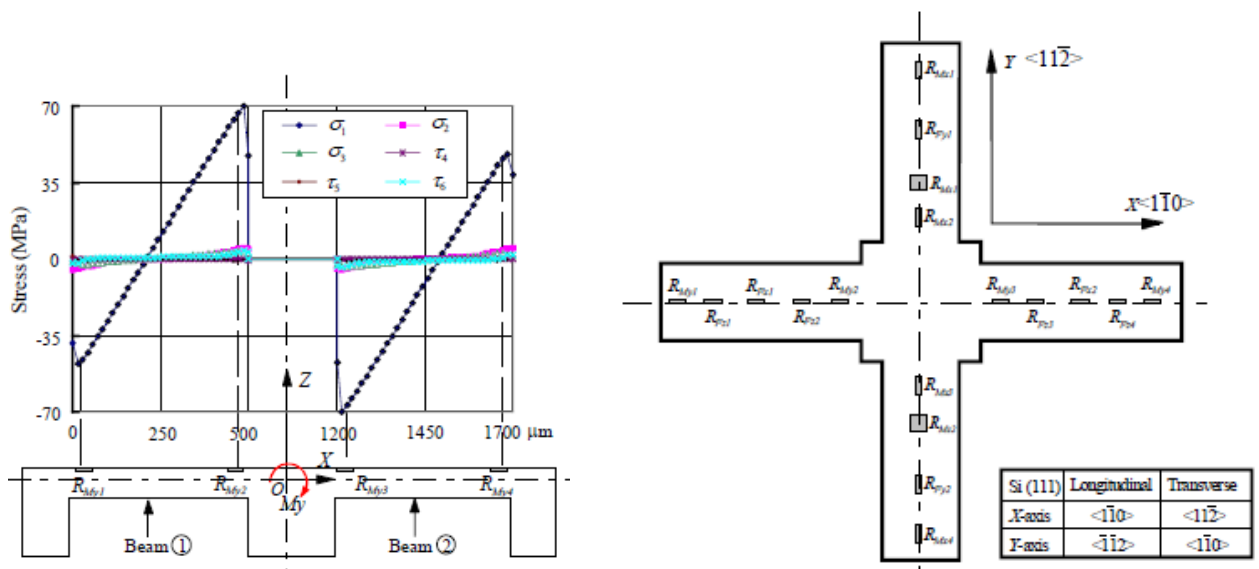


Figure 1.9 Stress diagram and resistor distribution (Dao et al., n.d.)

With the algorithm and depending of the voltage of its sensor we can distinguish between force directions and movements. This enables the system to accurately differentiate between movements such as pushing, pulling, or lateral shifts, providing valuable data for motion analysis and force characterization. The following table explains how the system manages to distinguish between directions establishing a sequence of movements that enables certain signals.

	Fx Bridge		Fy Bridge		Fz Bridge				My Bridge				Mx Bridge				Mz Circuit	
	R_{Fx1}	R_{Fx2}	R_{Fy1}	R_{Fy2}	R_{Fz1}	R_{Fz2}	R_{Fz3}	R_{Fz4}	R_{My1}	R_{My2}	R_{My3}	R_{My4}	R_{Mx1}	R_{Mx2}	R_{Mx3}	R_{Mx4}	R_{Mz1}	R_{Mz2}
Fx	+	-	0	0	+	+	-	-	+	+	-	-	0	0	0	0	+	-
Fy	0	0	+	-	0	0	0	0	0	0	0	0	+	+	-	-	0	0
Fz	=	=	=	=	+	-	-	+	+	-	-	+	+	-	-	+	0	0
My	0	0	0	0	+	-	+	-	+	-	+	-	0	0	0	0	+	-
Mx	0	0	0	0	0	0	0	0	0	0	0	0	+	-	+	-	0	0
Mz	+	+	+	+	+	+	+	+	+	+	+	+	+	+	+	+	=	=

Figure 1.10 Algorithm of the device in function of the resistances value. (Dao et al., n.d.)

Based on the table 1, piezo resistors are connected to form the measurement circuits so as the sensor can detect six components of force and moment independently. The Wheatstone bridge is a useful circuit to convert a change in resistance to an output voltage. The general measurement circuit for measuring the five components, (Fx , Fy , Fz , Mx , and My), is created by connecting in parallel five independent detecting potentiometer circuits together and with a potentiometer circuit to form five Wheatstone bridges sharing a common half bridge. (Dao et al., n.d.)

1.6 Working principle and commercial Ideas

Firstly, we need to explain how piezoresistive materials work and establish the differences between piezoelectric ones. A piezoresistive material is a type of material that changes its electrical resistivity as a result of mechanical stress, in my case, compression stress, in the other hand, piezoelectric materials generate a current when pressure is applied. Using that principle (piezoresistive), my objective is to create a 6 degree of freedom touch sensor, that is be mounted in a robotic arm, and will be used for calibration, Due to the importance of measuring in all directions, and the compression only working way, we need to create a physical device that fulfils all these requirements regarding design and characteristics, and also the algorithm to distinguish between touching directions, all together in a reduced and simple design made of a touch probe and a number of sensors, everything printed in a 3D machine.

Looking to the available market options for having an idea of what should I need for my project, I found similar projects that can be helpful for my creation. Starting with a simple one to understand the principle of piezoelectric sensors and how they work.

1.6.2 Kistler triaxial force transducer:

In this commercial example device made by Kistler group, a complex force detection device will be presented for useful knowledge.



Figure 1.11 Image of the Kistler triaxial force transducer (Group, 2021)

This device is a piezoelectric ring force transducer for tensile and compression forces from 3kN to 80 kN. It's a more complex example that covers all directions of force measuring. These triaxial piezoelectric force transducer are piezoelectric load cells for the exact measurement of all forces on the three orthogonal components acting in an arbitrary direction. These sensors are suited for measuring dynamic force and direct force and they work in a range of temperatures from -20°C to 200°C . Its especially small size is ideally suited for installation in structures such as force plates, fitting strips and tools. The sensor is used in industrial production processes in which forces are monitored or measured. Used in combination with a control monitor, the sensor is ideal for quality control and monitoring in industrial processes. Using quartz as the piezoelectric material, the 3-axis load cell is mounted under preload between two plates and measures both tensile and compression forces in all directions. Based on the piezoelectric principle, a force produces a proportional electric charge. This is conducted via an electrode to the appropriate connector. The simple and vibration-resistant design of the force link is very rigid resulting in a high natural frequency, which is a requirement for highly dynamic force measurements.

The sensitivity of the device is 8 pC/N for x and y directions and $3,7 \text{ pC/n}$ for the z direction. Combining the data of all the sensors, the resultant force will be calculated as a vector, using the correct algorithm using a device after the sensor called summoning box. For the part of measuring and signal processing, Charge amplifier channels are still required for the complete measurement system. These convert the measurement signal into an electrical voltage. The measured value is exactly proportional to the acting force. The multichannel charge amplifier Type 5167A was specially built for multiaxis force measurement systems. The advantages of this device are the precision, and the fact that it is previously calibrated. Also being steel is very hard and not influenced by external vibrations. (Group, 2021)

1.4.3 Tekscan Flexiforce standard model A502:

In this chapter a soft commercial touch sensor made by Tekscan is analysed for future additional information will be optimal for thesis design ideas.

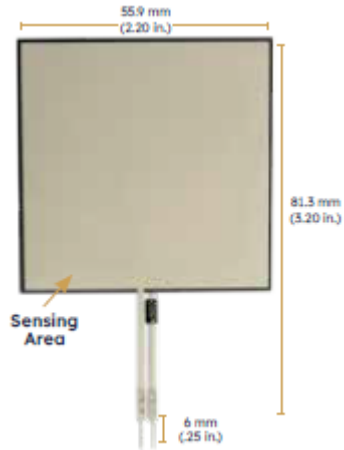


Figure 1.12 Image of the Tekscan Flexiforce device (Tekscan, n.d.)

The Flexiforce A502 is a square sensor with the dimensions shown in the figure and a sensing area of 50,8 mm². This particular sensor has multiple benefits, such as its small size, flexibility and being very thin. It permits the integration in tight spaces for non-intrusive force measurement between mating surfaces. It is very easy to use and it is made for testing, prototyping or even embedding.

The substrate is made out of polyester. It has a linearity error of 3% going from 0 to 50 percent of maximum load. Hysteresis is 4,5% from 80% of the maximum scale force. It works in the temperature range from -40°C to 60°C and has a response time of 5 picoseconds.

Table 1.1 Parameters of resistance in function of force (Tekscan, n.d.)

Voltage (V)	Force (lbs)	Resistance (kΩ)	Conductance (μS)
0.5	20	34.36	29.11
0.5	40	17.14	58.33
0.5	60	11.57	86.41
0.5	80	8.71	114.76
0.5	100	6.97	143.54

We can see from the chart the working principle, at a constant voltage, when the force varies, we have different resistance values. We can use this idea for knowing how the system works and the approach to a silicon material, similar as the piezo resistive material provided in Vilnius Tech.(Tekscan, n.d.)

1.5. Substantiation of the decision

In conclusion there are lots of examples of piezoelectric and piezoresistive force sensors, learning from the ones that I have analysed in this paper, but also knowing the differences, I will make my own touch sensor. One of the biggest differences is the piezoresistive material. The one that is provided for my project is a soft (biodegradable) material, while the majority of the commercial examples or ideas on the market, use quartz. This material suits better for this project because of the purpose it will be used. We need simplicity and response to a stress in the material combined with a simple electrical circuit that uses the variation of resistance for detecting de contact, so in addition we need a soft material. Next, we have a comparison table that shows the differences:

	Piezoresistive	Piezoelectric
Working Principles	Piezoresistive Effect (strain after stress)	Piezoelectric Effect
Physical Quantity	Resistance	Electric Charge
Elements Materials	Piezoresistive materials such as silicon, metal, etc.	Piezoelectric crystal or ceramic
Measurement Type	Static	Dynamic
Application	Industrial process, medical equipment	Aerospace, Acoustic measurement
Advantage	High precision, reliability, durability	High sensitivity, fast response time

Table 2.12 Comparison between piezoelectric and piezoresistive options

This means that in my project I will need to take into account deformations of the material and tolerance limits, which is an important thing, for design and future specifications. Another difference is the design, as shown in a previous article, the design will have a spherical touch probe for the measuring, and also the material, instead of steel, it will be made of PLA and 3D printed. It must be simple and at the same time accurate.

Another thing to take into account is the algorithm for combining the information of all the sensors and calculate the resultant vector. In my project, the type of piezoelectric sensors is piezoresistive, due to the better characteristics explained on the table, which are the ones that suit better my project. An algorithm must resolve, making a simple circuit, the changes in resistance that mean if one direction is touched, also my will is to integrate it in the robot control unit for robot connection at every time which will communicate the touch sensing for further calibration as well it must include safety stop reasons for hazardous situations like impact forces.

As seen in some examples, the circuit must contain a control unit, for example an ESP32 NodeMCU for calculating the variation in resistances. Also, we must need to measure the linearity of the measurement, the drift and the hysteresis of the material. Being a soft material, we have to take into account possible deformations and a maximum force of contact.

This leads to the security part, which all personal risks and machine risks should be included, such as impact forces in the machine or accidental forces that may occur within the work environment. This consideration naturally leads to the aspect of operational safety, which encompasses both personnel-related risks and machine-related hazards. A comprehensive safety assessment must account for potential sources of injury or malfunction, including the impact forces generated by the robotic system during normal operation, as well as accidental or unexpected forces that may arise within the work environment. These may include unintended collisions, human error, or the failure of system components. In collaborative robotics applications, such as the one involving the Yaskawa HC20SDTP, safety becomes especially critical due to the close physical interaction between human operators and the robotic arm. Therefore, appropriate safety measures such as force and torque sensing, speed limitations, emergency stop mechanisms, which comes with the robot, and workspace zoning must be implemented to minimize the risk of injury and ensure compliance with industry safety standards (e.g., ISO/TS 15066 for collaborative robots).

Additionally, risk assessments should be conducted to identify and mitigate hazards related to environmental conditions, system malfunctions, and improper use, thereby ensuring a safe and reliable operational setup.

For concluding this introduction, we must end with the most important and first point of this work, the mechanical design. Based on specifications and characteristics that must be specified later, such as maximum force of impact, deformation tolerances and touch sensitivity between much others, I will need to design the correct physical idea and establish the correct constraints that allow the measurement in all directions.

2. OVERVIEW OF SPECIFIC NODES

2.1. Device design, general view and function.

This chapter provides an overview of the device's general design, highlighting its main components, and overall functionality. By examining the general configuration and the role of each part within the assembly, this section sets the base for understanding the device's performance and how it works generally.

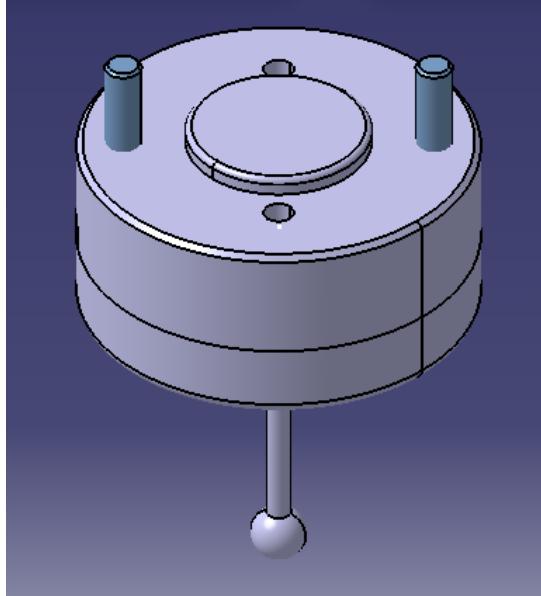


Figure 13 General view of the device.

The object of this device is to measure contact with a touch probe and to be able to distinguish all the directions of the orthogonal space. In this point I will present the overview of it, without entering in details that later will be specified. The device, made of PLA, will be cylindrical shaped in the base, specifically the dimensions of the robot that will be attached, and with a spherical probe that will be in charge of the contact. The finality of the device is to make robot calibration easy, cheap and also versatile, because it can be attached to more robots, of the same characteristics with simple portability and calibration

The algorithm must contain the necessary parameters to use and compound a vector with all de sensing options directions and also to send to the control unit when contact is made for its processing. The circuit must detect changes in the resistance of the material that means contact has been produced for each sensor and to provide this information to the robotic arm for contact calibration purposes.

The first part to analyse and calculate is the design and functionality. We have to take into account to describe first the specifications. The sensors must detect contact in all directions, in other words, have 6 degrees of freedom. Before any measure, I must study the design to make it possible. First it must contain a spherical probe, that makes contact with the surface perpendicularly in every situation. Then, connected with a cylinder to a spherical head, that permits the movement in any direction. Then 4 cylinders come from the sphere to make the connection with the sensors in the allowance.

Then this part is introduced in a matrix where the sensors are mounted. The shape is very similar to the probe part, but slightly bigger to permit the movement with a small tolerance. When the sensor makes contact, it moves inside the part bending and compressing the sensors correctly disposed for making additional contact force with all the directions.

This will be attached to the robot that later will be described with screws in the base of the matrix. The matrix will be made in two parts for being able to mount and access to the inside for assembling or if anything fails or needs to be repaired and also for calibration issues. Inside it there are channels correctly disposed for wiring that go from the sensors to the exterior. A simple view of the inside of the device is shown.

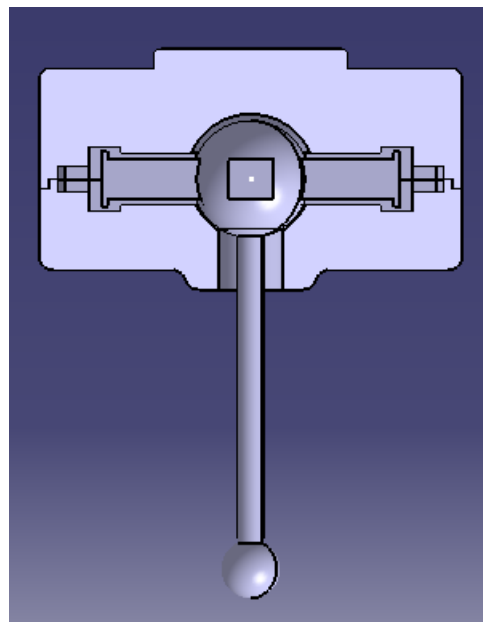


Figure 14 Section view of the device.

In conclusion, the design of the two-part matrix not only facilitates secure attachment to the robot but also ensures quick and easy assembly, maintenance, and makes calibration accessible. The division into two parts allows practical access to internal components if setting is required, while the integrated wiring channels support efficient and organized sensor connectivity, sending the wires to the exit part. This functional construction approach gives us both the reliability and serviceability of the device, contributing to a more robust integration within the overall system.

2.1. Material of the sensor and robot

The piezoresistive material provided by Vilnius Gediminas Technical University Tech will be integrated into the designated within the sensor matrix structure. This material is characterized by being soft and very thin, brown coloured material in which, when contact force is applied a change in the resistivity of it is produced, so we can take advantage of this property to provide electrical signal in a circuit. Consequently, this property makes the material an ideal candidate for applications in tactile sensing and force mapping in smart sensing systems.

The robot to be attached is the Yaskawa Cobot (collaborative robot) HC20SDTP developed by Yaskawa electric corporation. A human collaborative robot designed specifically for confined spaces or limited access environments. This model is part of Yaskawa's Human Collaborative (HC) series, which prioritizes safety, flexibility, and ease of use in close proximity to human operators. It has 6 axes and a maximum payload of 20kg. It weights 97kg and a working range of 1412mm, with a repeatability of 0.05mm which is very precise. Depending on the axis it has different speeds but the can be up to 180 °/s.



Figure 15 Yaskawa HC20SDTP robot. (Yaskawa, n.d.)

These specifications, combined with its collaborative safety features, make the HC20SDTP a robust and versatile solution for research and industrial automation, as for my thesis project, being also easy to work with it. Its ability to work safely alongside human operators without the need for protective barriers not only enhances workplace efficiency but also supports flexible deployment in dynamic environments. (Yaskawa, n.d.)

3. CALCULATION OF PROJECT

3.1. Specifications, calculations and accuracy

The first thing to explain is the general dimensions and characteristics. The device will be cylindrical shaped with a maximum diameter of 65mm and a total vertical longitude of 85mm. It's weight, without attachment screws and wiring, is 0,131 kg. The material used is PLA (polylactic acid filament). This material is optimal for its use object and design because it permits an easy fabrication method, which is 3D printing. Not only that, performance characteristics comply with the technical requirements of the measurement process and construction, such as mechanical resistance, working temperature ranges and weight. Disadvantages, its moisture absorption from the air which can be 1968 ppm (ISO 62), so it is recommended to store the device in a dry place with desiccant to keep the properties of the material. Following the table of the material characteristics as well as the construction parameters for its fabrication in a 3D printer:

Table 3.1 Properties of PLA.(BCN3D filaments, n.d.)

PLA PROPERTIES	
PROPERTY	VALUE
Tensile strength at yield	70 MPa
Strain at yield	5%
Strain at break	20%
Tensile modulus	3120 MPa
Density	1200 kg/m ³
Thermal expansion coefficient	68e-6/°C
Impact strength-Charpy method 23°C	3,4 kJ/m ²
Melting temperature	115 °C ± 35 °C *

Polylactic Acid (PLA) is a biodegradable thermoplastic polymer widely used in additive manufacturing due to its ease of processing, good mechanical properties, and environmental sustainability. In the context of this project, PLA was selected as one of the structural materials due to its balance between strength and printability. The material exhibits a tensile strength at yield of 70 MPa, with a strain at yield of 5% and a strain at break reaching 20%, indicating moderate ductility. Its tensile modulus is measured at 3120 MPa, reflecting a relatively high stiffness compared to other commonly used thermoplastics. PLA has a density of 1200 kg/m³, contributing to a lightweight yet mechanically stable structure.

The coefficient of thermal expansion is $68 \times 10^{-6}/^{\circ}\text{C}$, which is relevant for dimensional stability under temperature variation. Impact resistance, evaluated using the Charpy method at 23°C , is approximately 3.4 kJ/m^2 , indicating moderate impact performance. The material's melting temperature is reported as $115^{\circ}\text{C} \pm 35^{\circ}\text{C}$, a range that must be considered during thermal processing and application in environments where temperature control is critical.

*Melting temperature has a big variation value, that is because of its amorphous plastic characteristics. Glass transition temperature is 57°C and the Vicat softening temperature is 60°C (ISO 306). That is the temperature at which a flat-pointed needle penetrates the sample to a thickness of 1 mm when loaded with a 10 N or 50 N load.

Table 3.2 Printing properties of PLA.(BCN3D filaments, n.d.)

PRINTING SETTINGS	
PROPERTY SETTING	VALUE
Extruder temperature	190 °C - 220 °C
Bed temperature	65°C
Speed	10-70 mm/s
Retraction speed	40 mm/s
Retraction distance	4 mm
Cooling fan	Yes
Minimum layer height	0.05mm (precision)

To ensure optimal print quality and mechanical performance when working with PLA, specific printing parameters must be carefully selected and maintained. The extruder temperature is typically set between 190°C and 220°C , depending on the printer model, filament quality, and desired print resolution. This temperature range ensures proper melting and flow of the PLA filament through the nozzle without degradation. The bed temperature is maintained at approximately 65°C , which helps with first-layer adhesion and minimizes the risk of warping during the initial phases of printing.

The printing speed varies between 10 mm/s and 70 mm/s, where lower speeds are used for detailed or precision components, while higher speeds may be acceptable for simpler geometries or drafts. Retraction settings, including a retraction speed of 40 mm/s and a retraction distance of 4 mm, are important for minimizing stringing and ensuring clean transitions between segments of the print. The use of a cooling fan is recommended, as it helps to solidify the material quickly after extrusion, improving dimensional accuracy and surface finish. For having an optimal finish in the place which it is required (see drawings), such as the joining plane between the two matrixes, or the probe sphere joint, sanding is used, first 180, 400 and then 800 grit. With this we ensure correct functioning of the assemble and comply with surface requirements.

Lastly, the minimum layer height of 0.05 mm enables high-resolution printing, allowing for finer detail and smoother surfaces when precision is required.

Operating temperatures go up to 40 °C. At that temperature thermal expansion compromise precision as later shown in the finite element analysis with a maximum displacement arrow of 0,05mm of expansion. That expansion will affect sensing capabilities by making false contacts with the sensors (see tolerances in kinematics drawings).

The force range of contact the device is designed for is from 1 N to 10 N of force. Maximum limits withstand the maximum compression force the material can support. Piezoresistive material is soft so no big forces of impact could happen.

When the device is correctly calibrated pressure is maximum and gaps are minimum between the probe's arm and the sensing material, but a mobility diagram must be done to put a maximum range of it even if in its normal working conditions, it shouldn't go to that limit because of sensor placement (already in the limit of contact).

Assuming the material compression, the following calculus are made: The distance from the arm to the sensor placement for maximum angle of deviation needs to be calculated also for avoiding clash with the probe and the base part:

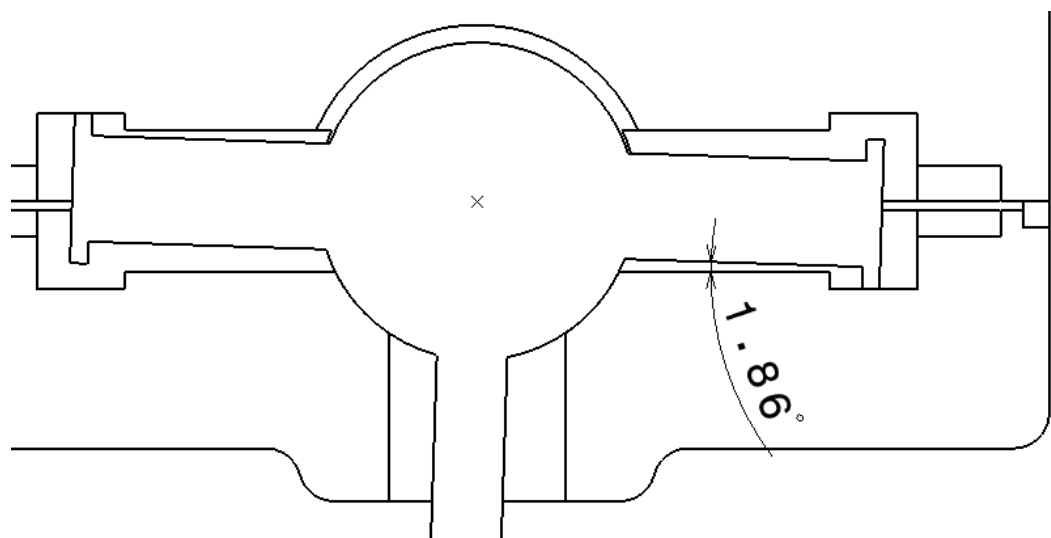


Figure 16 Angle of displacement of the probe

The maximum mobility of that arm should be inferior to the gap between the probe measurement part with the base part case, for having sensitivity and to not make crash. Thanks to computer calculations we can see the maximum angle probe can achieve does not make clash with the lower part.

This deviation also gives us the maximum deviation of the touch probe or maximum error for sensing contact in the limit case. It is the limit case because it is needed to remember that sensors will be un punctual contact so sensing comes after getting this error displacement. Making this calculus is important to have limits in error for specifications. Getting the distance from centre to centre of the spheres and establishing the same angle we get:

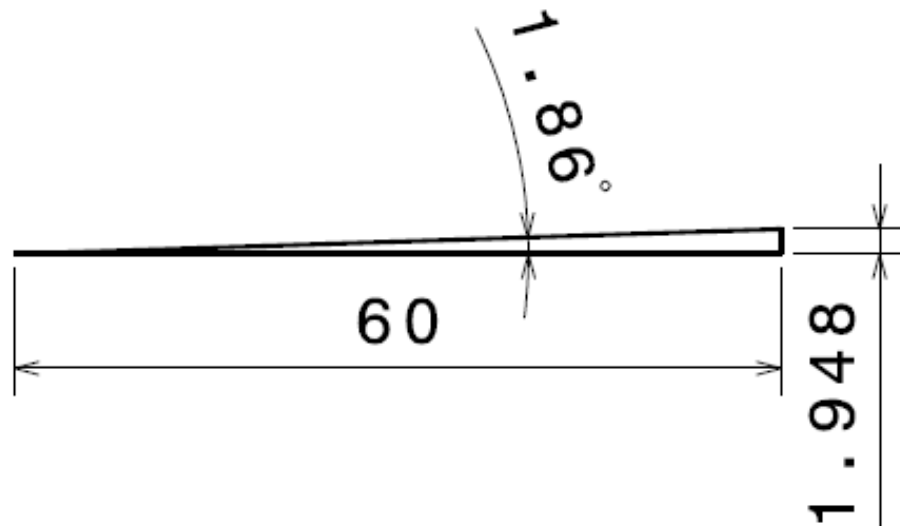


Figure 17 Calculation of maximum displacement

Next, we are also taking into consideration movements that are caused as a consequence of the touching procedure due the design of the fixed probe. This side-effect movements are very important to calculate, measure and establish tolerance limits or a range of the maximum movement, to ensure there is no fail during the operation and a design success. By doing so, we aim to minimize the risk of mechanical failure during operation and ensure the success of the probe design from both functional and structural perspectives.

When the probe moves for detecting a movement in one axis, inevitably, the opposite arms also twist in their axis due it is a fixed part, so it is necessary to analyse the clash possibility using the previous maximum angle of deviation which it is 1,86 degrees. It is also necessary to make these measures in the probe arm and in the sensing extreme, which is bigger. For that, we make the angle along the centre axis in one extreme of the probe arm, for example the bigger one because the displacement will be bigger, and the allowance is the same in both cases (probe arm and sensing part) so in conclusion, if it fits with the longer part it will fit with the shorter. The rotation is established and triangulation is made obtaining a maximum lateral displacement of 0,14 mm as shown in the calculus. It is sure now the part does not crash with the case.

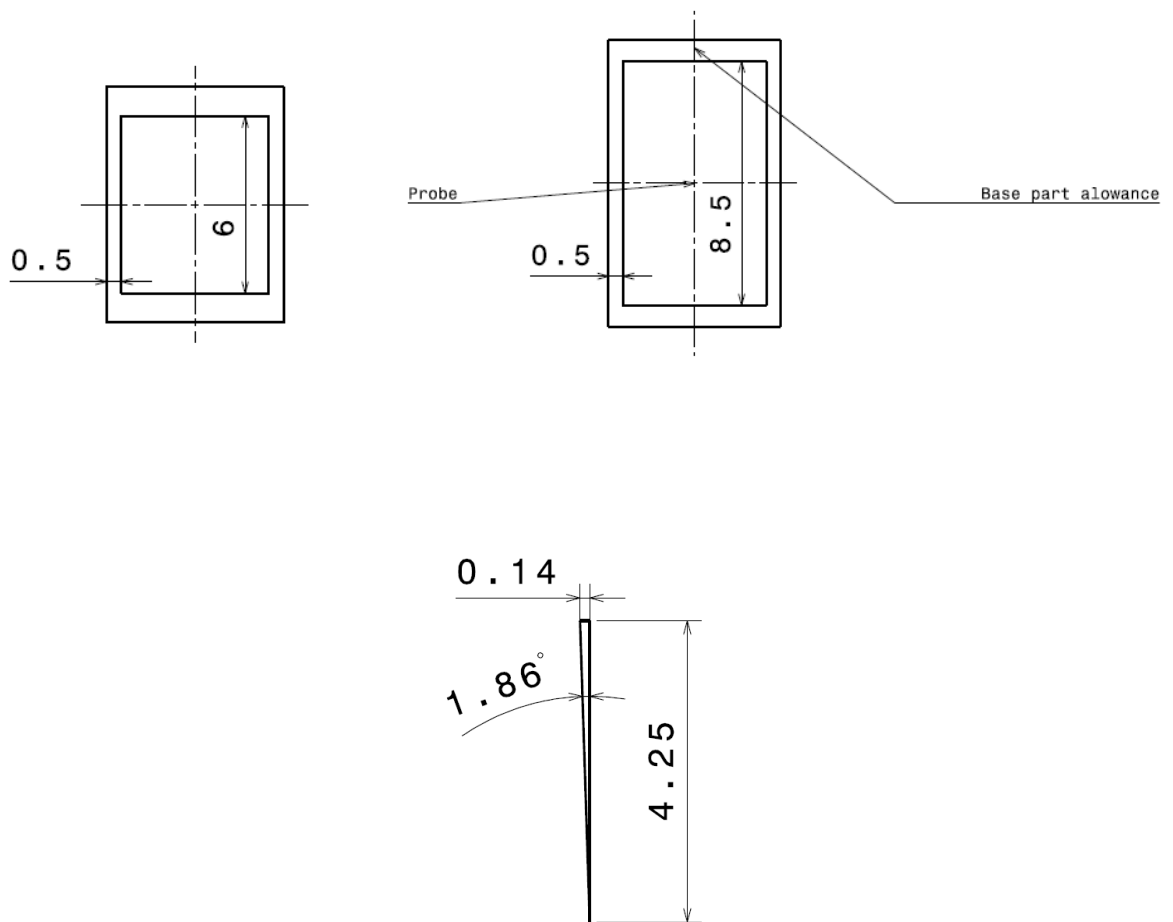


Figure 18 Calculation of the lateral arm displacement

When making this torsional calculations is also important to talk about sensor contact when making this lateral movement. For avoiding false contact a design feature is added. Sensor placing will be on the center and the dimensions will be narrow so lateral rotations input will not activate the sensor and if minimum contact is made the calibration algorithm (minimum resistive values) will withstand the possible lateral contact. Design is shown in the next figure:

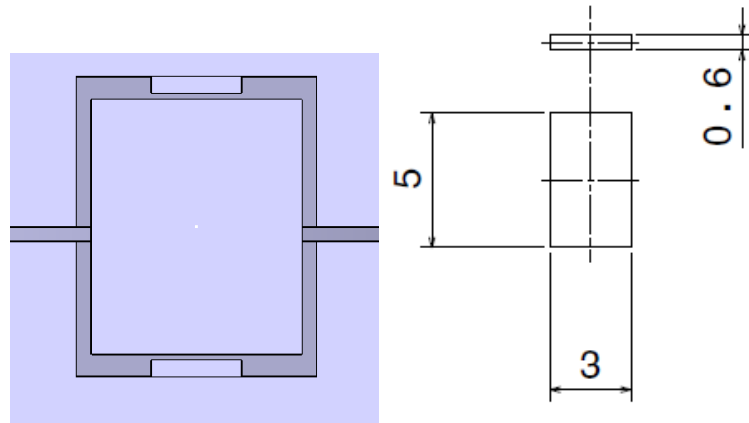


Figure 19 Sensor placement design

Now is precise to analyse the maximum moment applied in the sensor, by multiplying the maximum force by the distance of origin sphere. That moment divided by the distance of the probe arm will give us the applied force on the sensor:

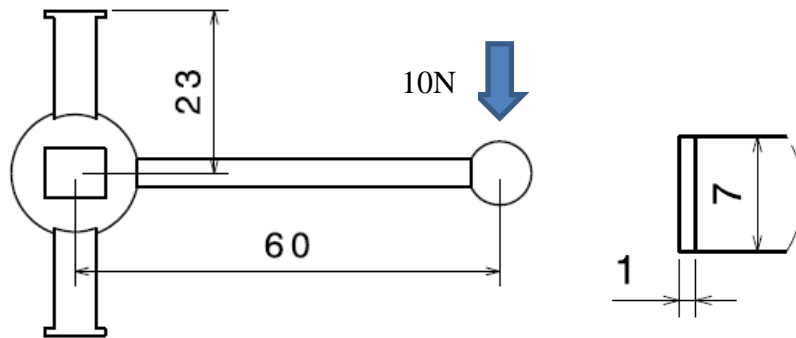


Figure 20 Moment and stress calculations.

$$60\text{mm} \cdot 10\text{N} = 600\text{N} \cdot \text{mm} \quad (1)$$

$$\frac{600\text{N} \cdot \text{mm}}{23\text{mm}} = 26,087\text{ N applied in } 7\text{mm}^2 \quad (2)$$

$$\frac{26,087\text{ N}}{7\text{mm}^2} = 3,727 \frac{\text{N}}{\text{mm}^2} = 3,727\text{ MPa}^* \quad (3)$$

Formula 3.1 Moment calculation (1) (2) (3).

*These values are calculated supposing flat contact with the sensors error in pressure can be 10% superior considering a lateral contact $\sim 6\text{mm}^2$.

Calibration method calculation: To reduce gaps and have a precision measurement, the need of a calibration method was necessary. A gap of 0,5mm between parts which can be shortened with two screws (mechanic explanation in kinematics) was the idea to have that margin of correction if necessary. Procedure of calibration is, first tightening the screws to get to the point of punctual contact.

Then making 1N of force in the -Z direction and establish the base point of start in the algorithm. The same procedure is also made to calibrate all the sensors in the same way and directions. The order is made in that way to compensate first self-weight of the probe possible values and errors.

3.2. Finite element Static analysis calculations

Inertia and mass analysis:

The following table shows the characteristic properties of the device such as Area, volume, density and mass and the contribution of each part of the device assembly. This gives us an idea of how parts are distributed and the correspondent density contribution.

These properties are essential for evaluating the mechanical behaviour of the overall system, particularly in terms of load distribution, structural balance, and dynamic response. By analysing the contribution of each individual part to the total mass and volume of the assembly, we gain valuable insight into how material is spatially distributed across the structure.

Table 3.3 Properties of the assembly elements

Component	Sub-component	Area [m ²]	Volume [m ³]	Density [kg/m ²]	Mass [kg]
Shell		0,025	9,2155e-05	1200,000	0,111
	Base	0,012	3,92868e-05	1200,000	0,047
	Superior part	0,013	5,28682e-05	1200,000	0,063
Probe		0,004	6,51428e-06	1200,000	0,008
ISO 4760 m6x40		0,001	1,51665e-06	7860,000	0,012
ISO 4760 m6x16		0,000701629	8,38065e-07	7860,000	0,012
Rubber protection		0,000229889	5,40688e-08	910,000	0,007
Total Device		0,033	0,000103433	Not uniform	0,155

Following the next table shows the inertia related parameters, which are basic in weight distribution which means a good design in terms of balance and operation stability, in the end precision in movements and detection. First, we have to describe the axis system, to analyse the distribution of the parts in the assembly, in the analytical weight. As shown in the next figure, the origin of the assembly is located on the lower centre of the base part and that means all the references to distance go from that point in the space:

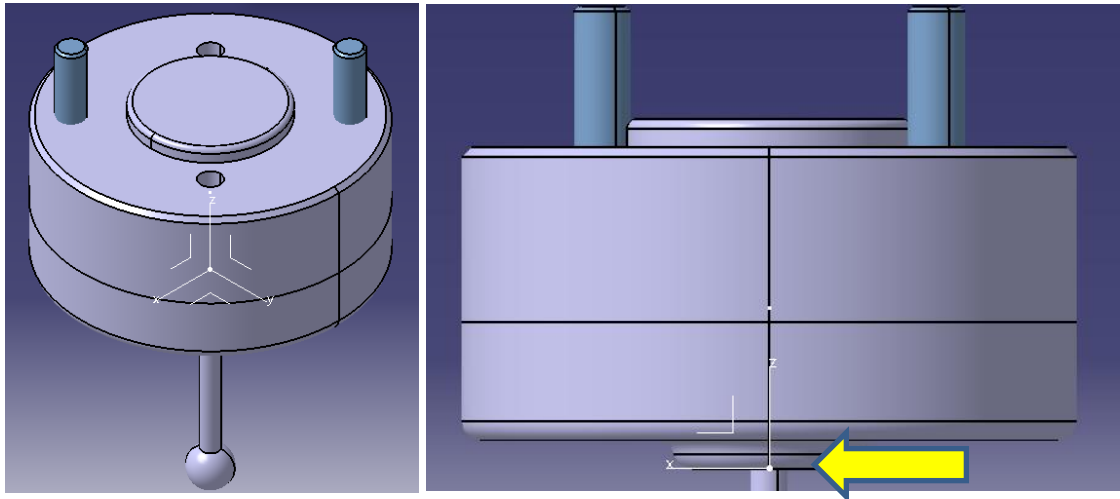


Figure 21 Origin of the assembly visualization.

Table 3.4 Inertia a centre of mass properties of the assembly.

Component	Sub-component	Gx[mm]	Gy[mm]	Gz[m]	IoxG[kgxm ²]	IoyG[kgxm ²]	IozG[kgxm ²]
Shell		-0,061	0,061	19,147	4,003e-005	4,003e-005	6,002e-005
	Base	-0,062	0,062	9,506	1,364e-005	1,364e-005	2,58e-005
	Superior part	-0,060	0,060	26,312	1,874e-005	1,874e-005	3,422e-005
Probe		-3,54274e-15~0	2,10819e-14	10,565	2,74e-006	2,74e-006	9,536e-007
ISO 4760 m6x40		17,678	17,678	23,110	2,405e-006	2,405e-006	8,366e-008
ISO 4760 m6x40		14,142	-14,142	11,984	3,02e-007	3,02e-007	5,966e-008
Rubber protection		24,6539	-24,653	17,000	3,109e-010	3,109e-010	3,042e-010
Total Device		-0,036	0,036	18,716	5,989e-005	5,989e-005	8,149e-005

We can observe G_x and G_y inertia contributions of each part are almost compensated resulting in a final $\pm 0,036$ mm of G displacement for each axis so that's a great result in terms of balance. That number is caused because of the wiring design that goes in one direction as shown in the figures, otherwise that are very good numbers that focus in the symmetrical balance for good precision specifications in measurement. When adding the sensors, the balance maintains itself due to the cross shaped allowance. With the Z axis is the opposite.

The characteristics of the design probe makes impossible to have a near 0 reference point of centre of mass, and its located in the middle of the upper part of the probe shell. That's because there is more material on the upper part of the device which means a higher centre of mass. When looking for the inertia values, the same logic is applied, but we can see, although the Z axis inertia is bigger as explained previously, the values are more or less the same magnitude, being identical in the X and Y axis because of geometrical and component material symmetry.

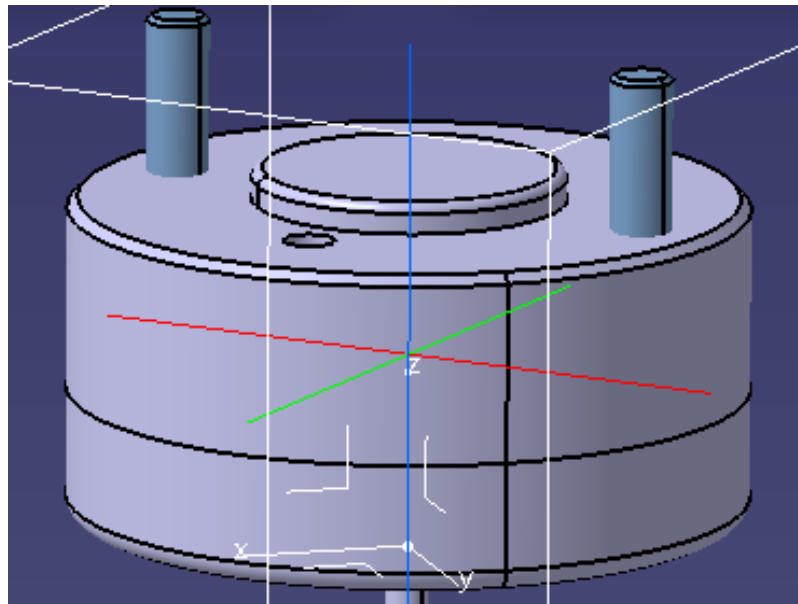


Figure 22 Centre of mass of the assembly visualization.

Static Von Mises stress analysis:

A stress test is required for ensuring the correct mechanical and operational performance during measurement, or even in the case of an accidental force, which needs to withstand some limit characteristics. In this analysis we are going to make different scenarios. The first one is the self-weight earth gravity acceleration analysis, attached to the robot, where the two screws that join the robot support all the weight here, therefore it's the place where the tensions are concentrated as logic will say. In the scale we can see the values of N/m^2 this device supports.

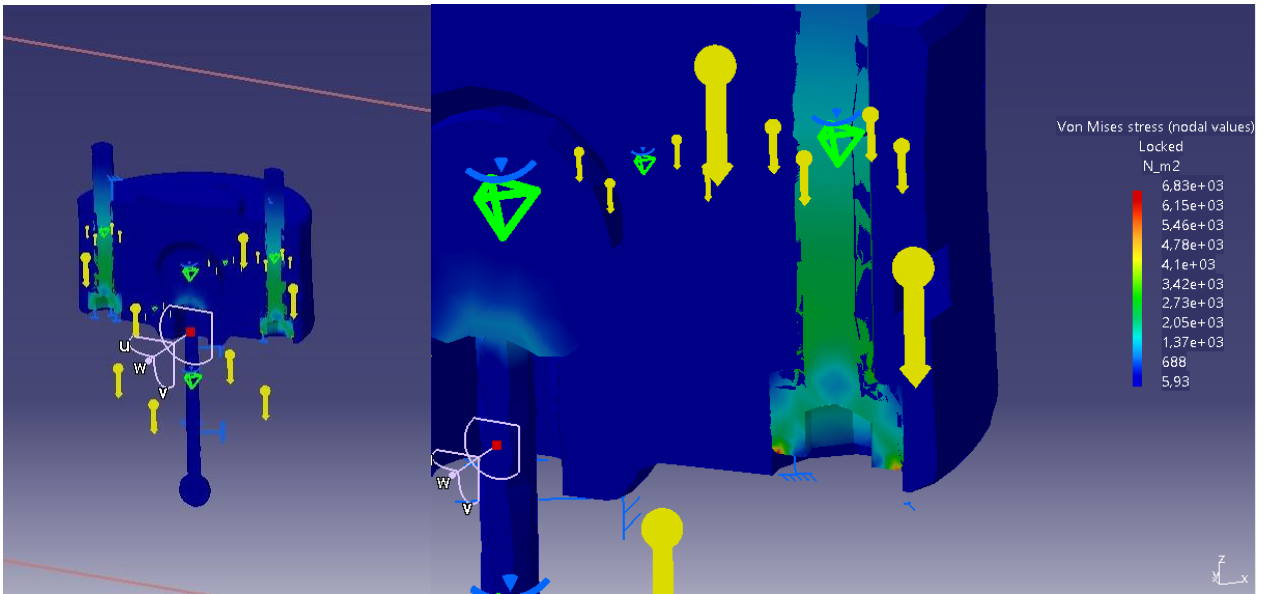


Figure 23 Self-weight stress analysis.

Now we are going to analyse some limit working scenarios. We are going to put first a lateral force of 30N which will be more of the limit of construction forces that de device is designed to support. Those are the situations that the need to be checked in case of accidental forces or crashes. Then we are going to analyse a combined force, vertical and horizontal, of 30N also, to see how the probe reacts in terms of tensional forces over the limit of the specifications, in a situation of a hole for example where two components x and z are involved:

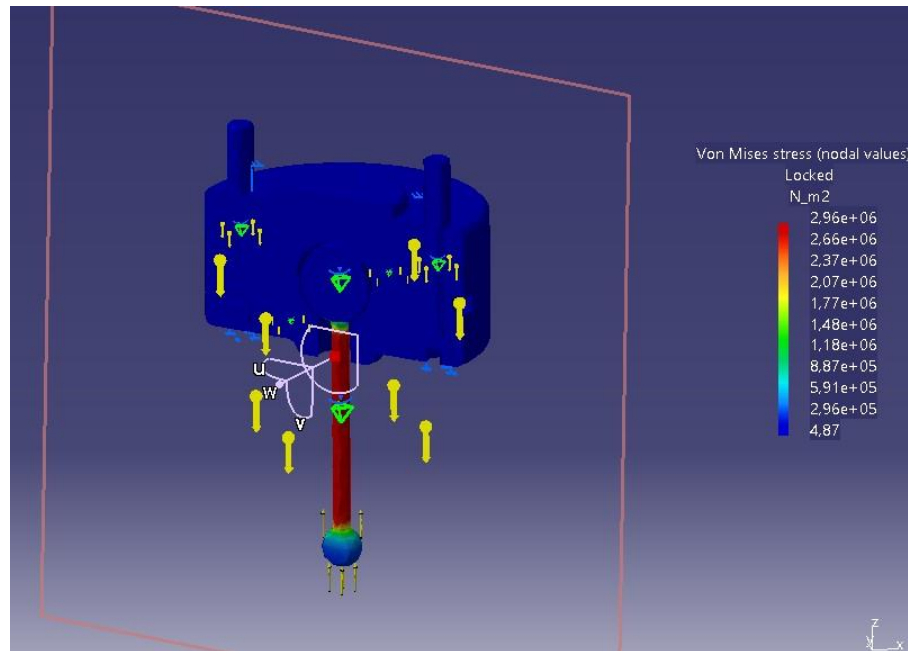


Figure 24 Vertical force of 30 N stress analysis.

In this image we can see how the probe responds at a vertical force of 30N. All the normal tensions are concentrated in the vertical part of the probe, that's because it is the longest and thinnest part of the device. Both of the spheres absorb the tension, or even the fluctuations of it when force is not static and variable, due its geometrical shape and permit to have low stresses on the parts where the sensors are located, which means high precision in measuring.

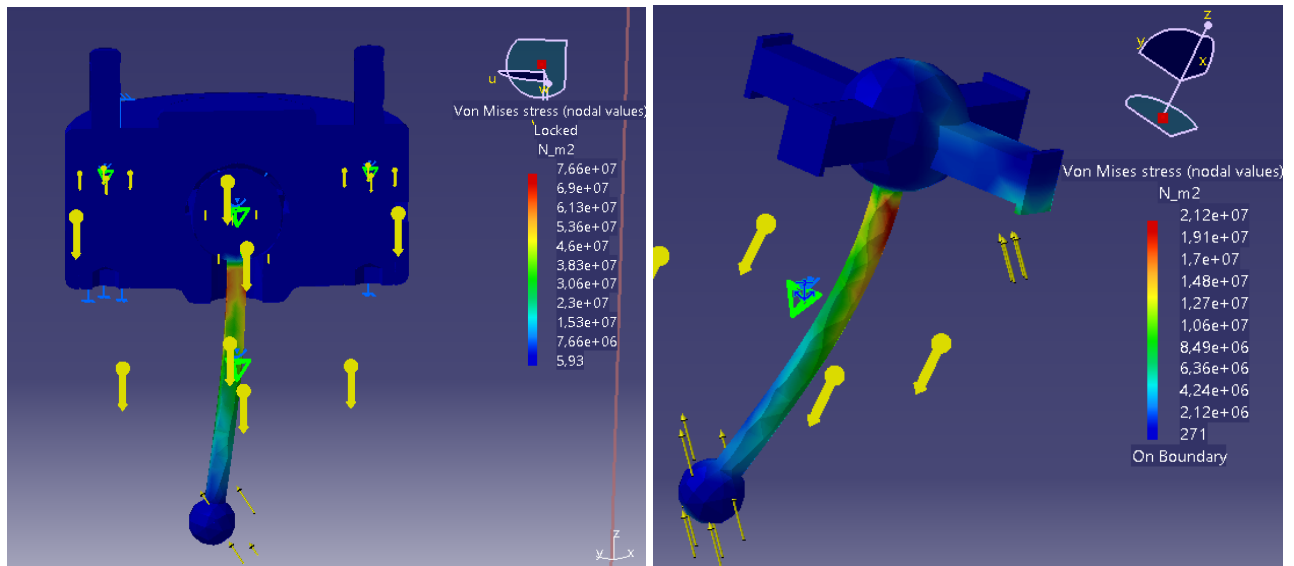


Figure 25 Combined force of 30 N stress analysis.

Following, the next case a combined force, x and z direction, with a combined normal of 30N as the previous case (21,213N each component) and the earth's gravity acceleration. Here we can see the stress is higher in in value but more distributed, comparing to the other case. Value is higher in the upper part due to the higher moment of force applied, bringing up to the limit yield strength (70 MPa) as shown in the material characteristics.

For the image on the left I isolated the probe itself for analysing the behaviour inside the case where the probe makes contact with the sensors. Due to the complexity of the program, I had to do a separated experiment in another scenario because it does not analyse the other part, but using the same force parameters, by using a force where the sensor is placed, simulating the reaction of the case, and fixing the other extreme of the probe, it behaves in the same way as the image on the left. The difference in the value of stresses is a matter of constraint definition and force distribution surface, so the analysis importance resides on how the probe responds inside de case.

It's curious to analyse the distribution of the tensions, higher compression stresses are located where the sensor is placed (as well in the others because it is a combined force), and where the arms of the probe connect with the sphere. That's an expected behaviour because it is where moment is higher due to force per distance formula. Also, we can notice higher stresses where the lowest arm

connects with the sphere, not as noticeable as in the other experiment, but that's because of the complexity of the different models (different value but not distribution) and the importance to analyse other part scenarios.

It's necessary to remark that is not an exact reproduction of the model on the left, and the value error is taken, to focus on the objective to make the similar distribution of stresses to make an idea of how the analytic correct values calculated in the previous point are divided, but in this case un the upper part of the probe which can't be analysed in the first way.

In conclusion, the critical points of the device are the points where the arms connect with the upper sphere, being more noticeable in the lower arm because of the longitude of it. Other important points are the places where the sensor makes contact with the probe arms.

3.3. Frequency analysis

Now a frequency analysis is been made. This analysis is very important in terms of early failure detect imbalances and preventive maintenance. In the end it prevents to detect any dangerous resonances or know where to reinforce the device. Also, a good designed device means an extended lifespan and a market success. These are the results of the analysis:

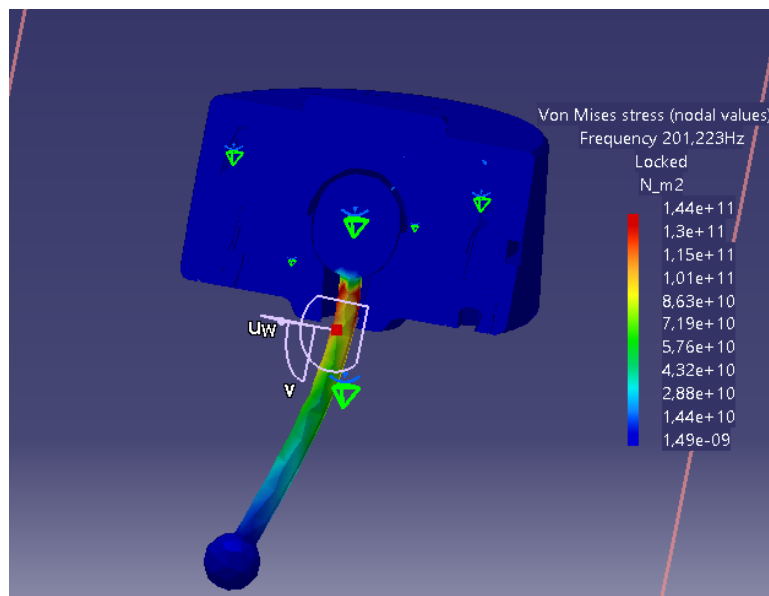


Figure 26 Frequency stress analysis.

The report says that at a frequency of 201,233 Hz, the biggest stresses appear, with the phenomenon of resonance. Those are located once again in the also critic static point, and that's where the dynamic forces vibrating at that frequency, compromise the structure as seen in the simulation making it to collapse, getting over the yield strength of 70 MPa, so either three ways, reinforcement,

change in material or avoid that frequency. This observation highlights the importance of identifying and addressing resonant frequencies during the design phase. Resonance significantly amplifies dynamic loads, especially at structural weak points, and can lead to rapid material fatigue or catastrophic failure if not mitigated. In this case, the simulation clearly indicates that the structure cannot withstand the amplified stress at the identified frequency without intervention.

The reality is that, this device is designed for not that high frequency dynamic forces, even mostly static forces, so there is not a problem in terms of risk of collapse, but a good analysis makes a good design. Moreover, this level of detail supports compliance with engineering standards and increases confidence in the reliability of the design, especially in scenarios where safety, consistency, and long-term operation are key priorities.

3.3. Thermal expansion calculation

This chapter addresses the calculation of thermal expansion in the mechanical structure of the system. Thermal expansion is a critical factor in mechanical design, especially in environments subject to temperature variations, as it can influence dimensional stability, alignment, and the integrity of assembled components. The chapter presents the theoretical background, relevant material properties, and applied formulas used to estimate dimensional changes due to temperature fluctuations. These calculations help ensure that the mechanical assembly maintains its performance and reliability under thermal stress, guiding material selection and tolerance planning in the design process.

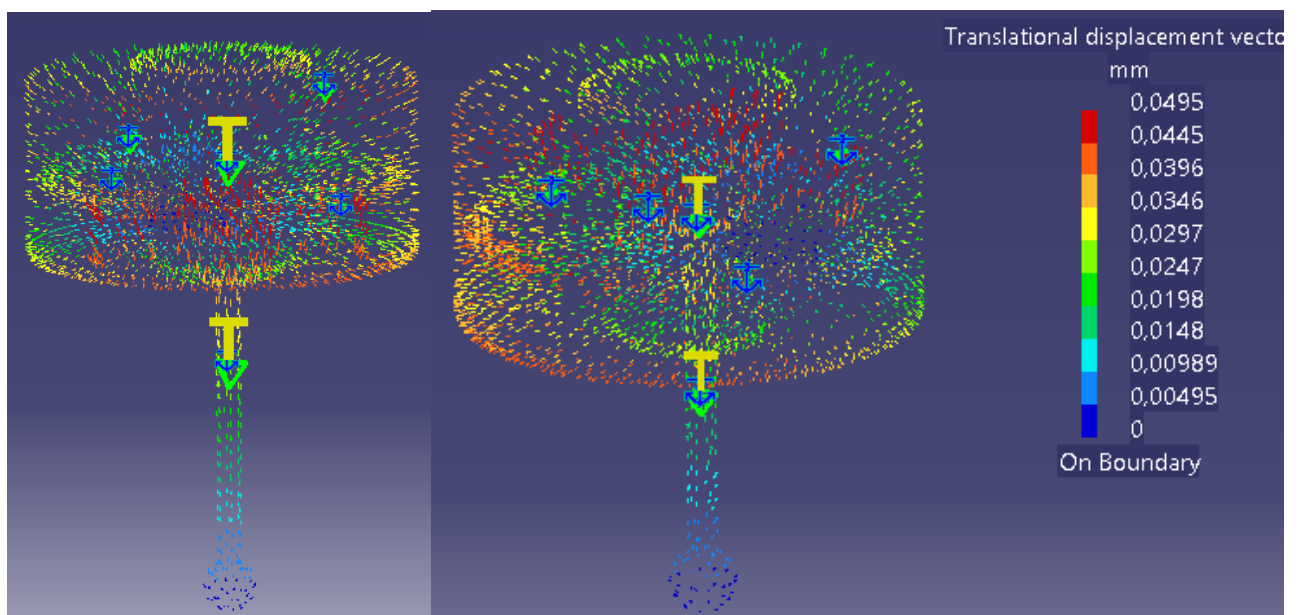


Figure 27 Thermal expansion displacement analysis.

In the first picture thermal expansion analysis is done at the reference temperature of 20°C, with the correct thermal expansion coefficient of the material which it is $6,84e-5/^{\circ}\text{C}$. This coefficient represents the material tendency to expand uniformly in response to temperature increases. This is a crucial factor for ensuring dimensional stability and mechanical integrity in precision devices such as the one in this project. This baseline will be used as a reference for normal temperature range working. The second one is the limit of specification temperatures for a good precision functioning, 35°C. At this temperature the effects of thermal expansion become more pronounced. We can see in red the most affected to displacement parts of the device, with a peak displacement of 0,0495mm which can be rectifiable with the calibration screws. This means the method allows us to manual fine tuning of the affected components which means high precision and reliability.

Overall, this thermal analysis highlights both the robustness of the design and the foresight in accommodating thermally induced mechanical deviations, ensuring sustained performance and system longevity through integrated calibration mechanisms, knowing the limits of the considered material which doesn't perform good in high temperatures.

4. DESCRIPTION OF THE CONSTRUCTION AND OPERATIONAL PRINCIPLE

4.1. Assembly construction scheme

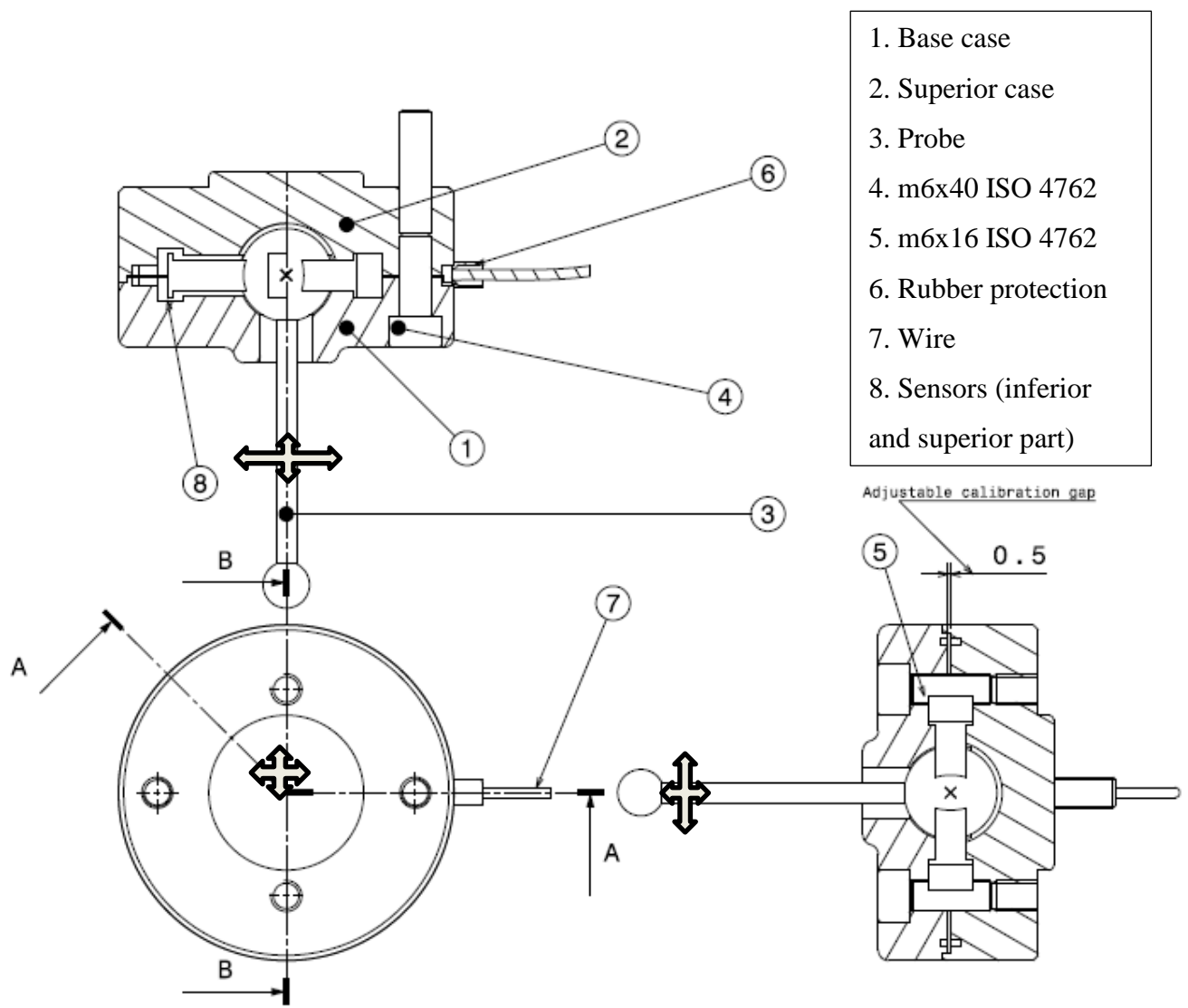
This chapter presents the assembly construction scheme, focusing on the mechanical integration of the system's structural components. It illustrates how individual mechanical parts are arranged, aligned, and fastened to form the complete physical structure. The scheme ensures clarity in the assembly process by highlighting component positioning, mounting methods, and connections between parts. This mechanical layout is critical for achieving structural stability, ease of maintenance, and proper functionality, serving as a practical guide for the physical realization of the system.

The first part to take into account is the assembly design. As previously mentioned, the exterior structure will be done in two separate parts for making the assembly possible and easy. The “disc” will be separated in two parts making it able to open it and access the interior for mounting the probe, sensors and wiring will be inside these parts.

The first part is the construction part, starting from the base part (1), wiring (7), and 4 sensors (8) must be introduced in the correct allowance as shown in the drawing. Wires are placed in the channels that exit the sensor allowance, designed for that. Then the probe (3) will be inserted from the top, leaving the bigger sphere on the upper part.

Next, put the final 2 sensors and wiring in the superior case part (2) and close the sensor with the rubber protection part (6) in the exit of the device's wires. Then to attach the device to the robot, two m6x40 (4) screws must be inserted, in the bigger diameter circumscriptive circumference. Finally, the last two calibration screws m6x16 (5) must be inserted in.

The calibration screws are shorter than the attachment ones because of their mechanical purpose. There is a gap between parts designed to undergo any sort of dilatation or sensor placement, which can be tightened by moving these screws. Being shorter it forces the two parts to go together while tightening the screws (making equal distances from both sides), resulting in a smaller gap. All the distances regarding this variable adjustment are correctly shown and established in the assembly drawing tolerances (included part material tolerance) The kinematic scheme of all of this is shown next:



4.1.1 Assembly scheme

Once the device is mounted, calibrated and connected to the power (and robot), its ready to use. Now the working principle will be explained. When the touch probe makes contact, for example in the x direction, the probe will move making the arm on the opposite place to apply pression on the piezo resistive sensor located in the specified allowance or gap. With the y direction or combination, it is the same working principle, but with the movements in z direction it has a difference. For -Z movements all four base sensors must be pressed or activated, and for the +Z movements, both two sensors in the upper case must also be activated. With this way we prevent from making mistakes in detecting the correct directions in an easy way and also in an optimized way by using the sufficient number of sensors for 6 degrees of freedom.

For not making mistakes with the self-weight of the probe, the movement for -Z is calibrated including it for not making false contact only if, in the calibration process, sensors detect pressure. The spherical hole in the base part is slightly smaller than the upper part, with the same nominal radius as the probe sphere with this, we obtain, a spherical surface that supports the probe but with a small tolerance gap that permits movement. Then the sensors must be placed as near to the probe's arm (almost contact point) to achieve high pression measurements, and at the same time being able to detect deformations in -Z. The key thing in here is the calibration screws, they can be applied till sensors make contact to ensure a high precision measurement. Lubrication during assembly in the lower sphere is key to have a precise movement and to keep straight the probe.

We know that 3D printers don't go that precise in tolerance values, but having this calibration screws solves the problem, and that's because of the capacity of the sensor's material. If there is a problem, material is moldable, so you can adjust the sensors to later on secure that distance with the calibration method again, always leaving the space for then adjusting. Also, the space between the sphere and the upper spherical hole permits us to have a gap for calibration issues in the point of punctual contact, ensuring allowance is no smaller and probe no bigger. Drawings show the nominal distance of adjustment before calibration.

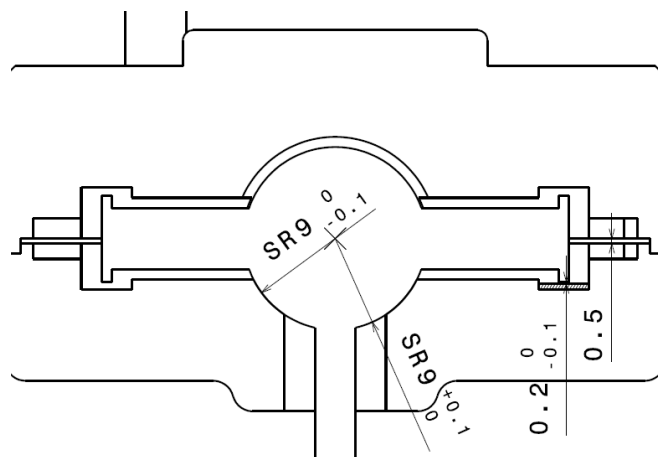
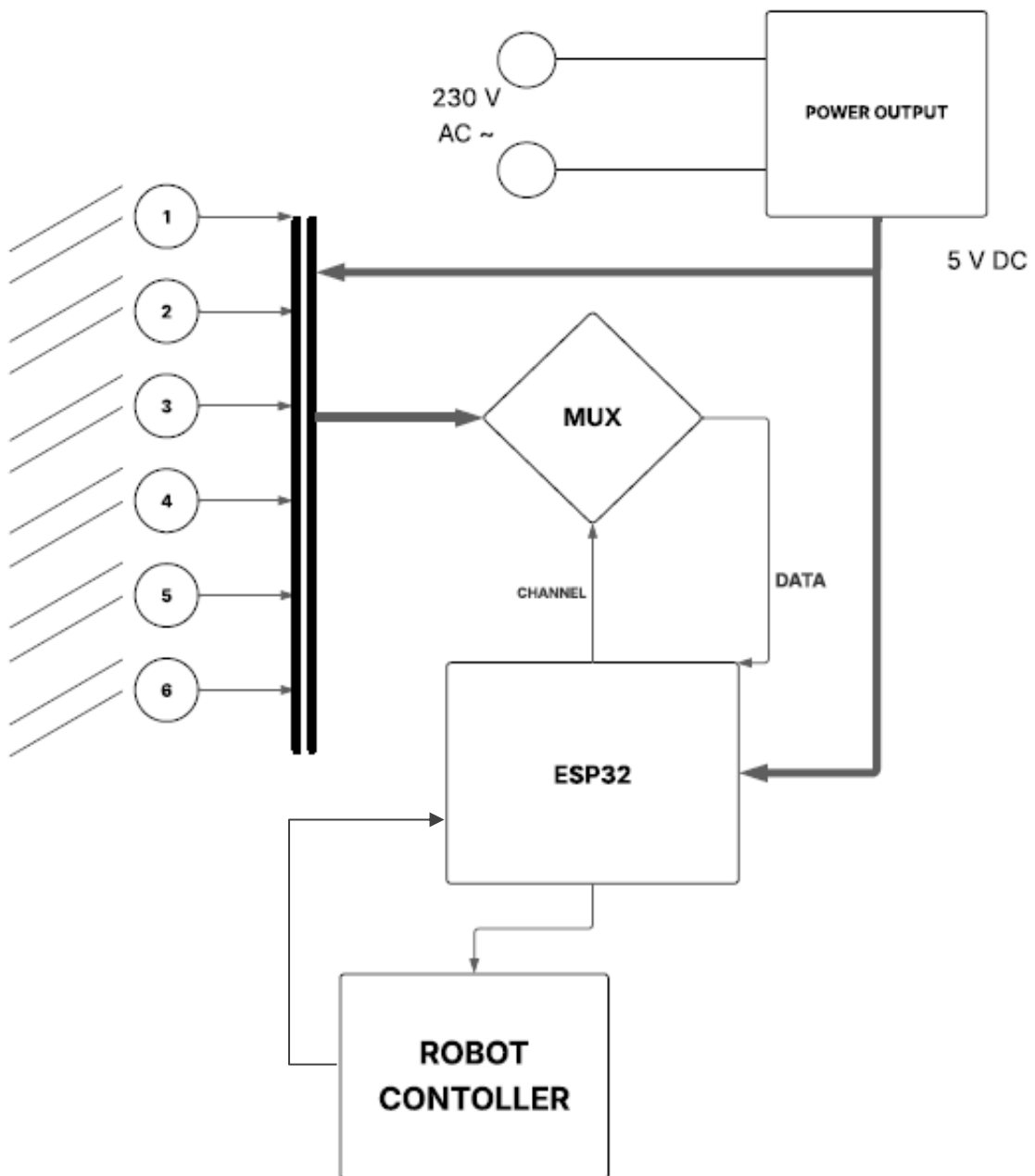


Figure 28 Kinematic movement assemble important tolerances scheme

4.2. Electric block scheme

This chapter presents the electric block scheme that defines the structural and functional organization of the system's hardware components. The block diagram serves as a high-level abstraction, illustrating the main electrical units, their interconnections, and the flow of signals and power throughout the system. It provides a clear overview of how each component, such as sensors, controllers, power supply units, and communication interfaces interacts within the overall architecture. Understanding this scheme is essential for both the design and troubleshooting phases, as it forms the foundation for the subsequent development and integration of the hardware elements.



4.2.1. Electric-block and control scheme

For the electrical and control scheme, starting with the power supply that gives electricity as the primary energy supply for both the sensors and to the ESP32 NodeMCU control unit, this power supply is responsible of transforming from 220 V alternate current to regulated 5V direct current as they are the values that the ESP32 supports, which is sensitive to voltage variations, and to provide sufficient current for stable sensor operation. Internally ESP32 regulates voltage to 3,3 V and current to an average of 250mA, depends on the working mode. These values are suitable for this type of devices.

The transformation from high-voltage AC to low-voltage DC is essential not only for safety and energy efficiency but also for the optimal performance of the connected electronic components. This is needed because of the way they work as piezoresistive sensors in which a change of resistivity is produced when contact force is applied so they need electrical current first for working.

We can see all the sensors connected to the data bus wires and this connected to a multiplexer due the amount of wires needed and this is where the signal previously commented is sent to the control unit.

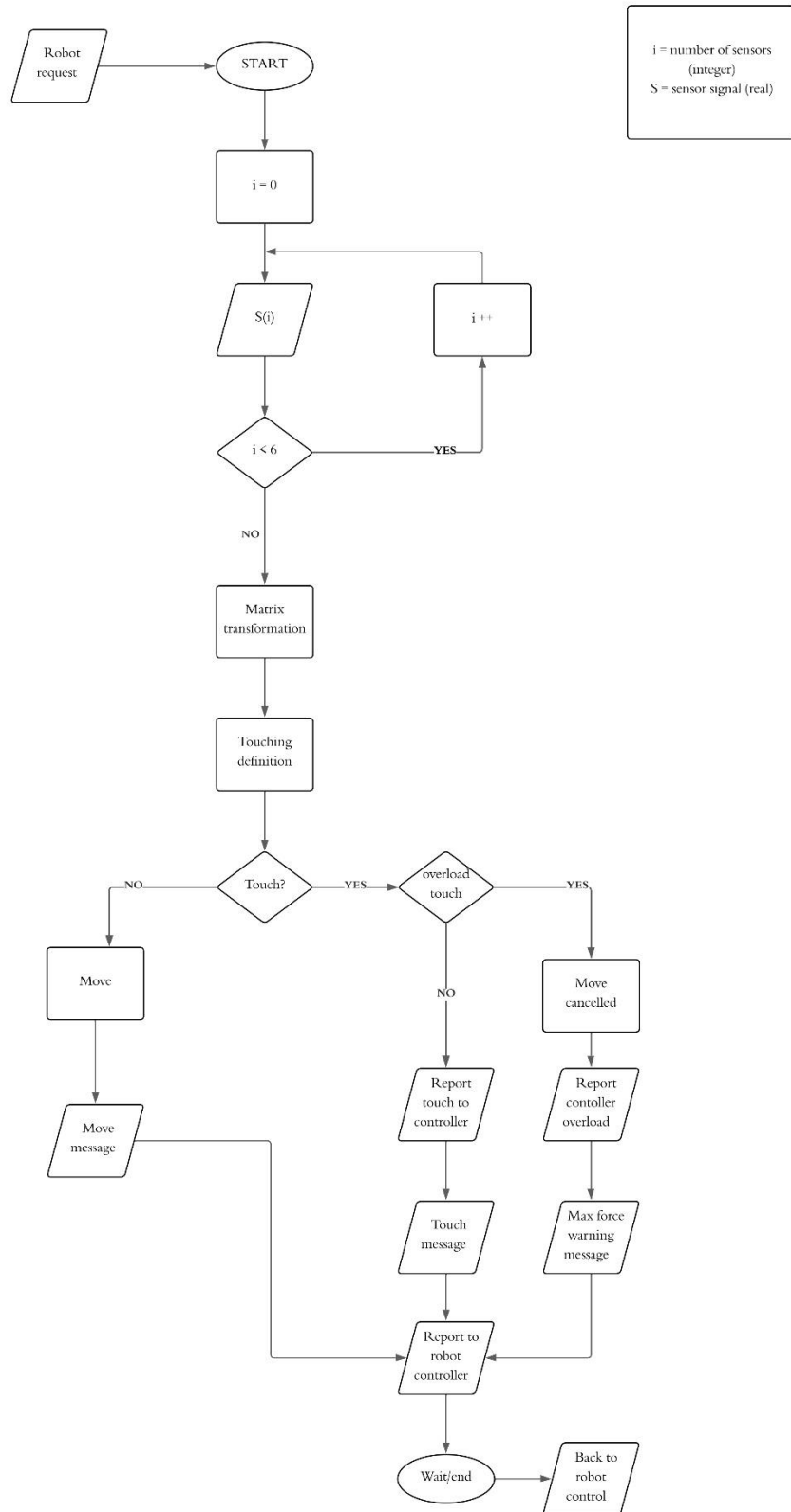
In terms of signal routing, each sensor is connected to a set of data bus wires that collectively serve as the communication pathway to the central processing unit. Given the number of sensors used and the limited input/output (I/O) capabilities of the ESP32, a multiplexer (MUX) is employed to manage these multiple inputs efficiently. The MUX acts as a channel selector, allowing only one sensor signal at a time to be routed to the ESP32 for processing. This greatly reduces the complexity of wiring and conserves microcontroller pins while still enabling full data acquisition from all sensors.

To facilitate proper signal flow and circuit completion, the ESP32 dynamically selects channels on the MUX, directing sensor outputs through the appropriate paths based on programmed logic. This interaction ensures that each sensor's data is accurately captured and forwarded in sequence. Once the sensor data has been acquired, it is processed by the ESP32 and then transmitted to the robot controller unit. This controller functions as the main processing and decision-making centre, where the data is analysed, visualized, and integrated into the robotic system's operational logic.

Finally, the information is sent to the robot controller for data processing and visualization of the operation this electrical and control scheme represents a compact, modular, and scalable system architecture that supports real-time tactile sensing and feedback. By integrating efficient power conversion, multiplexed sensor input management, and robust data transmission, the system achieves a high level of functionality suited for applications in robotics, automation, and interactive systems.

4.3. Algorithm of management of device or node

This chapter focuses on the design and implementation of the management algorithm responsible for managing the operation, communication, and coordination of devices or nodes within the system. In the next flow diagram the working sequence cycle is shown:



4.3.1 Algorithm of management of mechatronic system

A complete description of the developed device algorithm is provided. In this case we see algorithm is not closed, that's because this system forms part of the robot algorithm system, which is closed in the outside and its analysis is not the objective of this thesis. So, algorithm must start and end with a robot request and robot report and control respectively. First, we define the integer i for reading all the six sensors before starting the measurement. This is done for ensuring all the sensors work and to read them for the program. When this is done, the signal is transformed with a transformation matrix (3x2) in which later the touch direction is defined.

If a touch contact force is detected and its value doesn't exceed the limit of specifications, the signal is reported to the control unit (in the end also to the robot control unit) and the process stands by for making, waiting for the approval to start again the cycle as the position information is processed by the robot control unit. If the contact force exceeds the limits, a warning message is sent to the control unit and the cycle stops. The other case is when contact has not been produced, which means to report the move order to the control unit and starting again the cycle.

In summary, the described device algorithm provides a structured and robust approach to sensor data acquisition, signal transformation, and control feedback. By initializing the process with a verification loop using the integer i to sequentially read all six sensors, the system ensures complete sensor readiness before any measurement begins. The acquired data is then processed through a predefined 3x2 transformation matrix, which is critical for accurately determining the direction of an applied touch force. Depending on the magnitude and presence of the detected force, the algorithm follows distinct conditional branches: if a valid contact force within specified thresholds is detected, the transformed signal is relayed to the control unit subsequently interfacing with the robot control unit for further position analysis and approval to restart the cycle. If the force exceeds the defined safety limits, the algorithm triggers an immediate warning and terminates the cycle to prevent potential damage.

Conversely, if no contact is detected, a move command is issued to the control unit, and the robot system reinitializes the cycle. This logical flow ensures responsive, safe, and repeatable operation in touch-sensitive robotic applications.

5. WORK SAFETY

5.1. General provisions and requirements for safe working and environmental protection

The use of the robot Yaskawa HC20SDTP involves some risks that the user needs to take into account although the machine doesn't need a safety fence and that it comes with PLD's certification category 3 security. We can identify the following risks:

Mechanical risk: Crushing or entrapment due to unexpected arm movement which can cause harm to the user.

Electrical risk: Exposure to electrical currents or faulty connections during sensor integration or power supply management.

Collision hazard: Inadvertent contact between the moving manipulator and the surrounding equipment.

Measurement error risk: Miscalibration or signal noise in the force sensor may lead to erroneous force readings, potentially compromising task safety or research validity.

5.2. Work safety and environmental requirements of robotic calibration tool:

Due to the use of the robotic tool calibration equipment the following **safety protocols** must need to take into account:

- The system shall only be operated by trained personnel or under the supervision of qualified staff.
- Prior to handling or modifying system components, the power supply must be completely disconnected.
- During active operation, physical interaction with moving parts is strictly prohibited.
- The force sensor must be calibrated according to manufacturer specifications before each experimental session.
- If used in a shared space, visual barriers (not fence needed) must be installed to demarcate the robot's operating area.

Required personal protective equipment (PPE):

The use of appropriate PPE is mandatory during operation and maintenance:

- Protective gloves, when handling components, during assembly or conducting mechanical adjustments.
- Safety goggles, only in scenarios involving risk of mechanical debris or disassembly.
- Close fitting clothing, to prevent entanglement with moving parts or joints.

Emergency procedures:

In the event of an anomaly or incident:

- Emergency shutdown button needs to be activated, implemented in the control device of the robot (HMI elements)
- Incident reporting: Notify to the designated supervisor and secure everything before power is turned on again.

Maintenance and calibration:

Scheduled inspections and preventive maintenance of the robot, designed in the catalogue, is essential for safe operation:

- Periodic verification of electrical connections, mounting stability and mechanical joints.
- Cleaning of sensor interfaces and mechanical components using non-conductive tools and with power supply off.
- Calibration of the sensors using the standard procedure provided.

Training requirements:

Users must demonstrate competency in:

- Basic operation of robotic manipulators and related software interfaces.
- Interpretation and analysis of force of force sensor outputs.
- Laboratory safety procedures, including risk assessment and emergency response protocols.

Fire safety protocol:

Although the system operates at low voltage and current levels, fire hazards may arise due to electrical malfunctions or overheating components: The following fire safety measures must be in place:

- Ensure the robotic system is connected via a surge protected and properly rated power supply.
- Do not operate the system near flammable materials or in enclosed, poorly ventilated areas.
- A class C fire extinguisher suitable for electrical fires must be located within 10 meters of the workstation.
- In case of visible smoke, burning smell, or open flame: immediately disconnect power from the main supply, evacuate the area following the laboratory's emergency evacuation route, notify the emergency services and the building safety officer if necessary, and do not attempt to extinguish the fire unless it is safe to do so.

6. ECONOMIC CALCULATION

In this chapter an economic analysis of the project will be made, this includes the cost of every material involved in it or machinery needed for fabrication, fixed and variable costs. Economic viability is also important when a project is launched to the market. Based on this calculation, the payback point will be calculated and also the diagram of the distribution of costs. The bill of materials and total costs are:

Table 6.1 Economical cost of materials

Product	Units	Cost	Type	Total of material cost
UltiMaker 2+ connect	1	2.299,00 €	fix	2.299 €
Workshop rent	1	850€	fix	850€
Worker salary	1 per device	13,65€/h	variable	13,65€
PLA filament	0,131 kg/device	27,98 €/kg	variable	3,67 €
M6x40 ISO 4762	2 per device	0,27 €/unit	variable	0,54 €
M6x16 ISO 4762	2 per device	0,13 €/unit	variable	0,26 €
Piezoresistive sensors	6 per device	5€ per device	variable	5 €
Rubber protection	1 per device	0,50 €/unit	variable	0,5 €
Data Bus (sensor wires included)	1,8m per device	0,30 €/meter	variable	0,54 €
NodeMCU v3 ESP32	1 per device	6,51€ per unit	variable	6,51 €
Multiplexer (MUX)	1 per device	4,6€ per unit	variable	4,6 €
5V power supply to micro USB	1 per device	4,90€ per unit	variable	4,90 €
Electrical Cost	170W (6,5 h of 3D printing)	0,2135 €/kWh	variable	0,25 €
Total fix cost				3149 €
Total cost per device (variable cost)				40,42 €

The total fix cost corresponds to the 3D printer necessary for the fabrication process. The election of that model corresponds to the filament diameter, workspace dimensions and industrial performance (*UltiMaker 2+ Connect 3D Printer*, n.d.). Workshop rent is based on similar shared spaces available in the outskirts of Vilnius. Electricity prices are based on the average price for Lithuania in 2024 and the average electric consumption of the machine with the cooling fans and heating bed turned on (*Lithuania - Electricity Prices: Medium Size Households - 2025 Data 2026 Forecast 2010-2024 Historical*, n.d.). Printing time which is 6,5 h is simulated with Cura program made for controlling the printing process(*UltiMaker Cura - UltiMaker*, n.d.). For the worker salary, I estimated 1h of assembly and controlling 3D printing process for the average for a workshop worker in Lithuania (Trading economics, n.d.) Rest of the prices correspond to the Lithuanian market ones from internet catalogues available on the bibliography.(*Amazon.Com: DIYables 120 Multicolor Jumper Wires for Prototyping Arduino, ESP32, ESP8266, Raspberry Pi Electronics Projects: Industrial & Scientific*, n.d.; *Varžtų Pasaulis: DIN912 / ISO4762 - Hexagon Socket Head Cap Screws, Stainless Steel*, n.d.) (16 Channel Multiplexer Switch ICs – Mouser Lithuania, n.d.; NodeMCU V3 WIFI ESP8266, n.d.) (*Power Supply 5V 2A MicroUSB*, n.d.)

Next, the breakeven point is calculated, market cost of the device will be 72€. That price is selected due to the common margin of benefit characteristic for this technological devices. For that calculations with Excel will be done and the graph will show visually and analytically the point where inversion pays off and the number of units needed to sell for it:

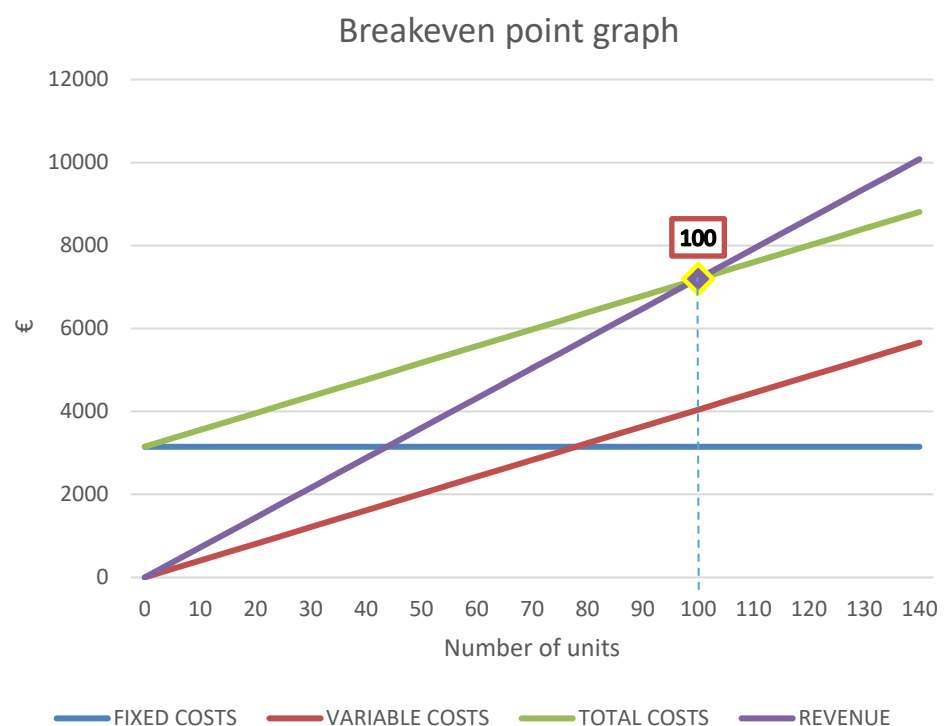


Figure 29 Breakeven point visualization

Table 6.2 Breakeven point exact parameters

Fixed costs	3.149 €
Variable costs	40,42 €
Selling price (bef. TAX)	72 €
VAT (21%)	15,12 €
Final selling price	87,12 €
Benefit margin	56,13 %
BEP	99,7150095 units

As we see the number of units necessary to sell for get back the inversion is 99,71 which equals to 100 physical units. Next, a distribution of costs of the project is made, this distribution will allow us to better understand the structure of the investment, evaluate the weight of each cost category, and identify potential areas for optimization or risk:

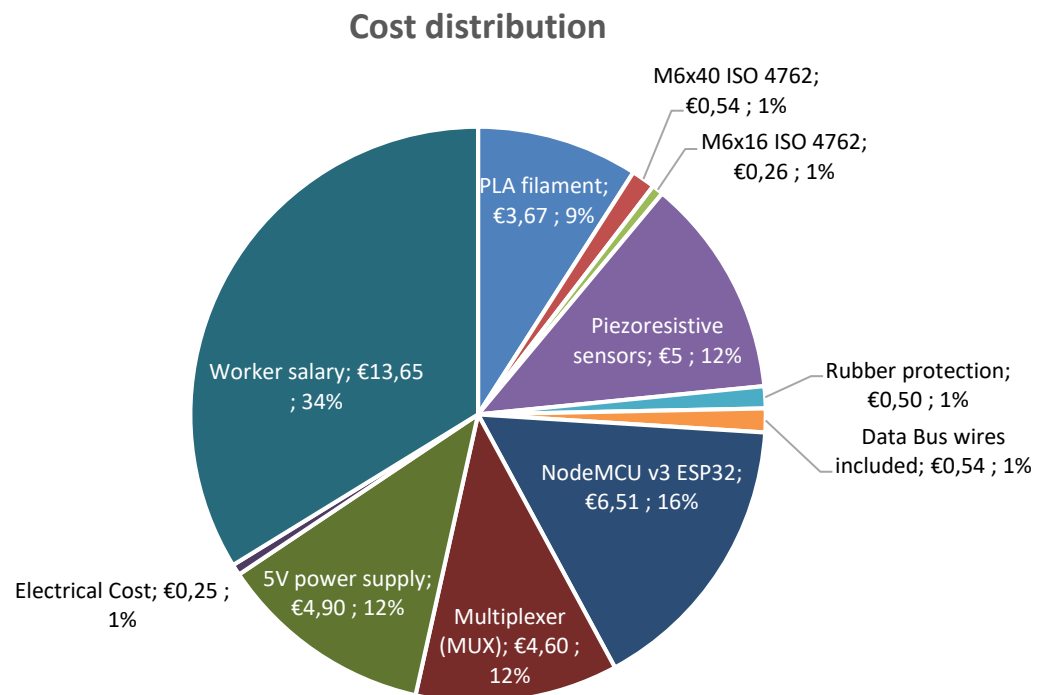


Figure 30 Distribution pie chart of device costs.

To conclude, we can analyse the cost distribution. Without the initial inversion of the 3D printer, and considering the device, as it is the object of this study, the bigger cost is the control unit ESP32 Node MCU with the 24%, then the piezo resistive sensors with a 19%, then the power supply with a 18% and then the multiplexer with a 17%. Last of the most representative costs is the PLA material, this reflects that the construction material is cheap compared to the first features. It is also remarkable to say the electrical cost is minimum so that puts into perspective how such a complex design can be done in a very economical way, without the cost of the machine, and how easy is to get back that inversion.

7. CONCLUSIONS

The study has presented the design of a touch probe for robot calibration issues, fabricated in a 3D printer and using the piezoresistive material provided by the Vilnius tech university for the sensing component. This thesis has presented the conceptualization, mechanical design, fabrication, and validation of a cost-effective touch probe device, manufactured from polylactic acid (PLA) through 3D printing manufacturing method for the calibration of robotic arms. The primary engineering goal was to explore whether additive manufacturing, combined with basic mechanical and piezo resistive components, could yield a sufficiently accurate and reliable tool for robotic calibration tasks typically dominated by costly commercial alternatives:

1. The integration of the device into a robotic system highlighted both the practicality of the approach and its potential application in educational or budget-constrained settings or even in an industrial application environment. In it there has been, most of all design challenges like the idea of making a touch probe in which sensors work only with compression in which the spherical cross shaped design was the election for completing the task due to its mobility properties and stress distribution nature. The biggest challenge was to create a calibration method that permits to adjust relative distance between parts so taking into advance the nature of the plastic material, the two-screw option demonstrated to be an easy and economical way to make adjustments when it comes to device sensor calibration. Gaps where needed to make for ensure a perfect fitting and optimal precision in every case. We can also talk about the fact that the device is composed by only three major parts which are the base matrix, superior matrix and probe so in comparison with the high cost alternative market options this project is simple and easier. Portability is also key in this project, the device could be used for various robots (of the same model characteristics) and also, being a reduced size part, makes it easy to transport it in a suitable protective case. When talking about robot integration we can highlight its simplicity in terms of electrical circuit scheme and algorithm, being at the same time easy and enough for the purpose this calibration tool was made for. This means that, for this first conclusion, a cheap but at the same time precise and accurate, simple integration device could be made. Design ideas where thoughtful and at the same time challenging, prepared for any case scenario and to permit assembly or even any maintenance operation, calibration and integration in a fast and simple way.
2. From a mechanical engineering perspective, the project involved addressing several core challenges: ensuring structural rigidity and repeatable deflection under low contact forces, minimizing backlash or play within the probe housing, and achieving a compact design that could be mounted and interfaced with existing robotic manipulators. The geometric

tolerances required for accurate calibration-imposed constraints on the design that were carefully balanced with the inherent limitations of 3D printing, particularly those related to PLA's mechanical properties such as stiffness, brittleness, and temperature sensitivity. This leads to thinking in other type of plastic material that withstands a more precise range of tolerance or even another process of fabrication in terms of mechanical design. In consequence, also means to have another type of material that achieves repeatability in dimensional tolerances and also a faster way of production, such as plastic injection which would be suitable for the probe part, maintaining 3d printing for it. Despite its advantages, the design exhibited limitations primarily associated with the mechanical and thermal properties of PLA, which may affect dimensional stability and long-term durability under certain operating conditions such as high humidity scenarios, high temperature working environments or big impact forces. These constraints suggest that while suitable for preliminary or low-precision tasks, further material optimization is required for deployment in more demanding scenarios. In this third conclusion we can talk about alternatives in terms of improvement of general characteristics and performance.

3. In terms of future engineering developments, several avenues are evident. Substituting PLA with more mechanically stable materials such as PETG, ABS, or nylon could enhance the durability and precision of the probe. Additionally, the integration of microelectromechanical systems (MEMS) sensors, capacitive touch elements, or strain gauges could improve the sensitivity and resolution of contact detection. On the systems engineering level, automation of the calibration process via robotic control algorithms (more complex), as well as the use of closed-loop feedback, could significantly increase both the usability and repeatability of the solution. Also, an automated retractable emergency stop movement which remembers the environment previous touch points and ensures no future collisions in the process will be a challenge for making a more advanced a complex device.
4. From the economical perspective, the device is intended to be low cost as it is made by 3D printing in comparison to the high-priced market calibration devices and also performing with enough precision for the purpose it is made for. This method significantly reduces production costs when compared to traditional manufacturing technics or different materials. Improvement could be made by buying more production equipment for reducing manufacturing time although initial inversion increases.
5. Although initial inversion is expensive mainly associated with the cost of prototyping, production equipment and development, variable costs for the fabrication procedure is economically acceptable, keeping the return of this first cost in the threshold of under one

hundred units of sales. This means that the entire initial investment can be recovered within a relatively short sales cycle, assuming a normal market demand. After reaching this threshold, sales contribute directly to profit, making the project not only technically viable but also economically sustainable.

Ultimately, this work contributes to the field of mechanical and robotic engineering by demonstrating that additive manufacturing can produce functionally effective, application-specific tooling for robotic systems. It validates a methodology wherein engineering design principles precision mechanics, systems integration, and material behaviour are synthesized with accessible technologies to produce real world, low-cost alternatives. The probe device developed in this thesis project serves not only as a practical tool but also as a case study in the broader application of engineering innovation to enhance accessibility and flexibility in robotic calibration processes.

LIST OF LITERATURE

- *16 Channel Multiplexer Switch ICs – Mouser Lithuania*. (n.d.). Retrieved May 9, 2025, from <https://www.mouser.lt/c/semiconductors/switch-ics/multiplexer-switch-ics/?number%20of%20channels=16%20Channel&srsId=AfmBOopFu5uSjcHVSCCgFSDXsRpmvEvYnwCnUsHxIoktkaY-hx3MLUKd>
- Albajez, J. A., Velázquez, J., Torralba, M., Díaz-Pérez, L. C., Yagüe-Fabra, J. A., & Aguilar, J. J. (2024). Development of a Six-Degree-of-Freedom Analog 3D Tactile Probe Based on Non-Contact 2D Sensors. *Sensors*, 24(9). <https://doi.org/10.3390/s24092920>
- *Amazon.com: DIYables 120 Multicolor Jumper Wires for Prototyping Arduino, ESP32, ESP8266, Raspberry Pi Electronics Projects: Industrial & Scientific*. (n.d.). Retrieved May 9, 2025, from <https://www.amazon.com/Jumper-Wires-Arduino-ESP8266-Raspberry/dp/B0BDFML3XD?th=1>
- BCN3D filaments. (n.d.). *pla properties*.
- Dao, D. V., Wells, J. C., Sugiyama, S., Toriyama, T., & Wells, J. (n.d.). *Silicon Piezoresistive Six-Degree of Freedom Micro Force-Moment Sensor*. <https://www.researchgate.net/publication/267304892>
- Fiorillo, A. S. (1997). A piezoresistive tactile sensor. *IEEE Transactions on Instrumentation and Measurement*, 46(1), 15–17. <https://doi.org/10.1109/19.552150>
- Group, K. (2021). *Piezoelectric force sensor SlimLine Piezoelectric ring force transducers for tensile and compression forces from 3 kN to 80 kN*. www.kistler.com.
- *Lithuania - Electricity prices: Medium size households - 2025 Data 2026 Forecast 2010-2024 Historical*. (n.d.). Retrieved May 9, 2025, from <https://tradingeconomics.com/lithuania/electricity-prices-medium-size-households-eurostat-data.html>
- *NodeMcu V3 WIFI ESP8266*. (n.d.). Retrieved May 9, 2025, from <https://www.anodas.lt/en/nodemcu-v3-wifi-esp8266>
- *Power Supply 5V 2A microUSB*. (n.d.). Retrieved May 9, 2025, from <https://www.anodas.lt/en/power-supply-5v-2a-microusb>
- Shi, Y., & Dai, J. (2025). Optimized Design of a Triangular Shear Piezoelectric Sensor Using Non-Dominated Sorting Genetic Algorithm-II(NSGA-II). *Sensors*, 25(3). <https://doi.org/10.3390/s25030803>
- Tekscan. (n.d.). *Tekscan_FlexiForceA502_2_0Datasheet_Rev_H-3574571*.

- *Tensile stress-strain curves of ABS and PLA for flat and upright... | Download Scientific Diagram.* (n.d.). Retrieved May 22, 2025, from https://www.researchgate.net/figure/Tensile-stress-strain-curves-of-ABS-and-PLA-for-flat-and-upright-printing-orientations_fig8_335060708
- Trading economics. (n.d.). *Lithuania - Industrial salaries | 2008-2024 Data | 2025-2027 Expectative.* Retrieved May 19, 2025, from <https://es.tradingeconomics.com/lithuania/wages-in-manufacturing>
- *UltiMaker 2+ Connect 3D Printer.* (n.d.). Retrieved May 9, 2025, from <https://www.crea3d.com/en/ultimaker-3d-printers/838-ultimaker-2-plus-connect.html>
- *UltiMaker Cura - UltiMaker.* (n.d.). Retrieved May 9, 2025, from <https://ultimaker.com/es/software/ultimaker-cura/>
- *Varžtų pasaulis: DIN912 / ISO4762 - hexagon socket head cap screws, stainless steel.* (n.d.). Retrieved May 9, 2025, from <https://www.varztupasaulis.lt/?locale=en#!gid=67759dda-e452-11e5-bdbd-000c299e27fc>
- Yaskawa. (n.d.). *Human-Collaborative Cobot Short-arm Variant for confined Spaces YRC1000 micro.* www.yaskawa.eu
- Zhang, Y., Ju, F., Wei, X., Wang, D., & Wang, Y. (2020). A piezoelectric tactile sensor for tissue stiffness detection with arbitrary contact angle. *Sensors (Switzerland)*, 20(22), 1–14. <https://doi.org/10.3390/s20226607>

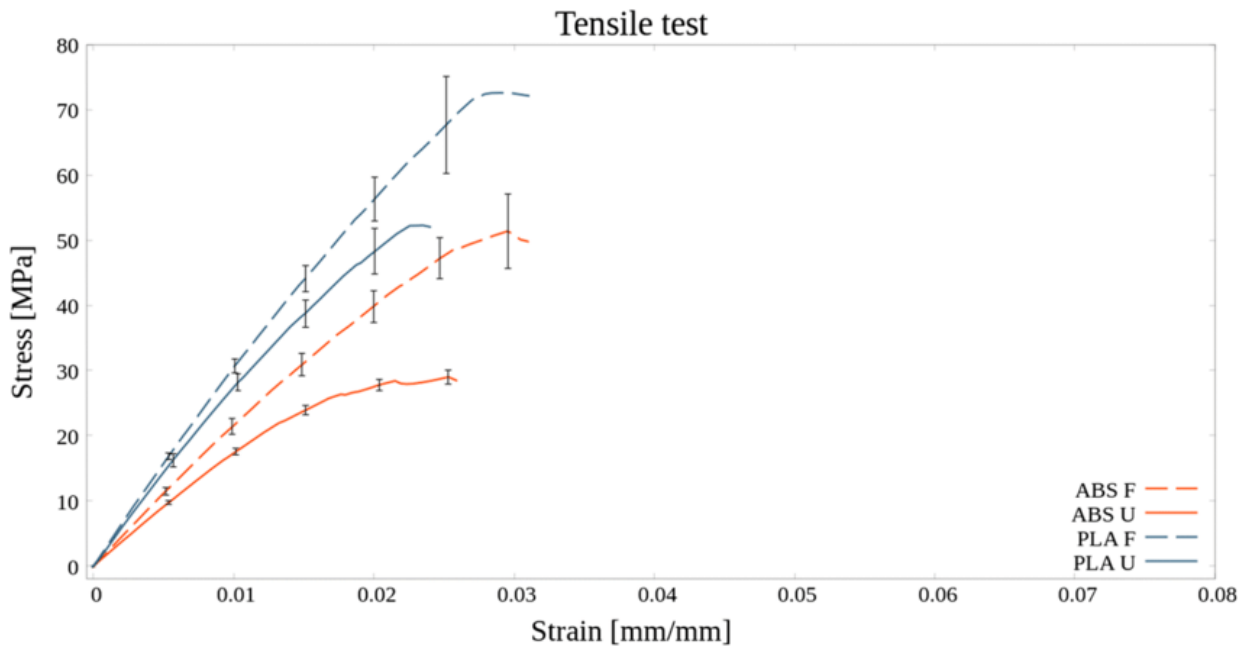
THE ANNEXES

Piezo resistive material provided by VGTU



Piezo resistive sensor material aspect and drying (VGTU)

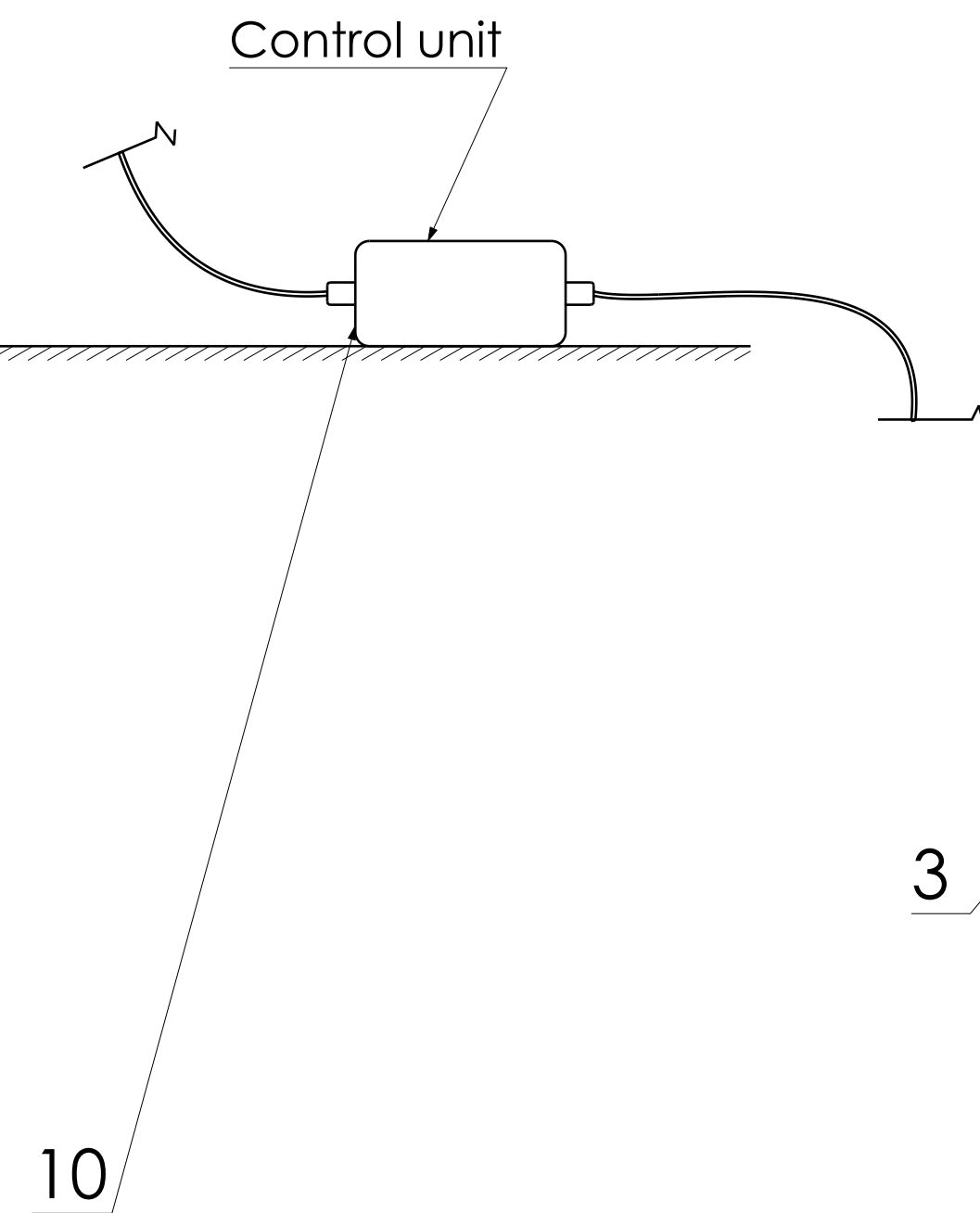
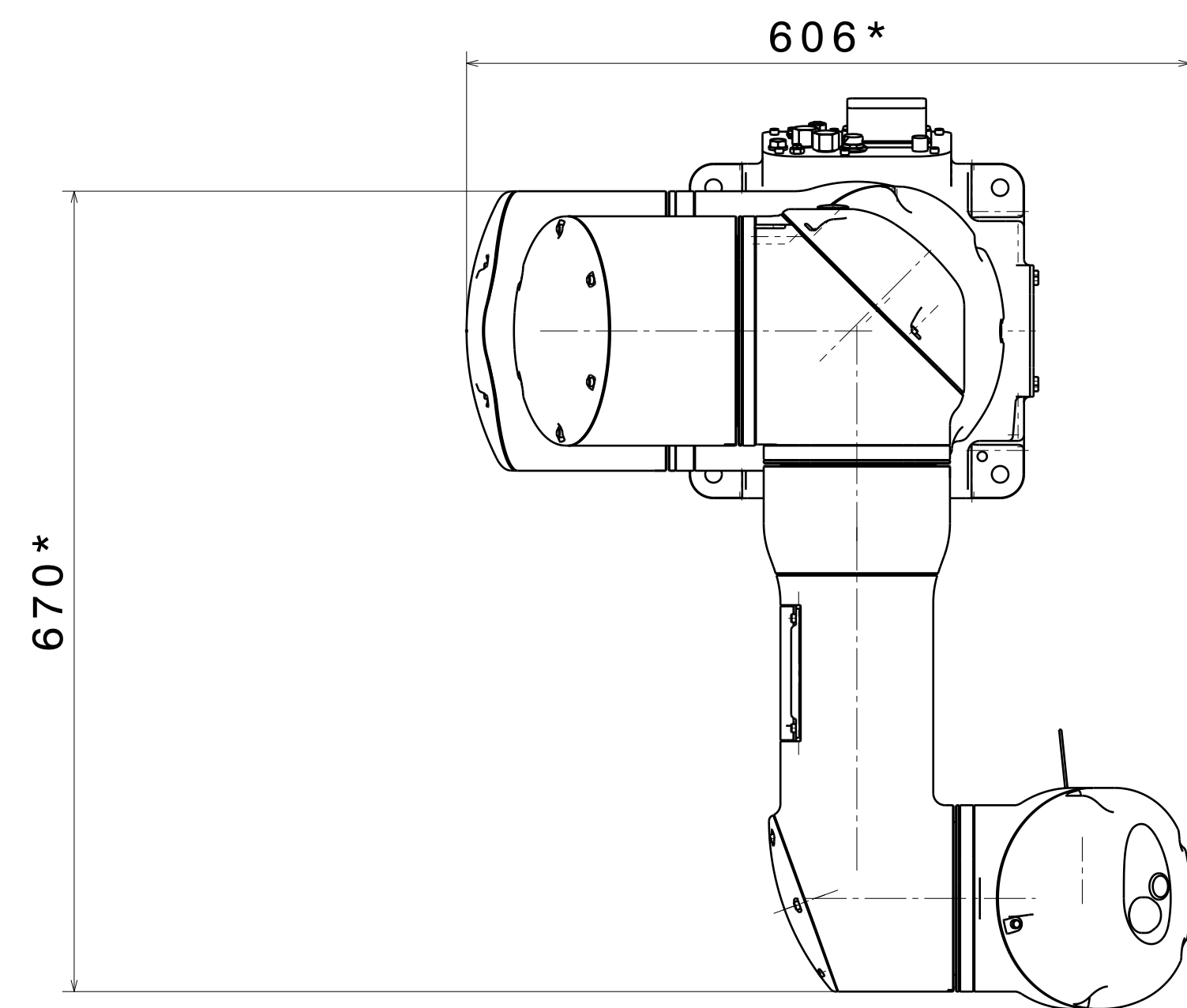
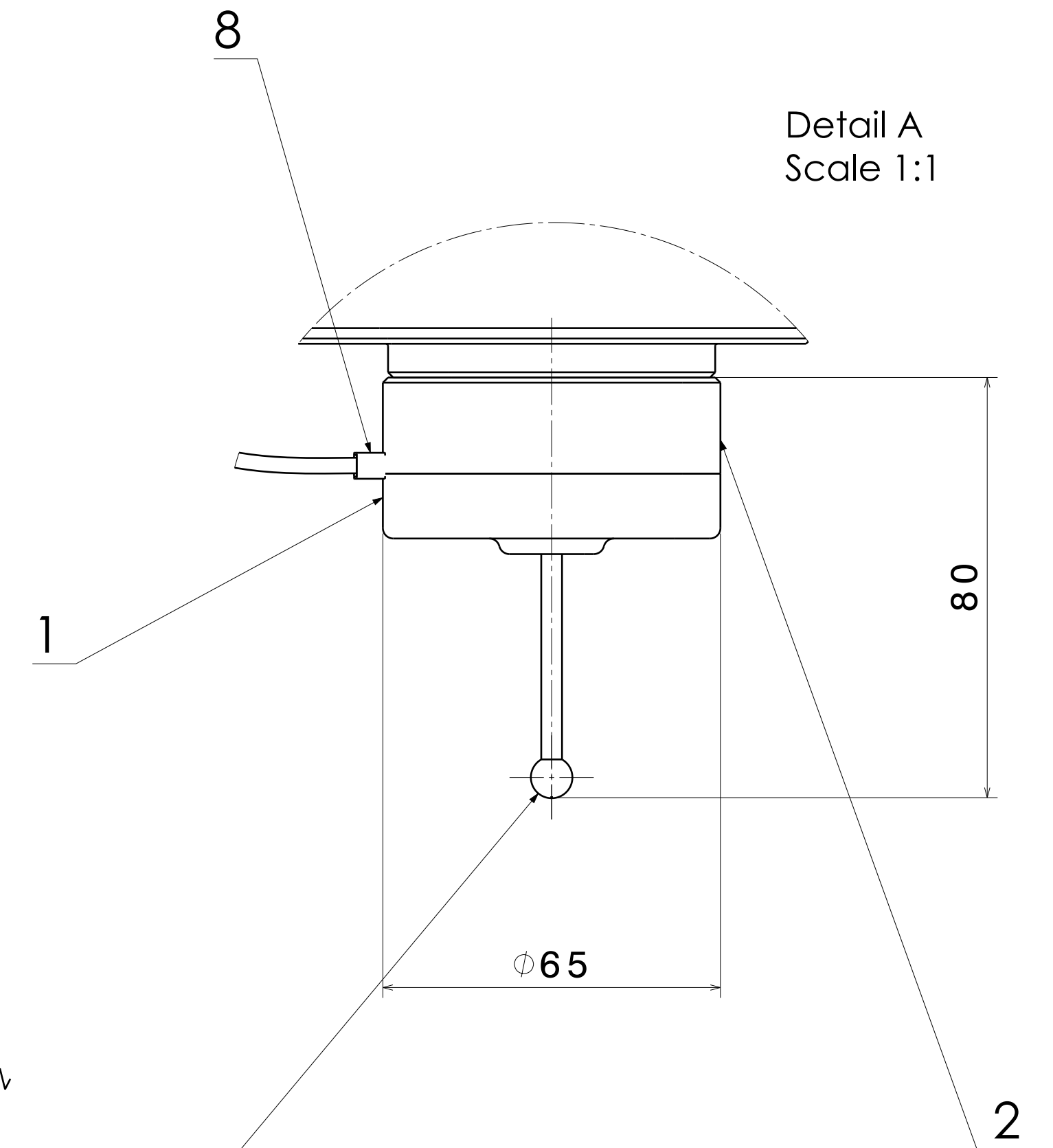
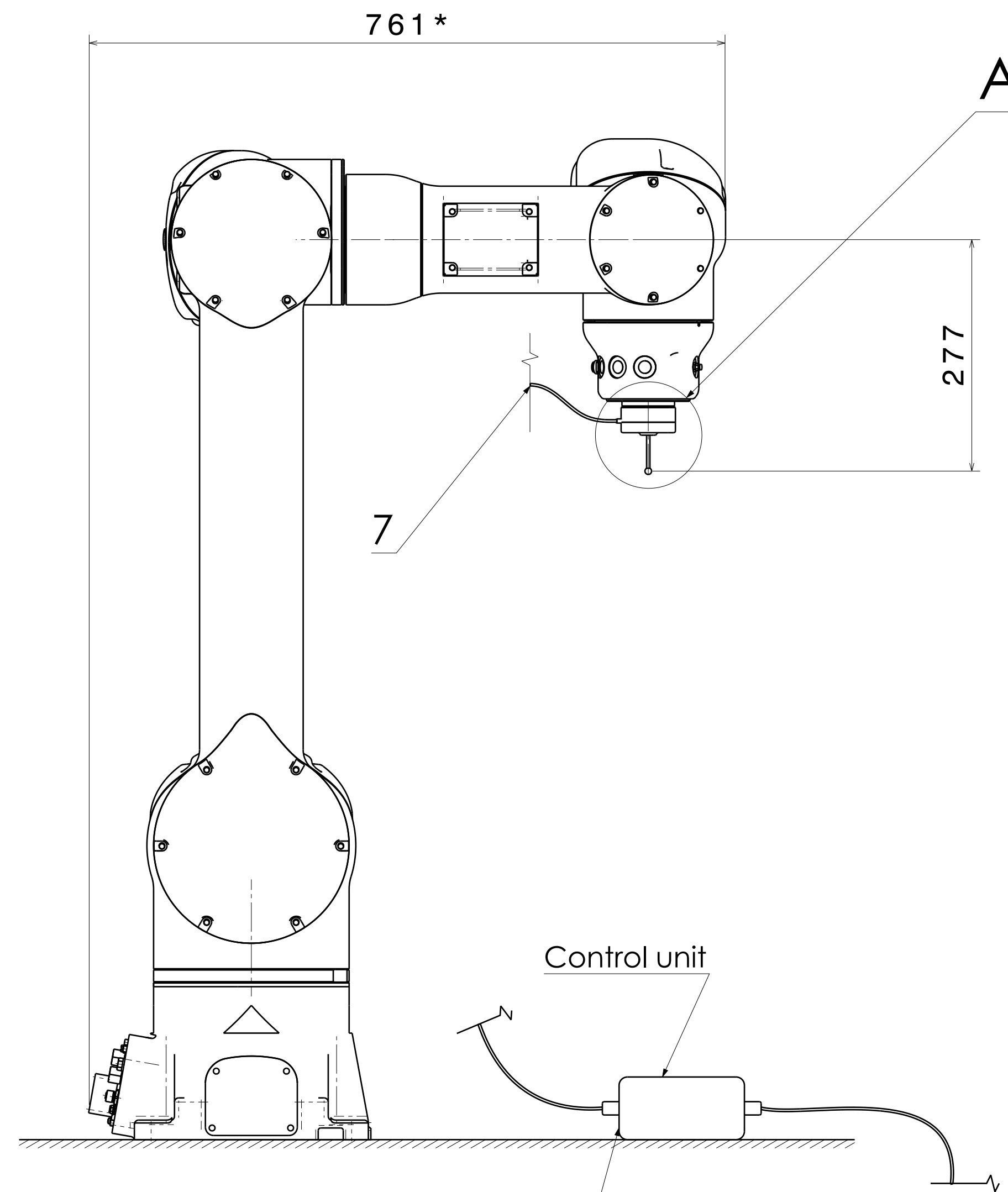
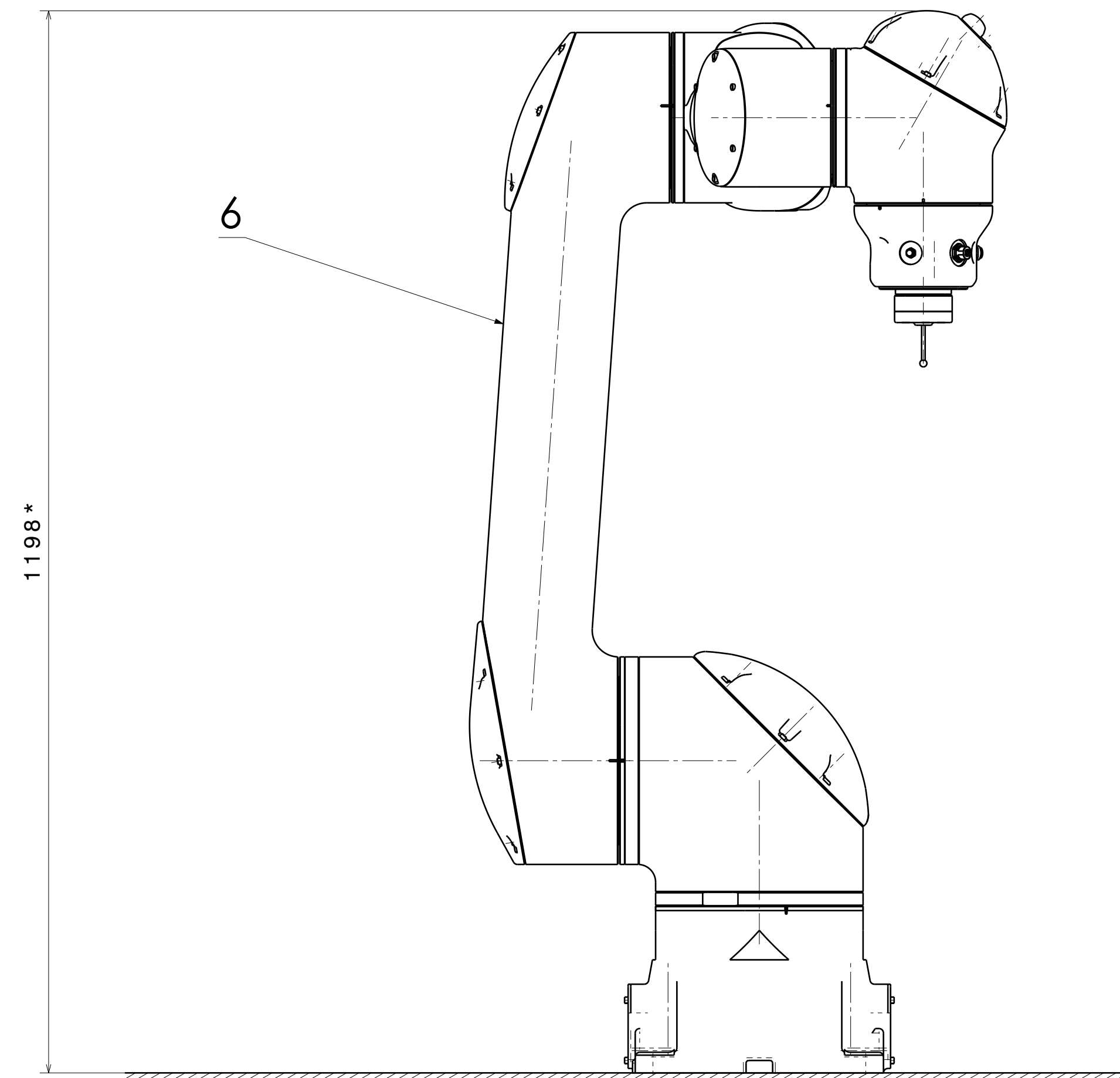
Tensile stress-strain curves of ABS and PLA for flat and upright printing orientations



(*Tensile Stress-Strain Curves of ABS and PLA for Flat and Upright... / Download Scientific Diagram, n.d.*)

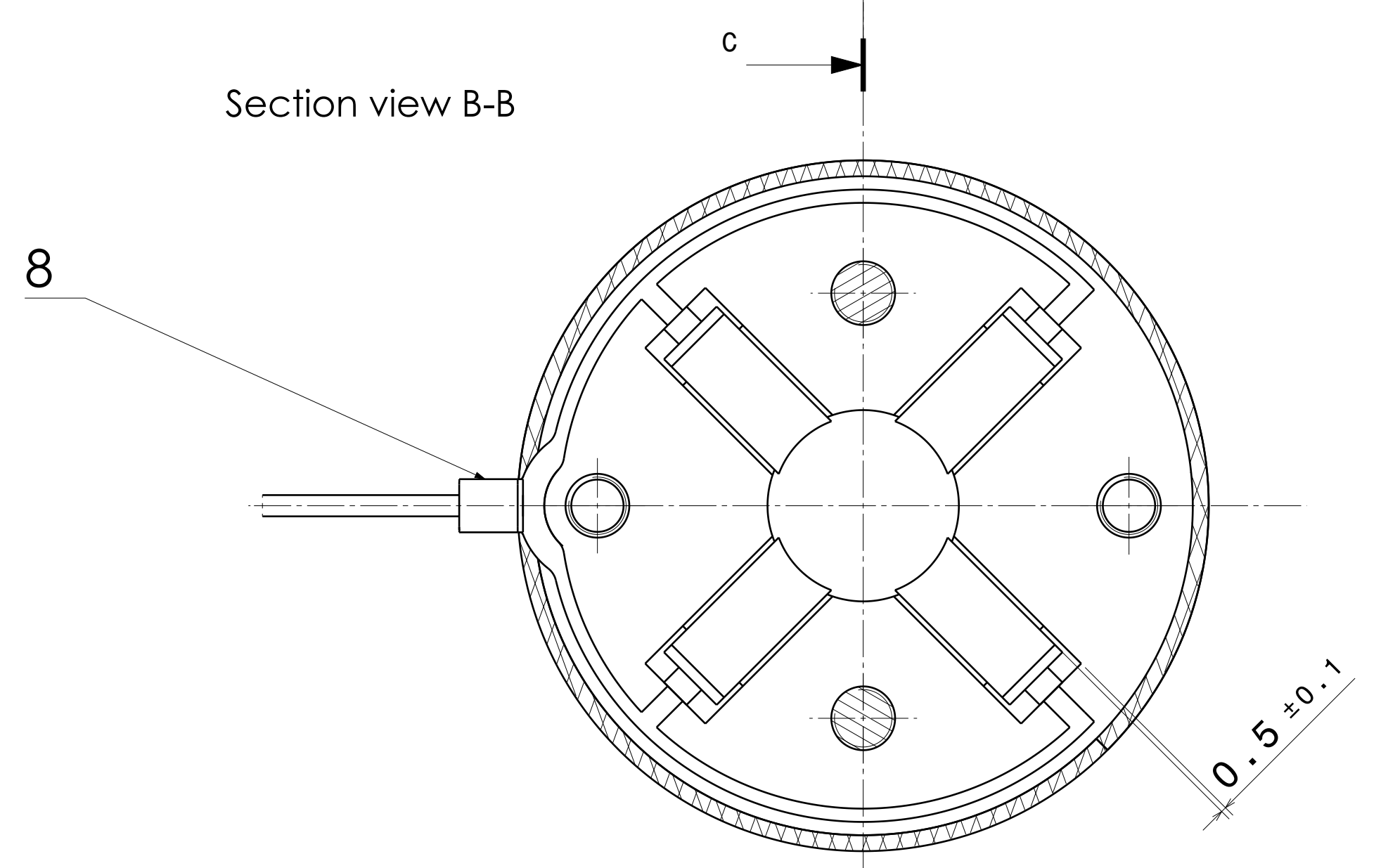
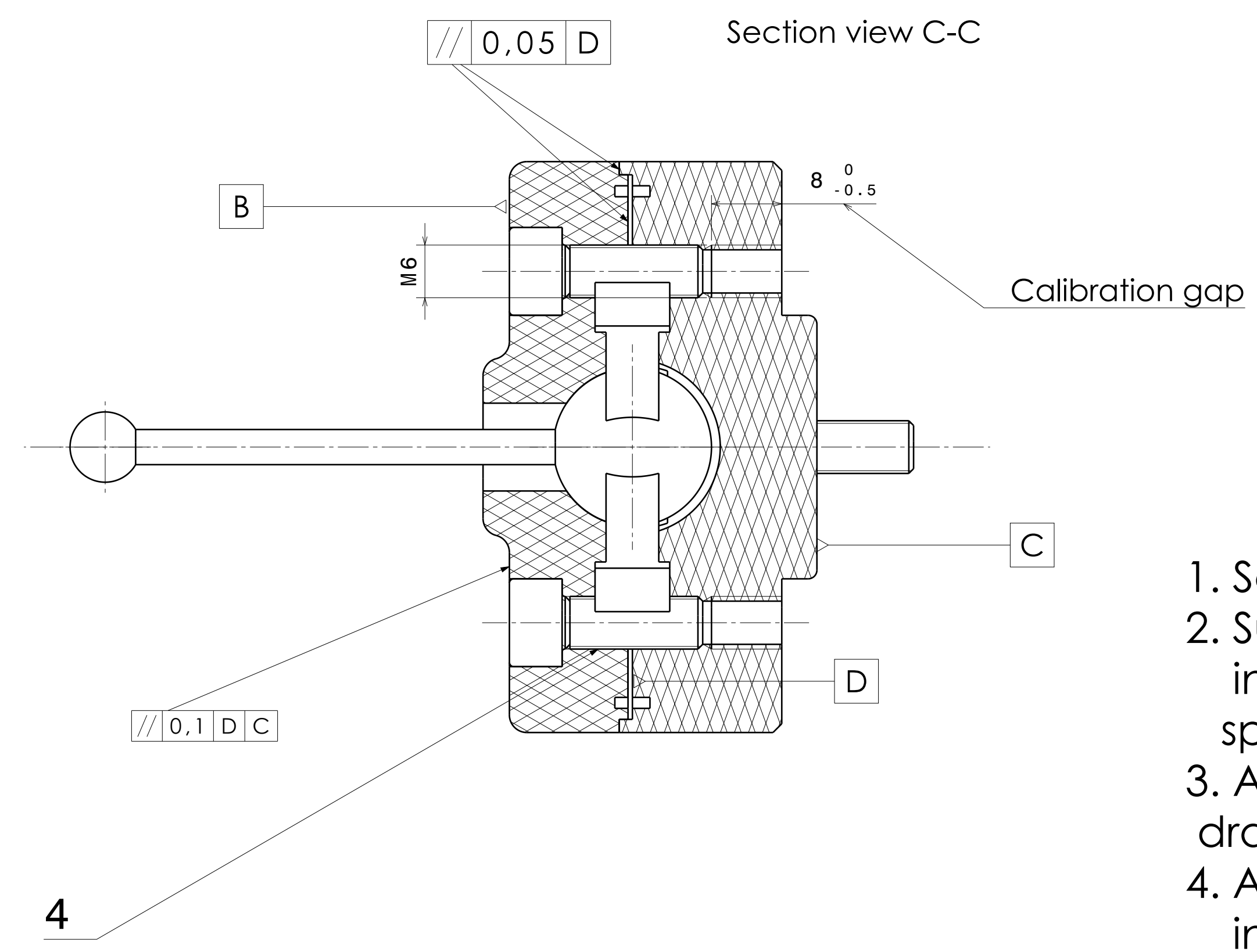
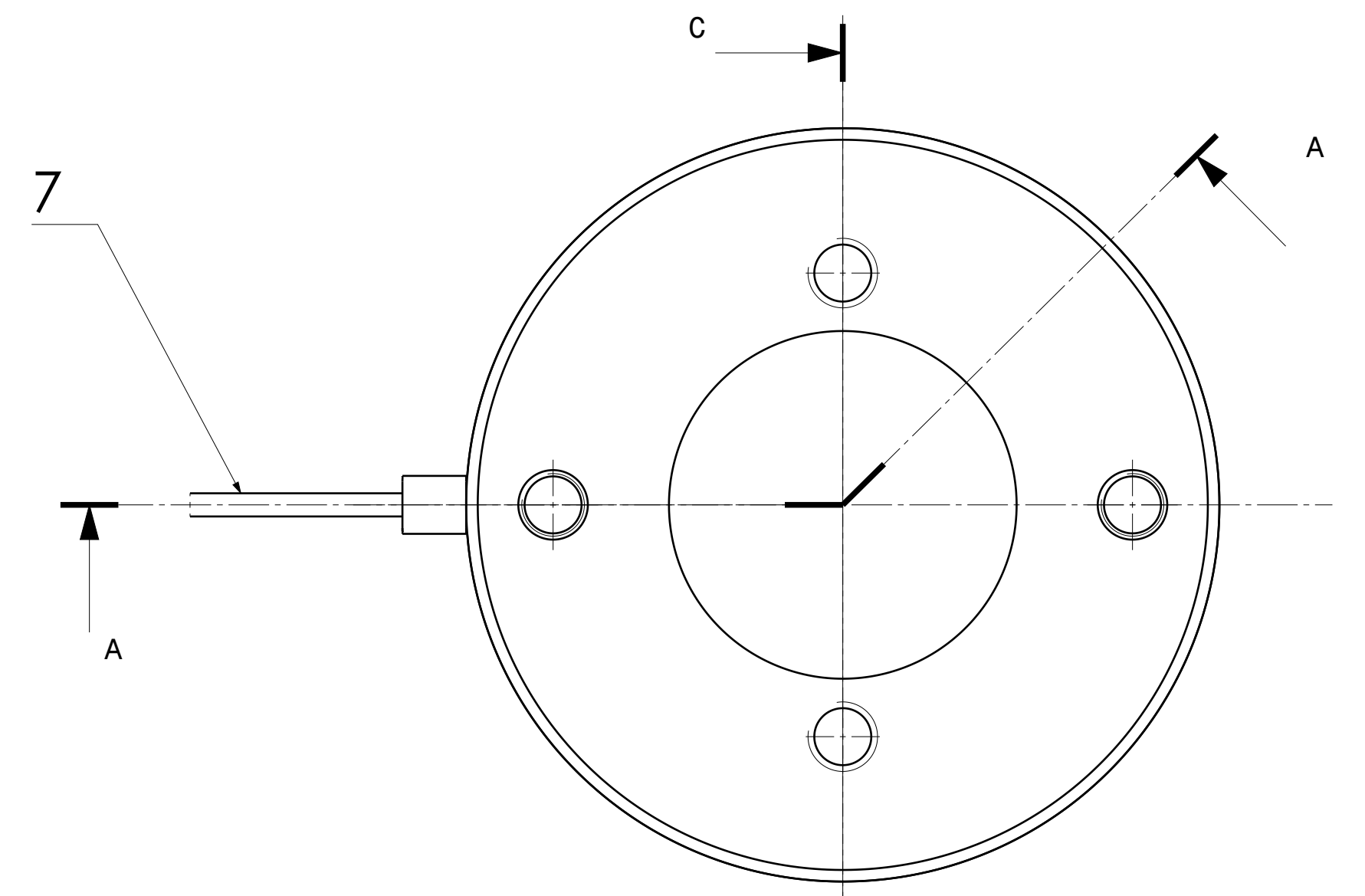
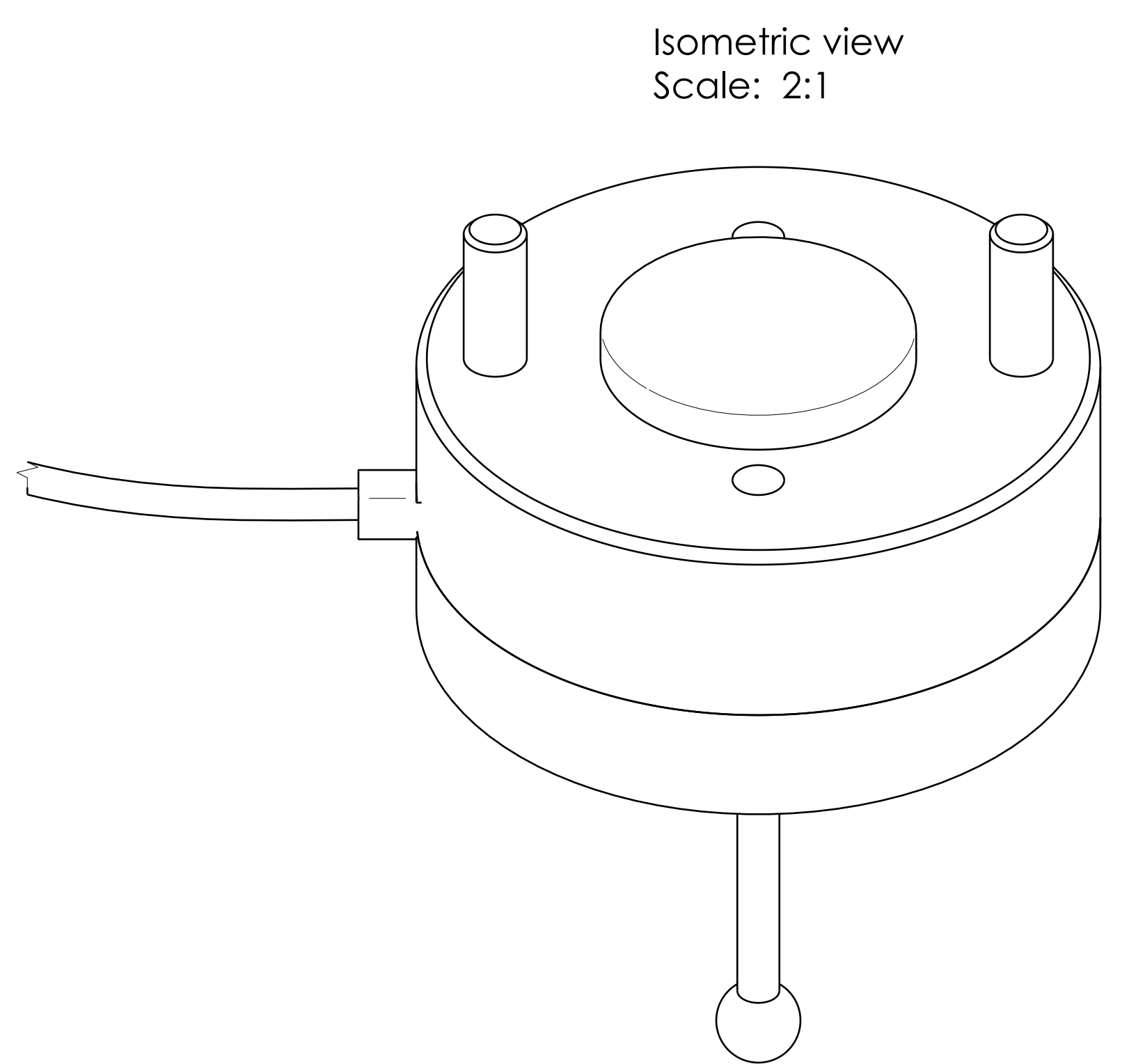
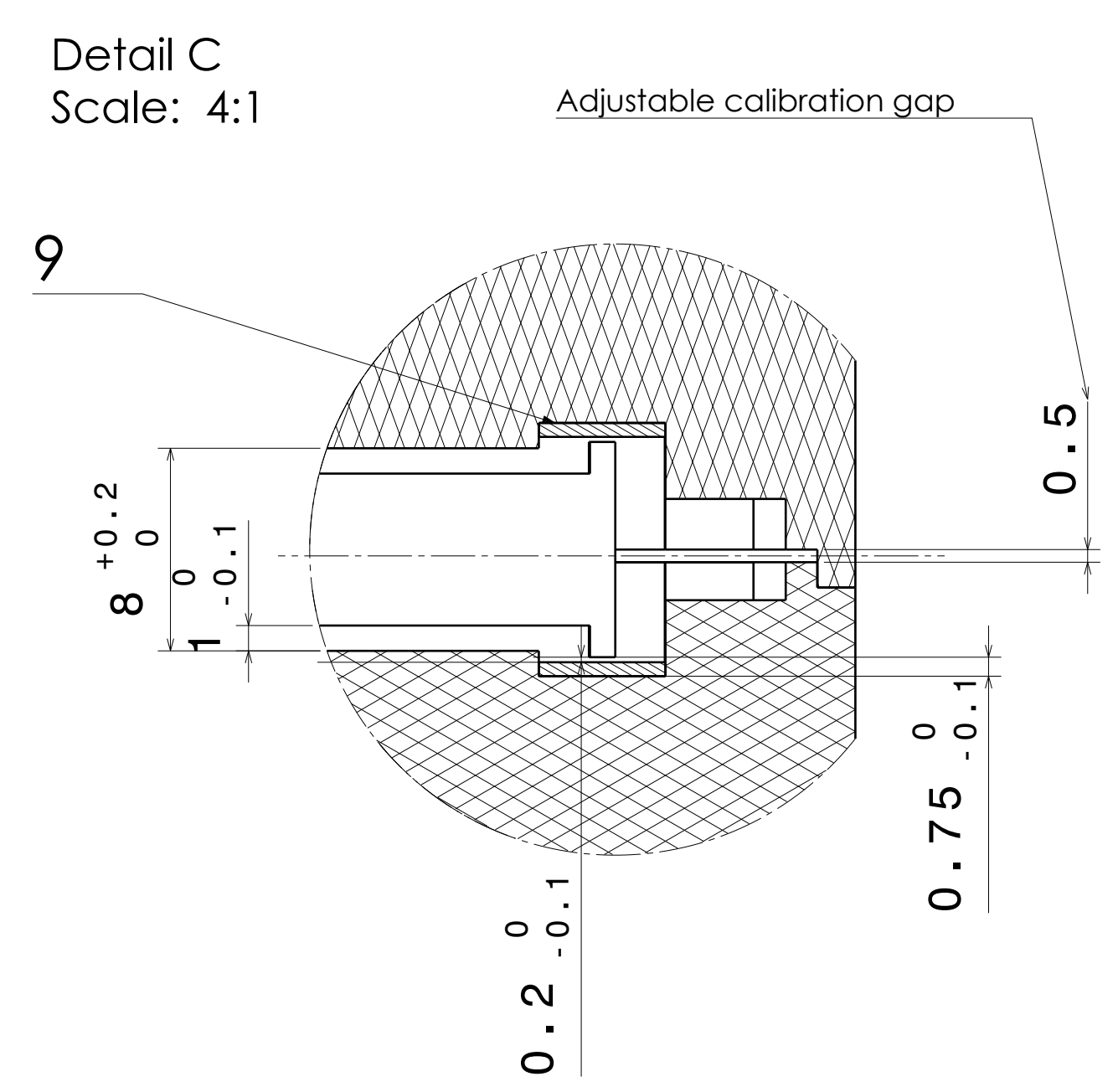
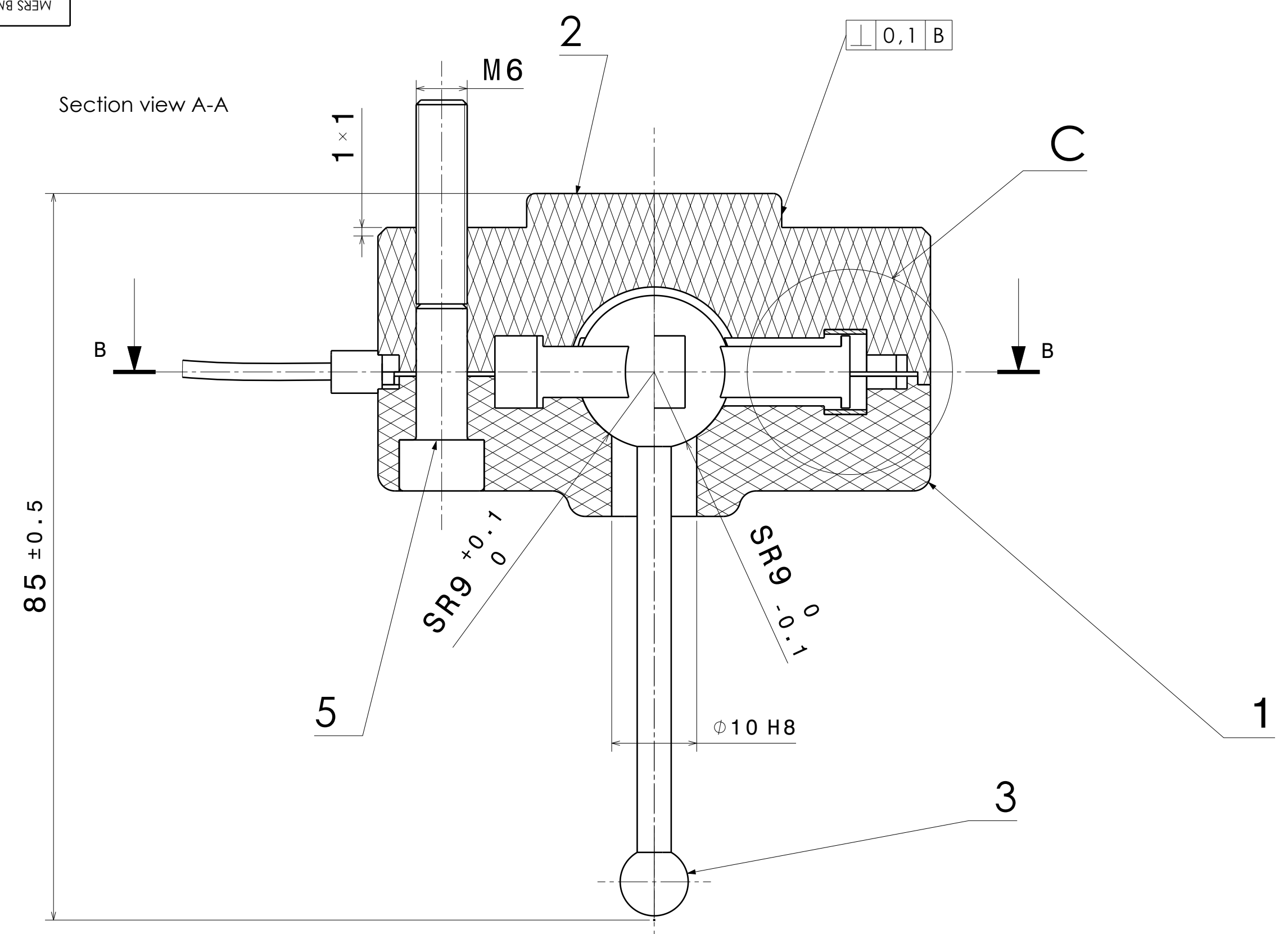
Drawings

Format	Zone	Position	Tag	Title	Qty.	Remarks			
				<u>Documents</u>					
A1			MERS BM 25 LP 01 01 00 00 GV	General view	1				
A1			MERS BM 25 LP 01 01 00 00 AV	Assembly view	1				
A3			MERS BM 25 LP 01 01 05 00 DV	Base matrix detail view	1				
A3			MERS BM 25 LP 01 02 06 00 DV	Superior matrix detail view	1				
A3			MERS BM 25 LP 01 03 04 00 DV	Probe detail view	1				
A2			MERS BM 25 LP 01 01 00 00 AM	Algorithm management	1				
A2			MERS BM 25 LP 01 01 00 00 EI	Economical indicators	1				
				<u>Parts</u>					
		1	MERS BM 25 LP 01 01 01 00	Base matrix	1				
		2	MERS BM 25 LP 01 01 02 00	Superior matrix	1				
		3	MERS BM 25 LP 01 01 03 00	Probe	1				
		6	MERS BM 25 LP 01 01 06 00	Yaskawa HC20SDTP	1				
		7	MERS BM 25 LP 01 01 07 00	Wire	1				
		8	MERS BM 25 LP 01 01 08 00	Rubber protector	1				
		9	MERS BM 25 LP 01 01 09 00	Piezoresistive sensors	6				
		10	MERS BM 25 LP 01 01 10 00	Control unit	1				
				<u>Standard parts</u>					
		4	MERS BM 25 LP 01 01 04 00	Hex head screw m6x16	2	ISO 4762			
		5	MERS BM 25 LP 01 01 05 00	Hex head screw m6x40	2	ISO 4762			
Respon.depart. Dep. of mech, rob and dig man		Adviser		Document type Specification		Status of the document Educational			
Owner Vilnius Tech		Prepared by Luis Palomero		Title Bill of materials		Tag			
		Approved by V.Bučinskis				Issue A	Date 05/05/2025	Lang. En	Page 1/1



1. Assembly must follow report instructions.
2. Calibration must be done according to the official procedure described on the report every assembly.
3. Attachment to the robot is made with the two m6x40 screws
4. Electrical parameters: 5V power supply
3.3 V (internal conversion) 250 mA (average) 0.825 W
5. Working temperature: up to 40° C
6. Force range: Max 10N
7. Weight: 0,131 kg

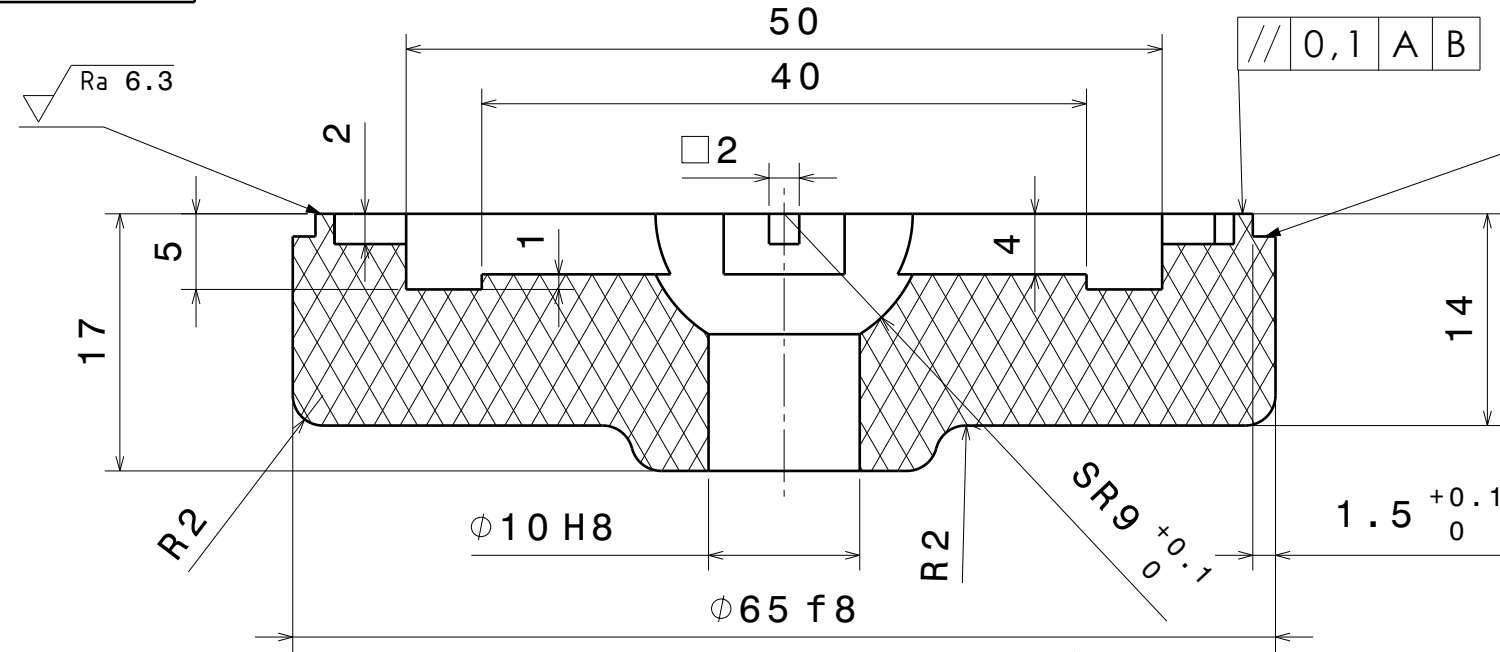
	File No.	Additional information	Material	Scale 1:5
Respon. depart. Dep. of mech., rob. and dig. man.	Adviser	Document type	Status of the document	
Owner VGTU	Prepared by Luis Palomero del Castillo	Title General view	MERS BM 25 LP 01 01 00 00 GV	
	Approved by V. Bučinskis		Issue 1	Date 05/05/2025
			Lang Eng.	Page 1/7



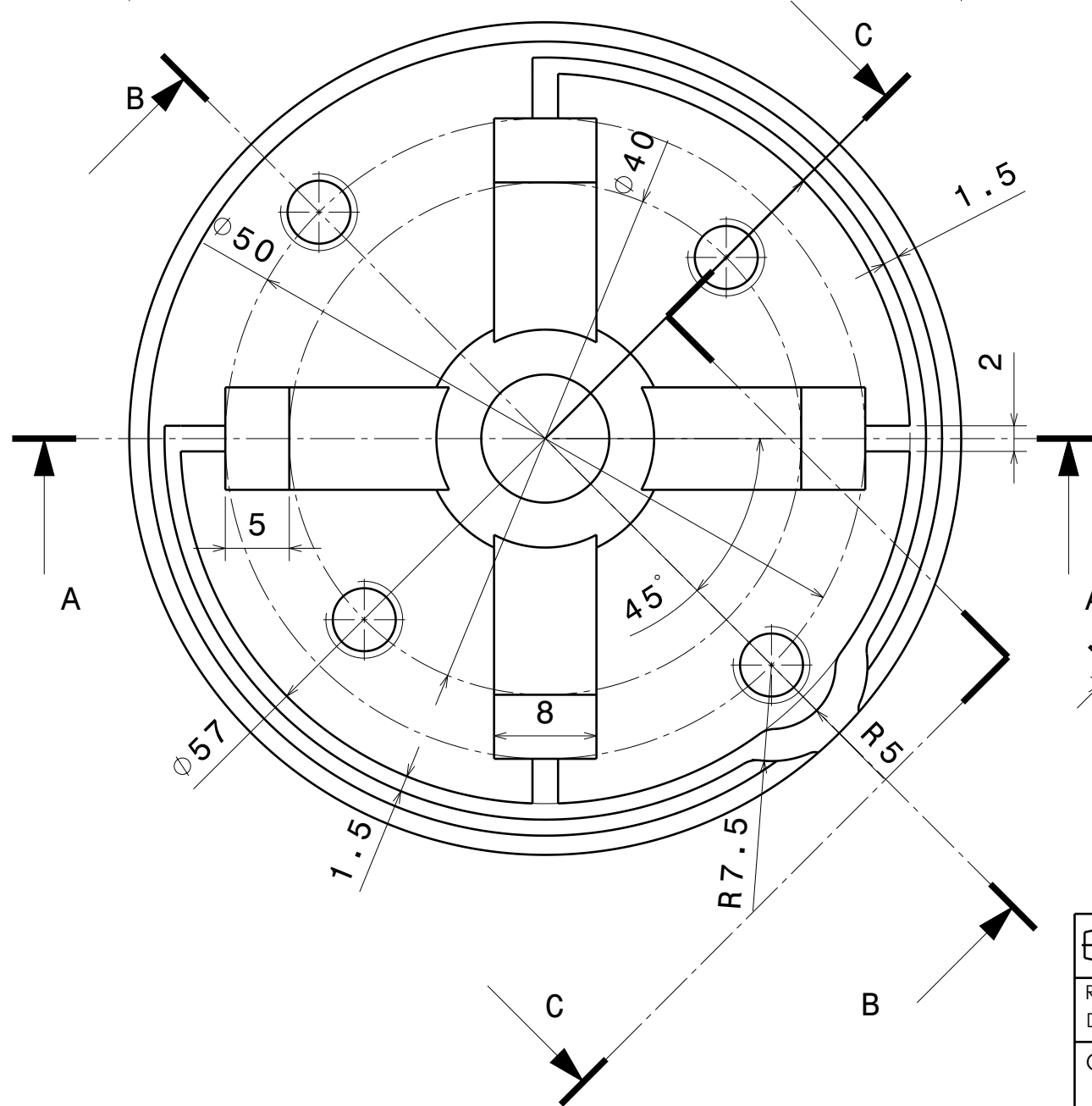
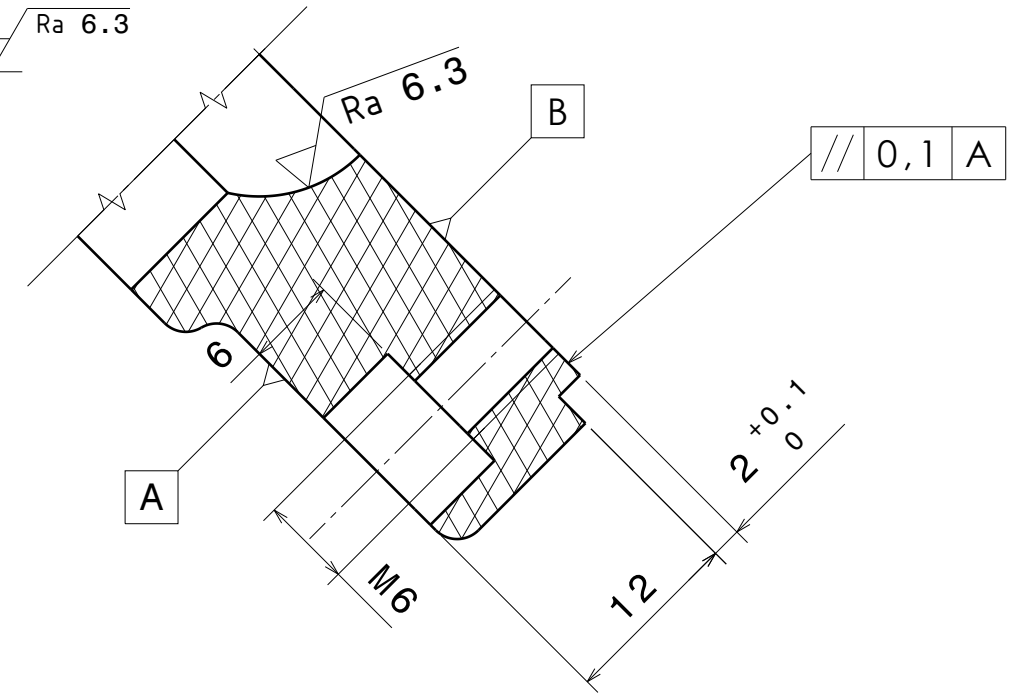
1. Scratches and dents are not acceptable.
2. Surfaces in contact with other parts as indicated must comply with roughness specifications on detail view drawings.
3. Assembly tolerances are required as the drawing indicates.
4. Assembly must follow the correct order instructions detailed on report.
5. Calibration must be done as indicated before use.

File No.	Additional information	Material	Scale 2:1
Respon. depart. Dep. of mech., rob. and sig. man.	Adviser	Document type	Status of the document
Owner VILNIUS TECH MRFU-21	Prepared by Luis Palomero del Castillo Approved by V. Bučinskis	Title Assembly view	MERS BM 25 LP 01 01 00 00 AV Issue 1 Date 05/05/2025 Lang. Eng. Page 2/7

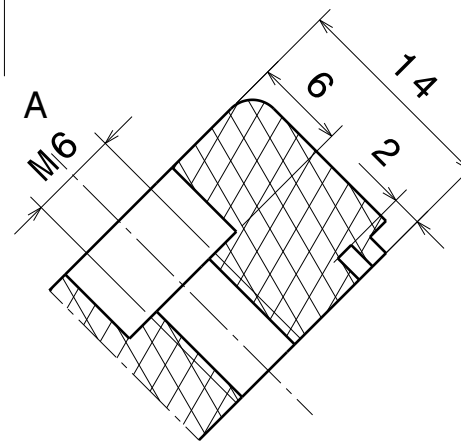
Section view A-A



Section view B-B



Section view C-C

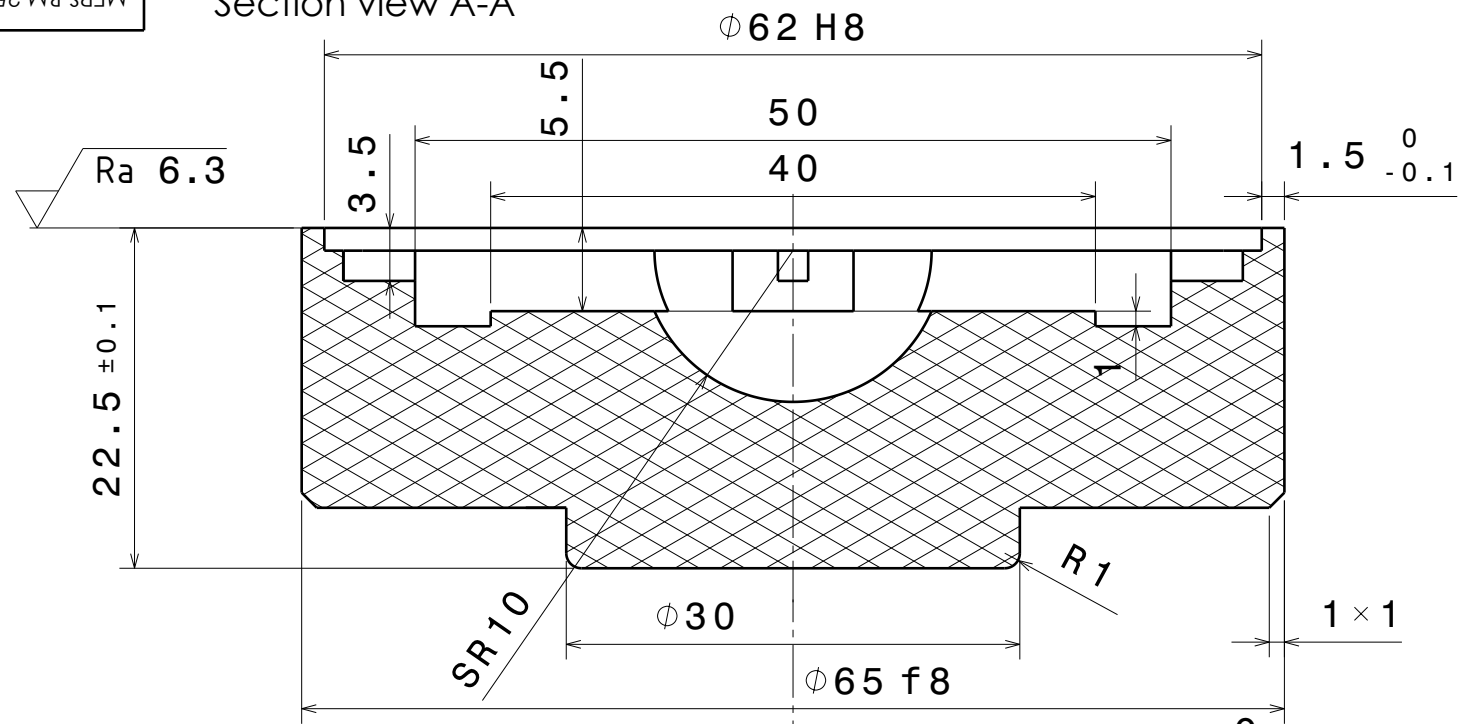


√ Ra 12.4 (Sanding Ra 6.3)

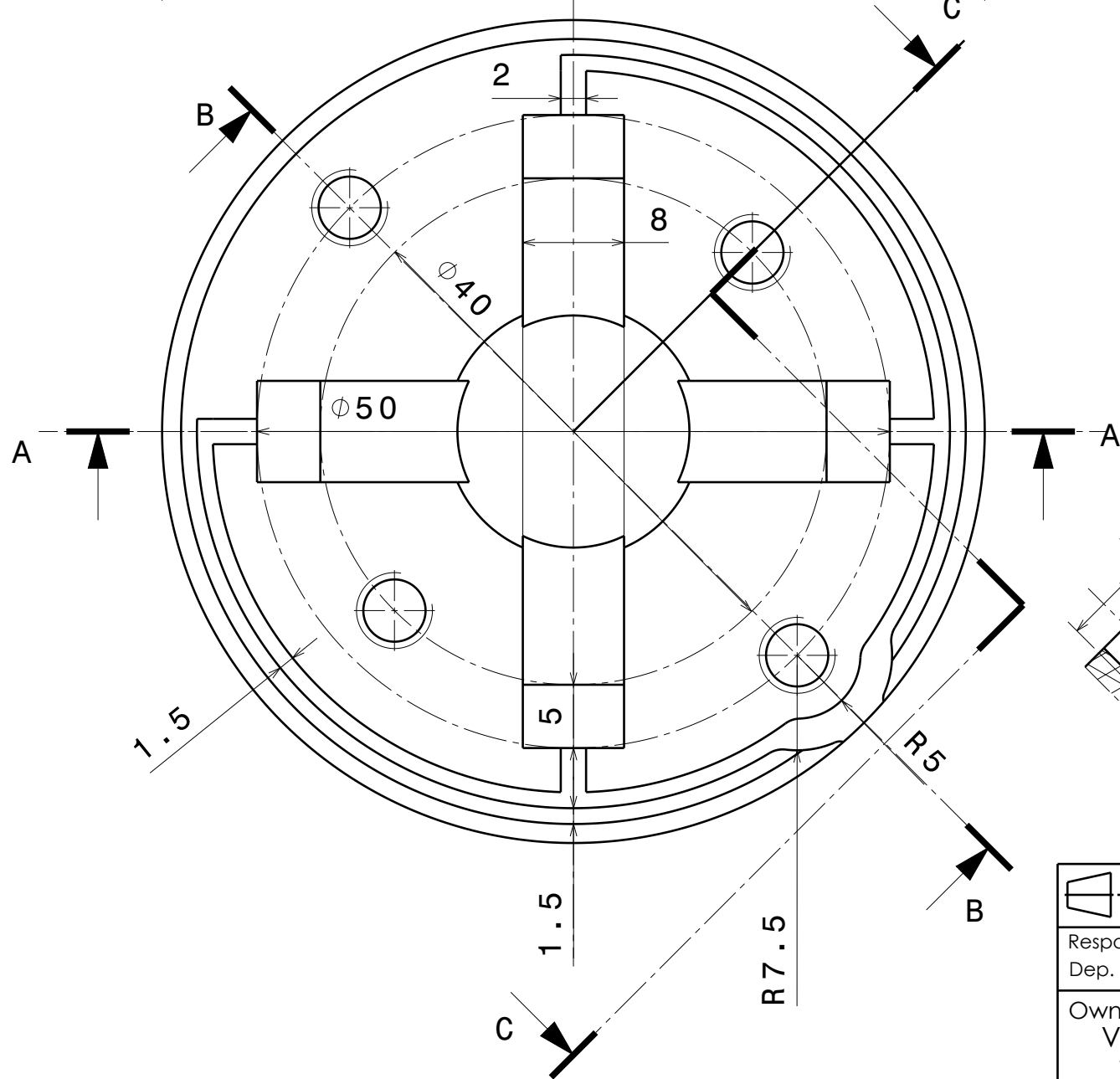
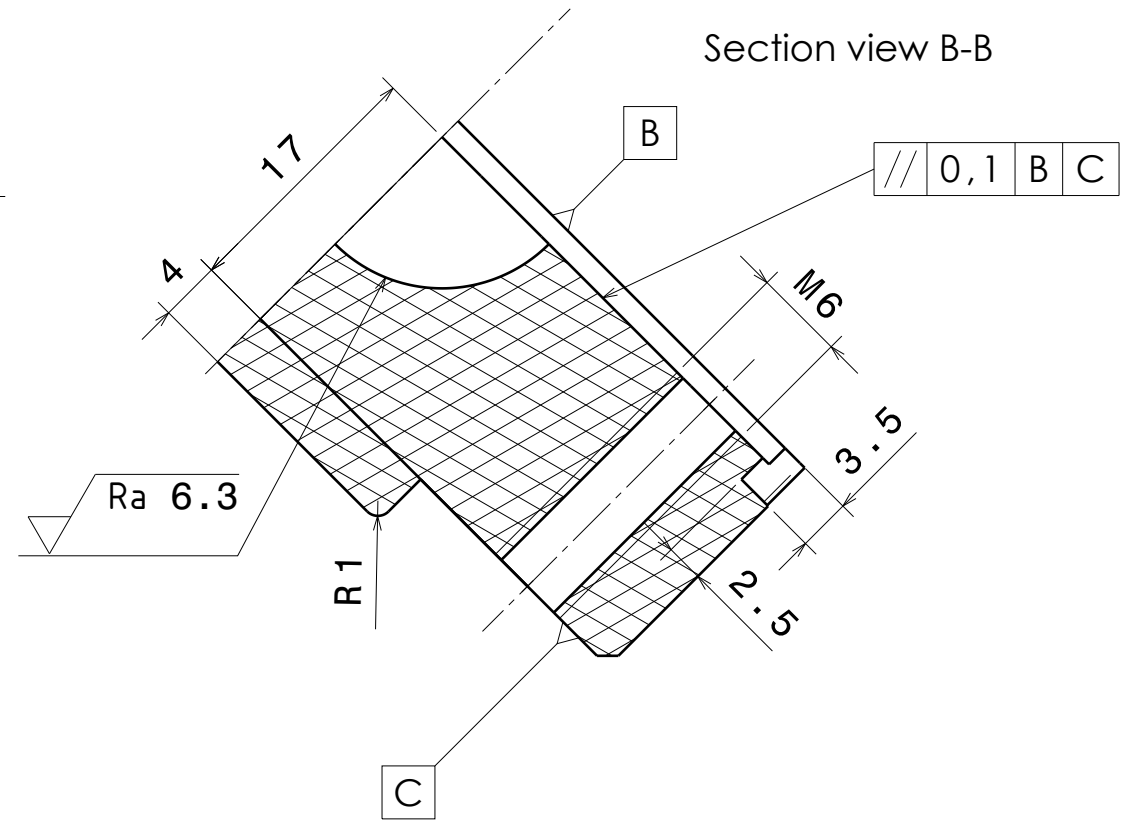
1. General tolerance according to ISO 2768-m
2. Scratches and dents are not acceptable.
3. Surfaces in contact with other parts as indicated must comply with roughness specifications.
4. Remove sharp edges or supports.

	File No.	Additional information	Material: Polylactic Acid (PLA)	Scale 2:1
Respon. depart Dep. of Eng. Graf.	Advisor	Document type Work drawing	Status of the document Educational drawing	
Owner VILNIUS TECH MRfu-21	Prepared by Luis Palomero del Castillo	Title Base matrix detail view	MERS BM 25 LP 01 01 05 00 DV	
	Approved by V.Bučinskas		Issue A	Date 05/05/2025
			Lang. Eng.	Page 3/7

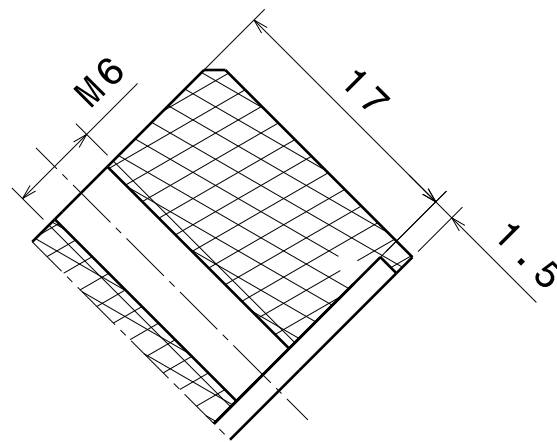
Section view A-A



Section view B-B



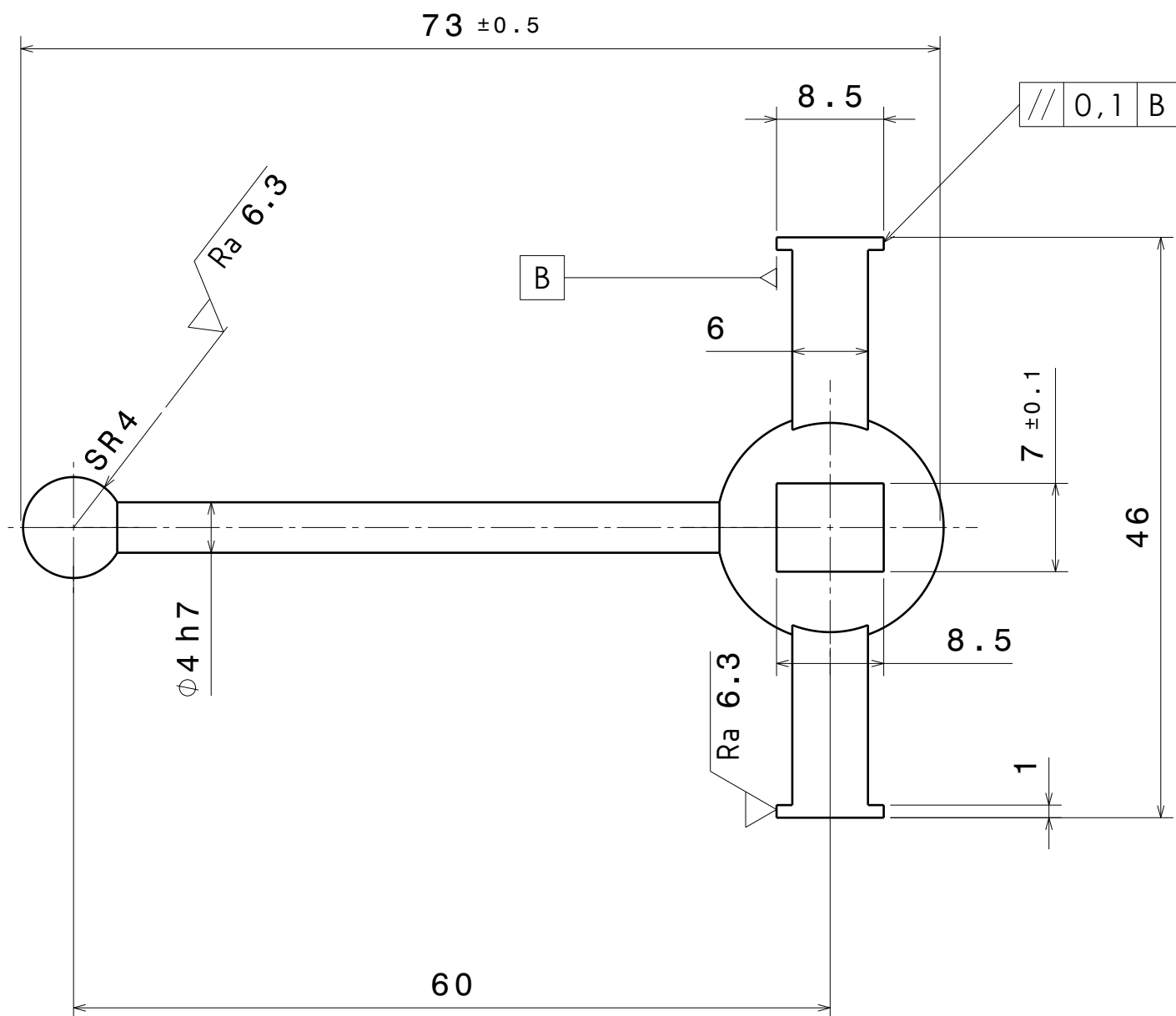
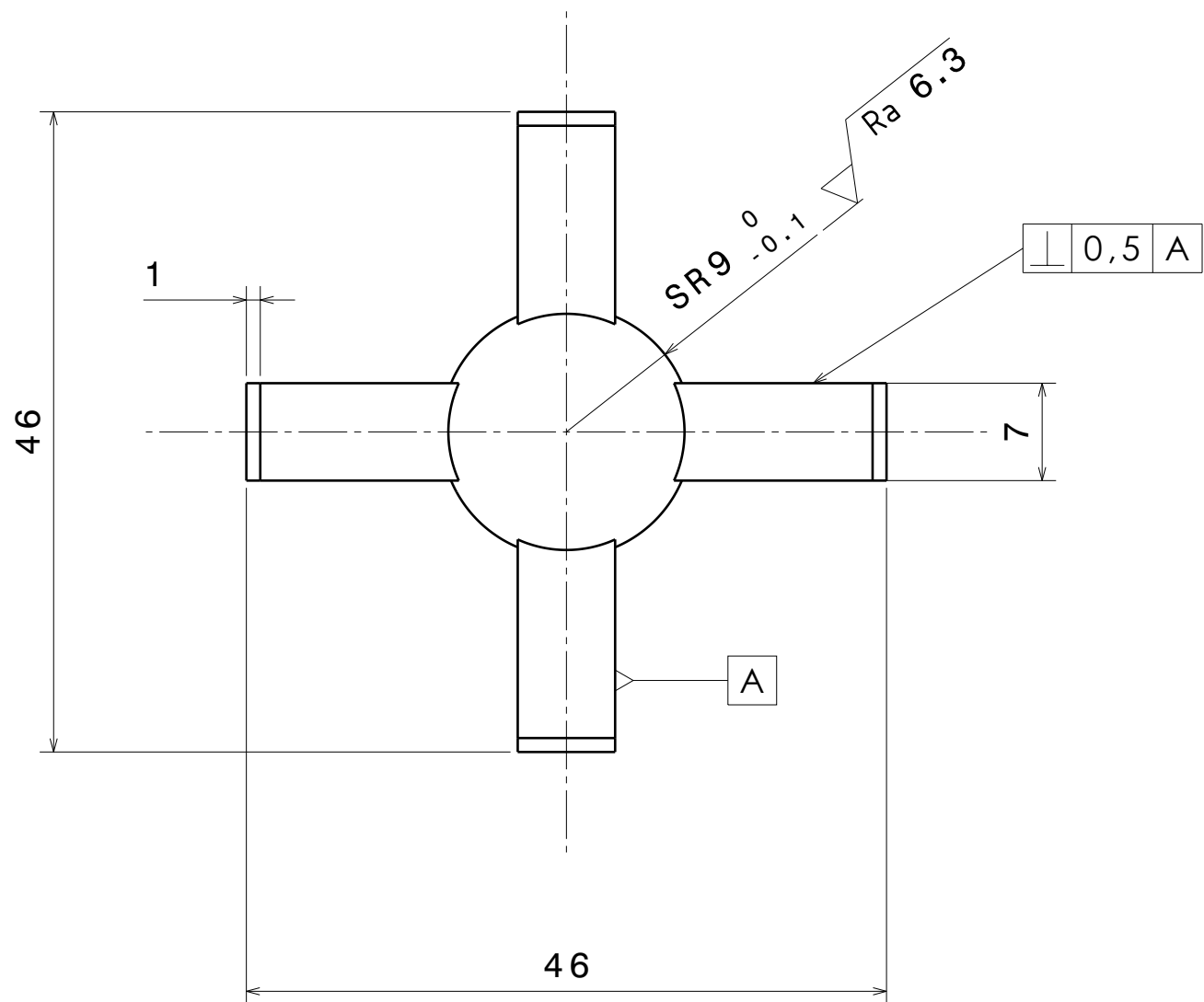
Section view C-C



$\sqrt{\text{Ra } 12.4}$ ($\sqrt{\text{Sanding Ra } 6.3}$)

1. General tolerance according to ISO 2768-m
2. Scratches and dents are not acceptable.
3. Surfaces in contact with other parts as indicated must comply with roughness specifications.
4. Remove sharp edges.

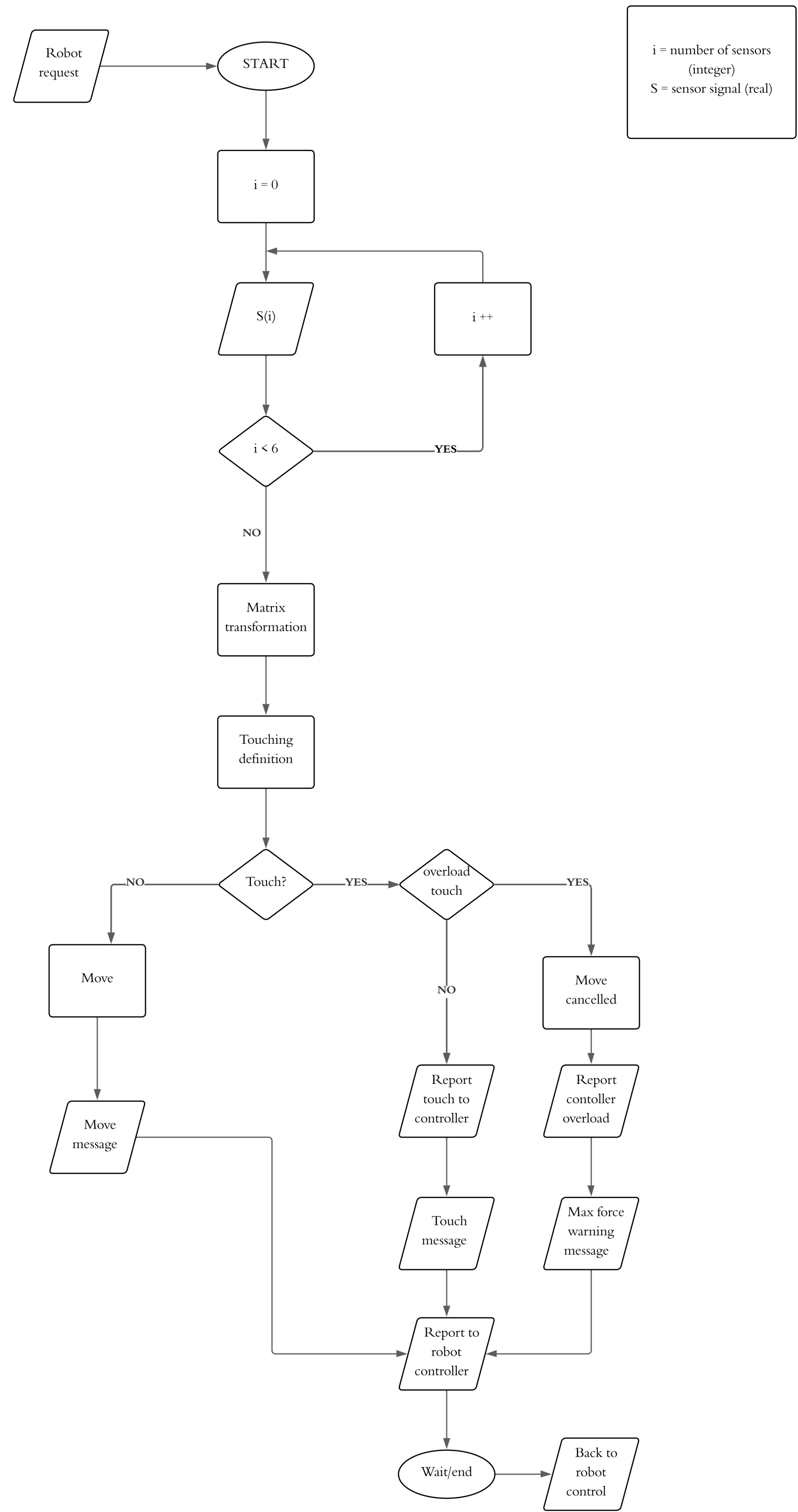
	File No.	Additional information	Material : Polylactic acid (PLA)	Scale 2:1
Respon. depart Dep. of Eng. Graf.	Advisor	Document type Work drawing	Status of the document Educational drawing	
Owner VILNIUS TECH MRfu-21	Prepared by Luis Palomero del Castillo Approved by V.Bučinskas	Title Superior matrix detail view	MERS BM 25 LP 01 02 06 00 DV	
			Issue A	Date 05/05/2025
			Lang. Eng.	Page 4/7



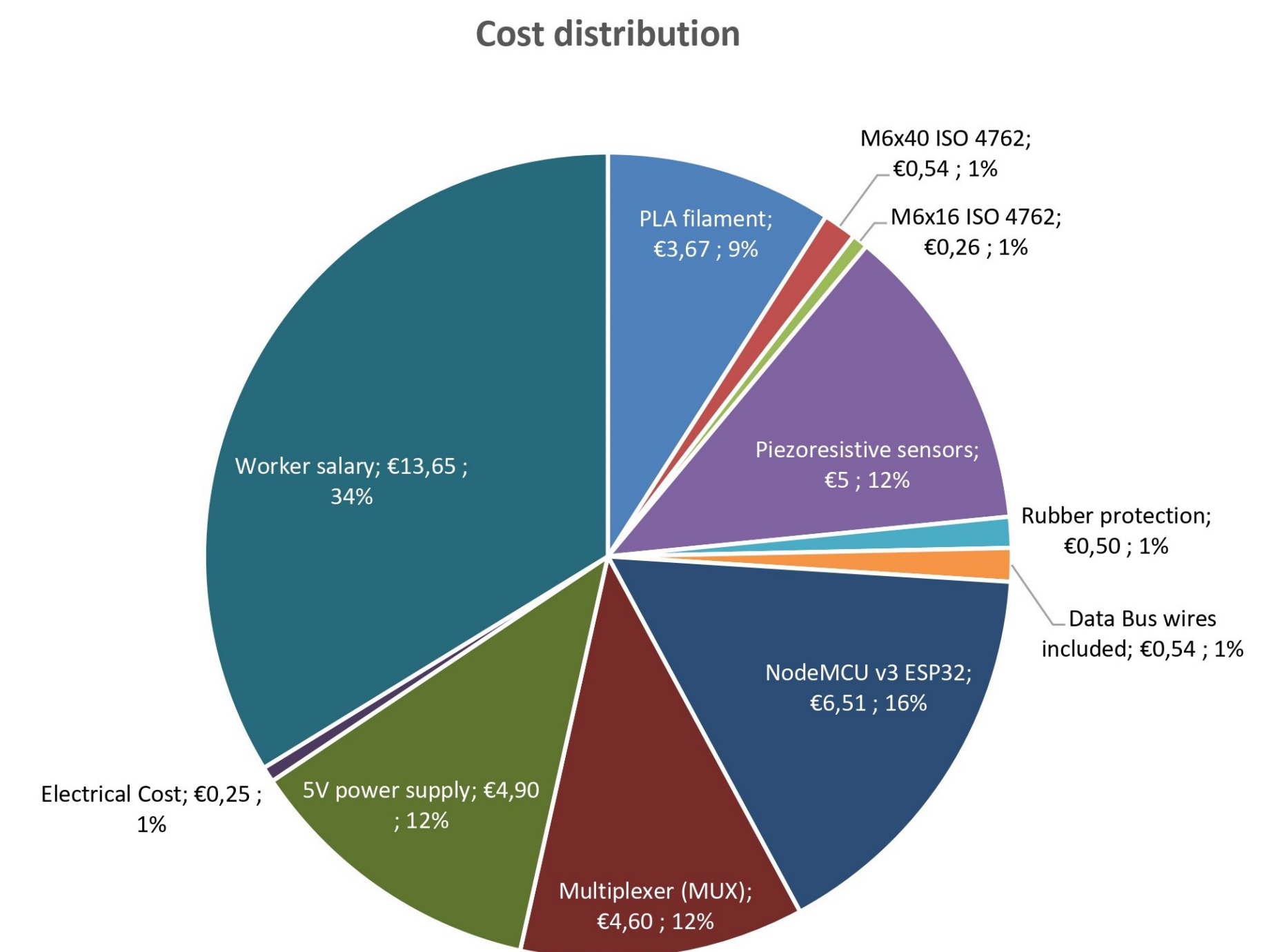
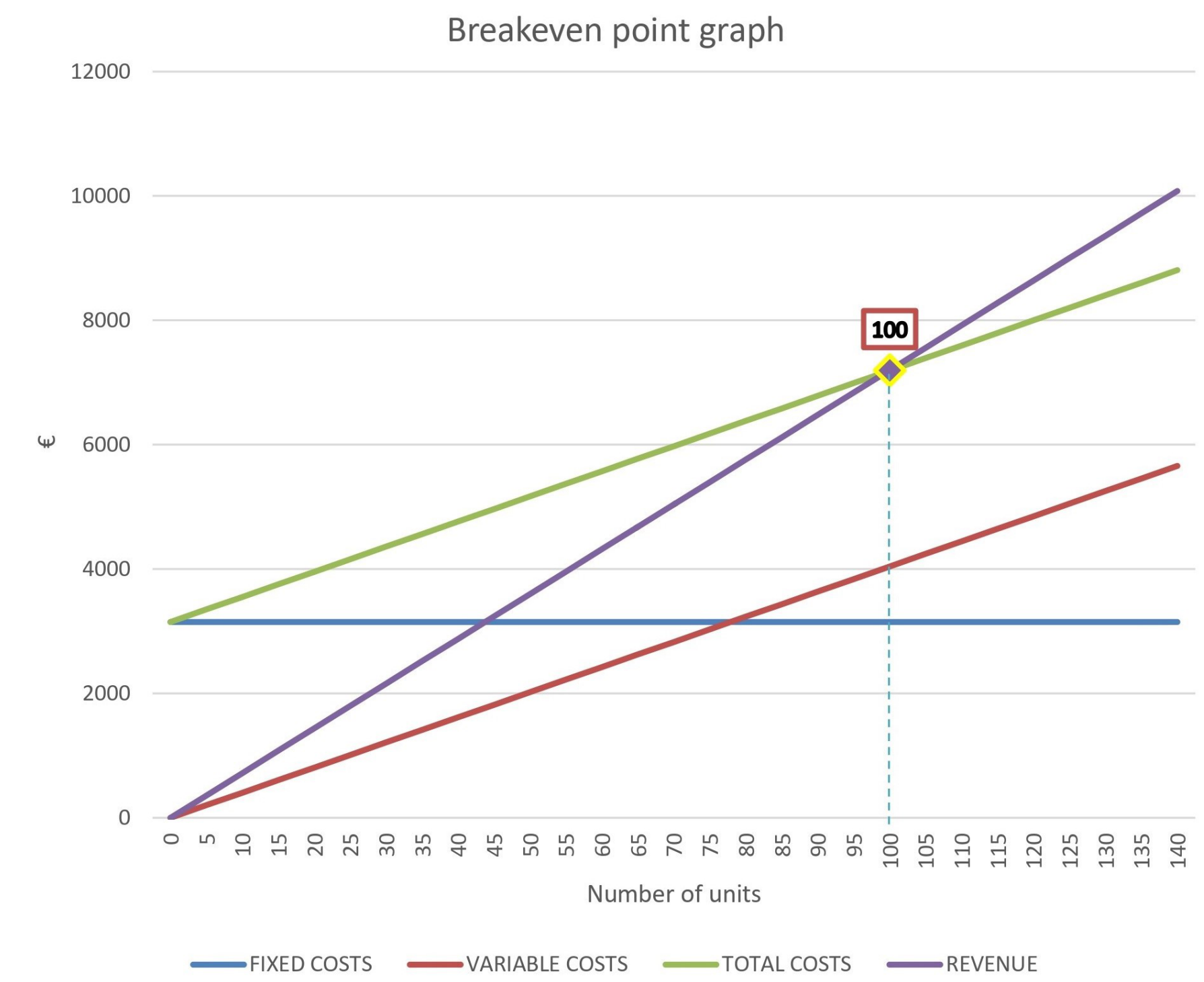
$\sqrt{Ra\ 12.4}$ ($\sqrt{Ra\ 6.3}$ Sanding)

1. General tolerance according to ISO 2768-m
2. Scratches and dents are not acceptable
3. Surfaces in contact with other parts as indicated must comply with roughness specifications.
4. Remove sharp edges (supports also).

	File No.	Additional information	Material: Polylactic acid (PLA)	Scale 2:1
Respon. depart Dep. of Eng. Graf.	Advisor	Document type Work drawing	Status of the document Educational drawing	
Owner VILNIUS TECH MRfu-21	Prepared by Luis Palomero Approved by V.Bučinskas	Title Probe detail view	MERS BM 25 LP 01 03 04 00 DV	
			Issue A	Date 05/05/2025
			Lang. Eng.	Page 5/7



	File No.	Additional information	Material	Scale 1:1
Respon. depart. mech. and dig. man.	Adviser	Document type	Status of the document Educational drawing	
Owner VILNIUS TECH	Prepared by Luis Palomero	Title	MERS BM 25 LP 01 01 00 00 AM	
	Approved by V. Bučinskis	Algorithm management	Issue A	Date 05/05/2025
			Lang. Eng.	Page 6/7



	File No.	Additional information	Material	Scale 1:1
Respon. depart. mech. and dig. man.	Adviser	Document type	Status of the document Educational drawing	
Owner VILNIUS TECH	Prepared by Luis Palomero	Title	MERS BM 25 LP 01 01 00 00 EI	
	Approved by V. Bučinskis		Economical indicators	Issue A
			Lang. Eng.	Page 7/7